Universidade de Lisboa
Faculdade de Medicina

The Role of the Ventral Telencephalon in Collective Motion

Renata Bastos da Silveira Pereira da Cruz

Orientadores: Gonzalo de Polavieja, PhD
Bruno Miranda, MD, PhD

Dissertação especialmente elaborada para obtenção do grau de Mestre em
Neurociências

2020

Universidade de Lisboa

Faculdade de Medicina

The Role of the Ventral Telencephalon in Collective Motion

Renata Bastos da Silveira Pereira da Cruz

Orientadores: Gonzalo de Polavieja, PhD
Bruno Miranda, MD, PhD

Dissertação especialmente elaborada para obtenção do grau de Mestre em
Neurociências

2020

"A impressão desta dissertação foi aprovada pelo Conselho Científico da Faculdade de Medicina de Lisboa em reunião de 26 de Novembro de 2020."

"*I am and always will be the optimist. The hoper of far-flung hopes and the dreamer of improbable dreams.*"

Doctor Who, Season 6, Episode 6

Resumo

Os humanos são organismos extremamente sociais que dependem de interações com outros indivíduos de forma a manter um estilo de vida funcional e saudável. O comportamento coletivo contribui para a criação de normas sociais que, por sua vez, têm o potencial de modelar consideravelmente as decisões e comportamentos de uma pessoa. Em contrapartida, comportamentos sociais primários, como agressividade ou reprodução, são também fundamentais para o nosso desenvolvimento. Como tal, torna-se importante perceber os mecanismos subjacentes a comportamentos sociais inatos e complexos.

O peixe-zebra (*Danio Renio*) é um modelo de particular interesse para o estudo de interação social em vertebrados. Apresentando um repertório bem documentado de diferentes comportamentos sociais e um conjunto impressionante de ferramentas genéticas disponíveis, este modelo animal permite uma abordagem reducionista no mapeamento de comportamentos sociais específicos em redes neuronais.

Estudos recentes sugerem que a região ventral do telencéfalo pode estar envolvida em comportamentos de caráter social, particularmente na atenção social. Contudo, este comportamento foi explorado num contexto estritamente visual. Isto é, um par de peixes, em regime de isolamento, foi colocado num tanque e separado por uma divisória transparente. A atenção social - interesse demonstrado pelo peixe vizinho - foi avaliada através da orientação entre os dois peixes enquanto estes interagiam visualmente através da divisória. Devido à simplicidade do paradigma descrito, torna-se relevante investigar o papel desta área do prosencéfalo no comportamento social do peixe-zebra, num contexto sensorial mais rico, no qual múltiplos peixes podem interagir fisicamente entre si.

Assim, o principal objetivo deste estudo foi avaliar o impacto causado pela ablação do telencéfalo ventral, na dinâmica de grupos de peixes-zebra, num contexto menos restrito. Para tal foi necessário otimizar um protocolo de ablação adequado para peixe-zebra em fase juvenil; perceber quais as características comportamentais que poderiam ficar comprometidas devido à ablação; e compreender que circuitos neuronais poderiam estar subjacentes a estas alterações comportamentais.

A ablação quimio-genética é uma técnica não invasiva que permite a ablação controlada de um alvo específico. Tem por base o sistema GAL4/UAS de modo a promover a expressão de um determinado gene apenas em locais onde o promotor GAL4 está presente. Um método popular baseado neste conceito é a ablação mediada por NTR/MTZ. Células que contém GAL4 expressam a enzima nitroreductase (NTR).

Ao entrar em contato com o pró-fármaco metronidazol (MTZ), a enzima produz compostos citotóxicos e induz morte celular nessas regiões. Neste estudo, utilizamos a técnica descrita na linha transgénica *y321*:GAL4. Esta linha em particular sinaliza o telencéfalo ventral (vTel) e o diencéfalo rostral, incluindo a área pré-óptica (POA), tubercular posterior (PT) e hipotálamo rostral (RH).

A rede do cérebro social (SBN) consiste em várias áreas cerebrais associadas à regulação do comportamento social. Foi originalmente proposta para mamíferos, exclusivamente. No entanto, com base em evidências de homologia funcional e anatómica foi sugerida uma conservação da SBN nos vertebrados, o que permitiu uma extensão do modelo. Em paralelo, a via mesolímbica (MRS) é um sistema fundamental que avalia a saliência de um estímulo. A integração das duas redes forma a rede social de tomada de decisões (SDN). O telencéfalo ventral do peixe-zebra, por sua vez, inclui estruturas cerebrais implicadas na SDN.

O peixe-zebra é um teleósteo de água doce encontrado no sul e no leste da Ásia. É uma espécie social que vive em extensos cardumes. O seu ciclo de vida é relativamente curto e a sua manutenção é bastante simples. O fato da maioria das estruturas envolvidas no SDN estarem conservadas no cérebro do peixe, conjugado com as vantagens anteriormente descritas, torna este animal um excelente modelo para estudos de comportamento social.

Os peixes têm tendência para se agregar em grupos coesos com fins sociais - cardumes - apresentando um comportamento social complexo conhecido como *shoaling*. A formação de cardumes confere diversas vantagens ao nível de proteção contra predadores, acasalamento ou na procura de alimentos. Os cardumes são sensíveis a fatores internos e externos, o que lhes conferem uma qualidade plástica. Não apresentam uma estrutura específica associada e facilmente sofrem alterações na sua conformação.

No entanto, existe um caso particular em que um cardume apresenta uma estrutura polarizada, onde os peixes se movem de forma coordenada. Neste estado específico de organização o cardume é considerado um *school*. Um coletivo de peixes pode alternar facilmente entre os dois estados de polarização, de acordo com suas necessidades. Por exemplo, com a habituação a um ambiente, os peixes tendem a passar menos tempo num estado polarizado e a tornar-se gradualmente mais desorganizados com o passar do tempo.

Comportamentos de agrupamento, como *shoaling* ou *schooling*, são formados a partir de interações locais entre os indivíduos. Sabe-se que os peixes ajustam seu comportamento de acordo com sua própria velocidade e com a velocidade e posição relativa dos seus vizinhos.

Por conseguinte, como foi referido anteriormente, utilizamos o método de ablação mediada pelo sistema NTR/MTZ. Este permitiu alcançar o telencéfalo ventral e o diencéfalo rostral, promovendo morte celular nesses locais. O tratamento de ablação foi avaliado através de técnicas de microscopia LightSheet. Posteriormente, exploramos o comportamento coletivo num paradigma sem restrições. A avaliação comportamental consistiu numa sessão de deslocamento livre em que cada grupo testado tinha um total de cinco elementos.

A otimização do protocolo de ablação foi relativamente bem sucedida uma vez que atingimos ablação parcial das regiões pretendidas. No entanto, a toxicidade associada ao MTZ foi mais elevada do que o esperado. A aplicação do tratamento nos peixes levou a complicações ao nível das funções motoras que se traduziram em claros sinais de acinesia e lentidão no movimento.

Por outro lado, os nossos resultados sugerem uma disrupção em comportamentos de ansiedade. Como esperado, os grupos controlo exibiram um comportamento ansioso ao serem introduzidos num novo ambiente. No entanto, os peixes que sofreram ablação não se mostraram tão sensíveis à nova situação. Curiosamente, peixes que não expressavam NTR mas que foram tratados com MTZ, exibiram um nível mais alto de proximidade do que os controlos, o que indica um comportamento ansioso mais forte. Acontece que a POA é considerada uma área importante em respostas ao stress e na regulação da ansiedade no peixe-zebra. Consequentemente, os resultados apresentados podem ser uma indicação de que a ablação da POA pode ser um fator contribuinte para a alteração da resposta normal ao stress e para a regulação negativa do circuito de ansiedade.

Além disso, enquanto a coesão do grupo foi preservada na sua generalidade, o alinhamento local entre os animais foi severamente alterado. As distâncias inter-individuais entre os peixes, uma medida útil para a avaliação da coesão, permaneceram praticamente inalteradas ao longo das experiências. Pelo contrário, enquanto todos os grupos testados exibiram uma diminuição gradual no alinhamento local ao longo do tempo, o grupo submetido à ablação não mostrou qualquer alinhamento à partida. Estes resultados sugerem que a ablação do vTel e da POA pode exercer um efeito local no comportamento, levando a mudanças no alinhamento individual dos peixes, enquanto mantém a integridade geral do grupo. Estas conclusões vão de acordo com estudos anteriores, pois indicam que o vTel pode estar particularmente envolvido no comportamento de orientação. Contudo, o papel da POA nesses resultados não se encontra claro.

Em suma, com o estudo apresentado demonstramos a importância de áreas ventrais específicas do prosencéfalo na plasticidade do comportamento social. O vTel e a POA

podem ser responsáveis por impulsionar o comportamento de orientação a nível local em ambientes sociais. Também confirmamos a importância dessas duas estruturas no circuito da ansiedade.

peixe-zebra; cardume; comportamento social; ablação quimiogenética; telencéfalo ventral

Abstract

Zebrafish (*Danio Renio*) is a favored model in neuroscience for studying vertebrate social behaviour. Fish display numerous complex behaviours depending on their environment and since they are a social species, valuable information could emerge when considering the entire collective and not solely the individual. Recent studies suggest that the ventral region of the telencephalon might play a role in social attention. However, this behavioural feature was explored strictly under a visual context where two isolated fish were separated by a transparent divider and could only interact visually. It remains unknown whether this area has a role in the dynamics of a collective under a richer environment, in which animals may physically interact with one another. Through chemo-genetic ablation, we were able to target the ventral telencephalon and rostral diencephalon, promoting cell-death on these locations. Subsequently, we explored the collective behaviour within an unconstrained paradigm. Our findings suggested a disruption in anxiety-typed behaviors. Furthermore, while group cohesion was mostly preserved, local alignment between the animals was completely impaired. In accordance with previous reports, our results indicate that the vTel might be particularly involved in orienting behavior.

zebrafish; shoaling; social behavior; chemogenetic ablation; ventral telencephalon

Acknowledgements

First, I would like to thank Gonzalo for accepting to be my mentor and giving me the opportunity to be part of this challenging project. You allowed me to work freely yet were always there to support and guide me whenever I needed.

To Paco, for being there since the very beginning. Thank you for your patience, availability and help throughout this journey. I learned so much from you and I wish you all the luck and success in the future.

To all the members from the Polavieja Lab, current and former, for being so welcoming, helpful and supportive. Also, a special thank you to our office of strong independent women, I had so much fun with all of you.

To everyone in the ABBE platform without whom the imaging part of the project would not have been possible. To Ruth for always being willing to help and listen to my numerous questions about zebrafish.

To the CCU community, because working within such a vibrant and dynamic environment was incredibly inspiring.

To my tea buddies Bernardo and Catarina, thank you for all the crazy and fun moments, you were my emotional support whenever I felt stressed or frustrated and I am so glad to take your friendships with me. To Filipa and Daniel, you were far away in distance but were as close to me as if you were here.

To my family, words cannot express how thankful I am for your unconditional support. To my extraordinary sister Mariana, you are my partner for the good, the bad and the uneventful. I am so curious to see the amazing things you will accomplish in the future! To my parents, you guided me to be the best version of myself and gave me the freedom to be my own person. You have always supported my decisions and trusted my judgement. Whenever I felt overwhelmed, you would say everything was okay and that all I needed to do was take a step back and breath. Thank you so much. I hope to make you all proud!

Finally, I would like to thank the examiners and everyone who took the time to critically read and comment the thesis: Gonzalo, Bruno Miranda, Paco, Daniel and Cátia.

Table of Contents

List of Figures

List of Tables

List of Abbreviations

AH	**A**nterior **H**ypothalamus
ATN	**A**nterior **T**uberal **N**ucleus
a.u.	**a**rbitrary **u**nits
BL	**B**ody-**l**ength
BNST	medial **B**ed **N**ucleus of the **S**tria **T**erminalis
BS	**B**ackground **S**ubtraction
BSA	**B**ovine **S**erum **A**lbumin
CB1954	5-(aziridin-1-yl)-2,4-dinitrobenzamide
CFP	**C**yan **F**luorescent **P**rotein
CNS	**C**entral **N**ervous **S**ystem
CZI	**C**arl **Z**eiss **I**mage
DMSO	**D**i**m**ethyl **S**ulf**o**xide
dpf	**d**ays **p**ost **f**ertilization
F	**F**ormamide
LBF	**L**aser **B**locking **F**ilter
LGF	**L**ocal **G**radient **F**ilter
IID	**I**inter-**i**ndividual **D**istance
KDE	**K**ernel **D**ensity **E**stimation
LS	**L**ateral **S**eptum
meAMY	**me**dial **AMY**gdala
MIP	**M**aximum **I**ntensity **P**rojection
MRS	**M**esolimbic **R**eward **S**ystem
MTZ	**Me**tronida**z**ole
NAcc	**N**ucleus **Acc**umbens
NGS	**N**ormal **G**oat **S**erum
NTR	**Ni**t**ro**reductase
OB	**O**lfactory **B**ulb
o.n.	**o**ver**n**ight
PBS	**P**hosphate-**B**uffered **S**aline
PFA	**P**ara**F**orm**A**ldehyde
POA	**Pre**optic **A**rea
PT	**P**osterior **T**uberculum
ROI	**R**egion **o**f **I**nterest
RTF	**R**apid clearing method based on **T**riethanolamine and **F**ormamide
SBN	**S**ocial **B**rain **N**etwork
SBS	**S**econdary **B**eam **S**plitter
SDN	**S**ocial **D**ecision-making **N**etwork
SDK	**S**oftware **D**evelopment **K**it
SumP	**Sum P**rojection

Str	**Str**iatum
tERK	**t**otal **E**xtracellular signal-**R**egulated **K**inases
TEA	**T**ri**e**thanol**a**mine
Tg	**T**rans**g**enic
UAS	**U**pstream **A**ctivating **S**equence
Vc	**c**entral **V**entral telencephalon
Vd	**d**orsal **V**entral telencephalon
VMH	**V**entro**m**edial **H**ypothalamus
Vs	**s**upracommisural **V**entral telencephalon
VTA	**V**entral **T**egmental **A**rea
VTN	**V**entral **T**uberal **N**ucleus
Vv	**v**entral **V**entral telencephalon
vTel	**v**entral **Tel**encephalon
W	Distilled **W**ater

1 | Introduction

Humans are extremely social organisms and greatly depend on interaction with others to maintain a functional and healthy lifestyle. Collective behaviour contributes to the creation of social norms, which might modulate considerably the decisions and behaviour of an individual [42][106]. However, the systematic study of human social behaviour and its corresponding neural and genetic correlates is still a great scientific challenge.

Trails of ants, flocks of birds or cockroach aggregations provide accessible examples of collective phenomena and complex systems. Indeed, collective behaviour renders great advantages to social species such as being less prone to predators or higher probability of discovering food sources. It can also have considerable impact on individual decision making. A good example are homing pigeons compromising their route exclusively when conflict on their directional preference is low [99].

Zebrafish (*Danio Renio*), due to their social nature and growing availability of genetic tools [67][26], are an increasingly popular model in neuroscience for studying vertebrate social behaviour. Zebrafish display numerous complex behaviours depending on their environment. For instance, under adverse situations fish tend to aggregate and exhibit a polarized and synchronous motion [77]. Notwithstanding, under similar conditions they may also assume a freezing typed behaviour. The collectives may switch between different behaviours according to their surroundings [57]. Nevertheless, the neural circuitry responsible for driving each of these behaviours and the influence that external stimuli might exert on them remain unexplored.

1.1 Rationale

Stednitz et al. (2018) presented a visually-mediated social study which focused on the level of engagement between two isolated zebrafish, separated by a divider. One of the animals was transgenic and had particular regions of the brain ablated to allow neuroanatomical studies.

In detail, animals were separated and could only interact visually through an electrochromatic panel. This partition could be switched from opaque to transparent upon cue, to activate the live stimulus according to protocol design (Figure 1.1 A). The animals performed a stereotyped orienting behavior towards each other which reflected social attention. In addition, three transgenic lines with different targeted areas underwent chemo-genetic ablation through the NTR/MTZ system (this technique will be further discussed in Chapter 3).

In their results, a particular line -*y321*- targeting the area of the ventral telencephalon, displayed significantly lower levels of engagement with their co-specific (Figure 1.1

C,D). Furthermore, this behavioral change observed in ablated fish, seemed to consequently affect the behaviour of their non-ablated neighbour, indicating a relevance on reciprocity. Thus, the stimulus fish required attention from the ablated fish otherwise, it would not manifest social interest towards the latter.

Note that in Figure 1.1 C, the *y321* line targets the hindbrain as well as the ventral forebrain, more specifically the ventral telencephalon. Two other transgenic lines with different anatomical targets were tested in the same experimental conditions. One of which - line *y299* - also included the hindbrain in its description. However, no changes in the behaviour were found in these ablated animals.

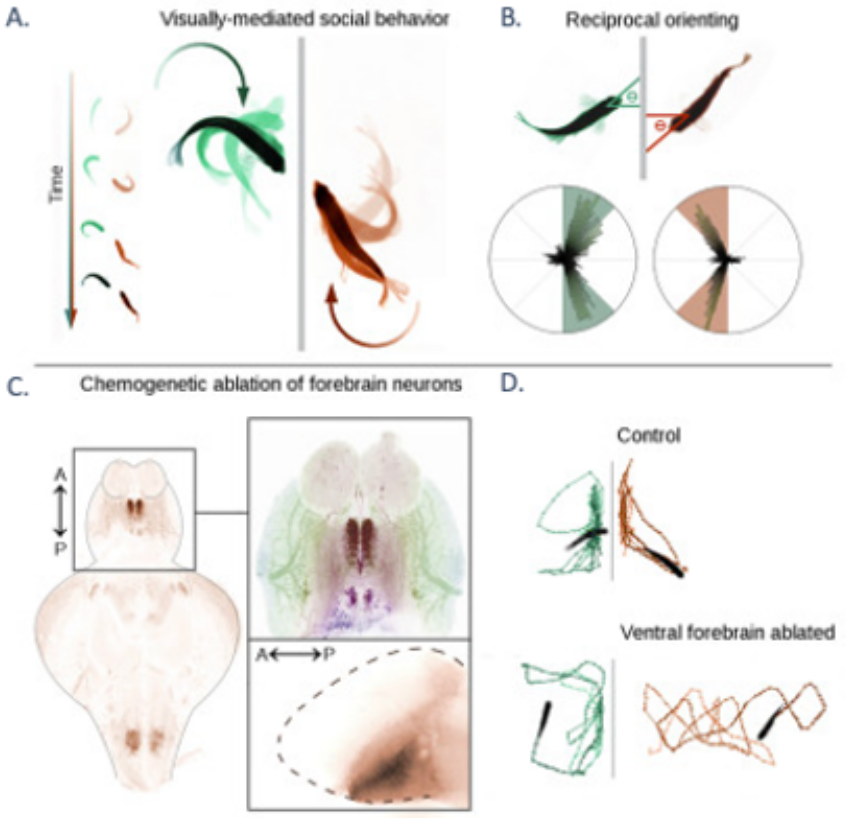

Figure 1.1. Social Behavior in Fish Dyads. Experimental design for a social behavior assay. (A) Visually-mediated behavioral assay of zebrafish dyads. Measure for social behavior is orientation over time. (B) Importance of reciprocity for social behavior. (C) NTR/MTZ-mediated chemical ablation on forebrain regions, including ventral telencephalic area and hindbrain (orange). (D) Trajectories from stimulus fish (green) and both control (orange, top panel) and ablated fish (orange, bottom panel). Figure adapter from Stednitz et al. (2018).

While these findings suggest that the ventral telencephalon might play a role in social orientation, it is important to note that behaviour modifies and adjusts according to the environment. As part of a richer social context where animals might physically interact, results for an individual might be different. Moreover, a noteworthy feature to consider in a social species is the size of the collective. Small groups of free-swimming fish, formed by two or three animals, may behave differently from larger

groups.

Tracking softwares (such as the idtracker.ai, developed in the lab [87]), allow for multiple individuals to be tracked across time without losing their identities. Combining this technology with genetic tools such as chemo-genetic ablation, provides the opportunity not only to study the social behaviour of a collective and its singular elements, but also gain insights on which brain areas might be involved in driving different behaviors.

1.2 Objectives

The main goal of this study was to evaluate the impact caused by the ablation of the ventral telencephalon in the dynamics of free swimming zebrafish collectives.

Assuming the ablation is successful and selectively damages the ventral telencephalon, the behavior of the fish within a social context might be significantly altered. If so, our hypothesis becomes whether this effect occurs in a local manner or instead, generates a global re-adjustment.

If the first, general group cohesion should be maintained but the local alignment of the individuals should be disrupted. If the second, inter-individual distances should increase and swimming should become more dispersed yet the alignment might remain unchanged.

Thus, the aims of this work were:

1. To optimize an ablation protocol appropriate for juvenile zebrafish. It had to successfully reach and ablate the targeted areas without generating any adverse consequences to the animals;
2. To assess which behavioural features might be particularly affected due to the ablation treatment;
3. To understand the anatomical correlates and neural circuitry underlying these behavioural changes.

1.3 Overview

The current dissertation is divided into eight main Chapters:

Chapter 1 introduces the project, including the reasons which led to its development, a small contextualization and the presentation of our initial hypothesis and main objectives.

Chapter 2 offers an insight on zebrafish as a model for social neuroscience, focusing on their ontogeny and anatomical and functional information.

Chapter 3 provides a brief clarification on the molecular mechanisms involved in a chemo-genetic ablation technique. Particularly, the strategies used to achieve specificity and cell death induction.

Chapter 4 focuses on the behavior of zebrafish as a collective and their local dynamics.

Chapter 5 describes in detail the methods employed for the development of this study.

Chapter 6 presents the results obtained following data acquisition and analysis. It is divided is two parts consisting on the imaging and behavioural data, respectively.

Chapter 7 features a thorough discussion on the previously described results. We seek to get a deeper insight on our findings and re-evaluate our initial hypothesis, always considering relevant literature.

Chapter 8 covers the main conclusions drawn from this study. It further reflects on the challenges and difficulties encountered and contemplates future work prospects.

2 | Zebrafish (*Danio rerio*): a Vertebrate Model for Social Neuroscience

As a species, humans are fundamentally social organisms. From complex social norms needed for co-habitation to basic social behaviors such as aggression or mating, social interactions are pivotal for our development. Therefore, it is extremely important to understand the foundations of both innate and complex social behaviors.

Social neuroscience is an interdisciplinary field that explores the close interactions between mind and brain in a social context, often focusing on concepts viewed as abstract, such as perception [14]. However, finding a suitable model which provides a proper social assessment while simultaneously, representing a good sample to study the biological systems of the brain, poses a great challenge.

Zebrafish is a model of particular interest for social neuroscience given its social nature. Presenting a well documented repertoire of different social behaviors and an impressive set of genetics tools available, they allow a reductionist approach on mapping specific social behaviors into neural networks [67].

In the following sections, we will revise relevant brain structures involved in the social networks of vertebrates and go through anatomical and functional information on the zebrafish brain.

2.1 Social Decision-Making Network

As originally proposed by Newman (1999), the social brain network (SBN) consisted on six nodes - the extended medial amygdala, the lateral septum, the preoptic area, the anterior hypothalamus, the ventromedial hypothalamus and a number of areas in the midbrain, such as the periaquedyctal gray (Figure 2.1 C, top yellow region). These core structures had to fulfill three basic criteria. First, they had to be implicated in the control of various forms of social behavior and be bidirectionally connected. Additionally, they had to contain sex steroid receptors important for sexual differentiation and temporal coordination of social behavior. Moreover, each node responded to a variety of stimuli depending on the social context, generating distinct patterns of activity across nodes, for different behaviors. This model was suggested exclusively for mammals. However, Goodson (2005) proposed an extension to all vertebrates provided by the increasing evidence for homologies which suggested the SBN is conserved in the vertebrate brain (Figure 2.1 A and B).

At the same time, it is important to note that regulation of social behavior comes in hand with an appropriate evaluation of stimulus salience. Animals need to integrate information from environmental and physiological cues and prior knowledge to make a proper assessment and produce a suitable action. In mammals, this is achieved by the mesolimbic reward system (MRS) and SBN. Subsequently, O'Connel (2011) proposed

the social decision-making network (SDN) as the integration of these two networks (Figure 2.1 C) [66]. As we can see from Figure 2.1 A and B, the SDN is relatively well conserved in the teleost brain [66][69].

In parallel, neuromodulatory systems such as dopaminergic, serotonergic and cholinergic pathways also seem evolutionary preserved (Figure 2.1 D, E and F) [71]. These systems are the basis of cognitive function and the interaction with the SDN give rise to social behaviors such as attention, emotion, goal-directed behavior and decision-making [7].

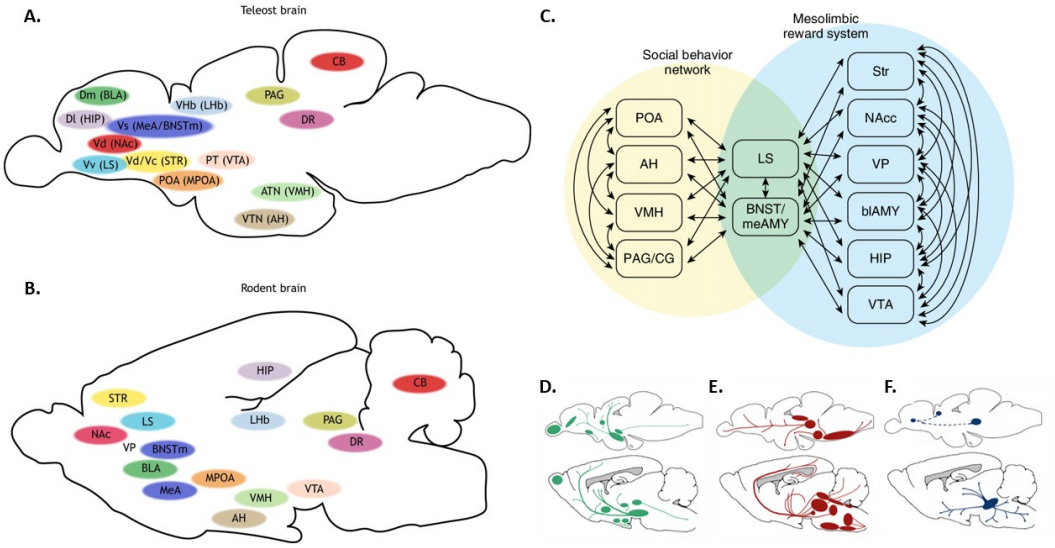

Figure 2.1. Social Decision-Making Network. Social behavior network (SBN) and mesolimbic reward system (MRS) in teleost fish and rodents. (A and B) Brain regions involved in both SBN and MRS mapped in (A) teleost fish and their homologous structures in the (B) mouse brain, coded by color. Figure adapted from Geng et al. (2019). (C) Brain areas associated to the vertebrate social decision-making network clustered by their role either in the SBN (yellow), MRS (light blue) or both (green). Arrows represent connections between brain regions. Figure adapted from O'Connell et al. (2011b). (D,E and F) Sagittal view of the (D) dopaminergic, (E) serotonergic and (F) cholinergic neuronal populations in zebrafish brain (top) and mouse brain (bottom). Figure adapted from Parker et al. (2013). AH, anterior hypothalamus; ATN, anterior tuberal nucleus; BLA, basolateral amygdala; BNSTm, medial bed nucleus of the stria terminalis; CB, cerebellum; Dl, lateral dorsal telencephalon; Dm, medial dorsal telencephalon; DR, dorsal raphe; HIP, hippocampus; LHb, lateral habenula; LS, lateral septum; MeA/medAMY, medial amygdala; MPOA, medial preoptic area; NAc, nucleus accumbens; PAG, periaqueductal gray; POA, preoptic area; PT, posterior tuberculum; STR, striatum; Vc, central ventral telencephalon; Vd, dorsal ventral telencephalon; VHb, ventral habenula; VMH, ventromedial hypothalamus; VP, ventral pallidum; Vs, supracommissural nucleus of the ventral telencephalon; VTA, ventral tegmental area; VTN, ventral tuberal nucleus; Vv, ventral nucleus of the ventral telencephalon.

2.2 Ontogeny of Zebrafish

Danio rerio is a freshwater teleost fish commonly known as zebrafish. The *Cyprinidae* family to which they belong also includes other known species in neuroscientific research such as the goldfish (*Carassius auratus*) and the carp (*Cyprinus carpio*). They are a social species that live in large shoals and can be found in South and East Asia [105].

Their life cycle is relatively short, as indicated by the schematic representation in Figure 2.2. At an early stage, larvae are transparent and swim in discrete short bursts of movements, generally known as bouts. While their transparency and small size are great advantages for imaging techniques, their social component is not fully developed yet [40][25].

However, by the time fish reach the juvenile stage, their social interactions are strong and they already display grouping behaviors such as shoaling [40]. They only achieve sexual maturity in adulthood, roughly three months after fertilization. From this stage on, they start to reveal social behaviors associated to sex differences such as aggression and mating [68][84].

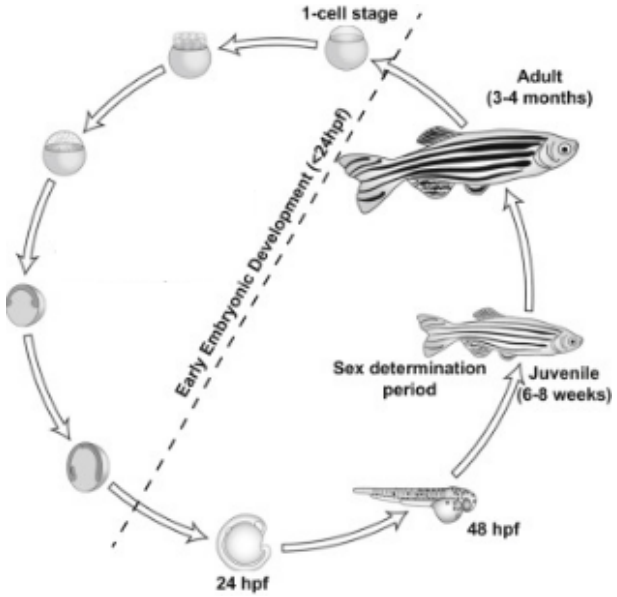

Figure 2.2. Developmental Stages of Zebrafish. The cycle begins at 1-cell stage after fertilization. Within the first 24 hpf the embryo develops all the major organs. At 48 hpf, embryos hatch and start swimming freely, beginning the larval stage. Approximately at 30 dpf, larvae become juvenile. At 45 dpf, the fish start a sex determination period. At 90 dpf fish are considered adults and become sexually mature. Figure adapted from Aluru et al. (2017).

Each stage of development has its unique set of advantages. Due to their large progeny, easy maintenance and relatively simple genetic manipulation, zebrafish are an ideal animal model for a diverse range of fields in neuroscience.

2.3 Zebrafish Brain: Anatomical and Functional Organization

The zebrafish brain is divided into four major sections: the telencephalon, diencephalon, mesencephalon and rhombencephalon (Figure 2.3).

The telencephalon is the most anterior part of the brain. It has been implicated in sensory and motor control, autonomic and endocrine functions and in cognitive activities such as memory and learning. This region includes the olfactory bulb and the dorsal and ventral telencephalon [105][75][4]. The diencephalon is essentially involved in the regulation of emotional and sexual behaviors and maintenance of homeostasis. It is where structures such as the habenula, pineal organ, thalamus and hypothalamus can be found. It has also been suggested to be an important part of the limbic system [105][18]. The telencephalon and diencephalon form respectively, the dorsal and ventral parts of the forebrain and are bounded by the preoptic area.

The mesencephalon, also considered as midbrain, is a set of three main sections primarily responsible for processing sensory information. While the optic tectum is an essential structure in the visual system [86], the torus semicircularis is mostly involved in the auditory system and mechanoreception [28]. The last structure is the tegmentum, mainly related to motor functions [105].

Finally, the most posterior region of the zebrafish brain is the rhombencephalon, also referred to as hindbrain. Formed by the cerebellum and medulla oblongata, this segment is implicated in balance and sensory and motor functions [60].

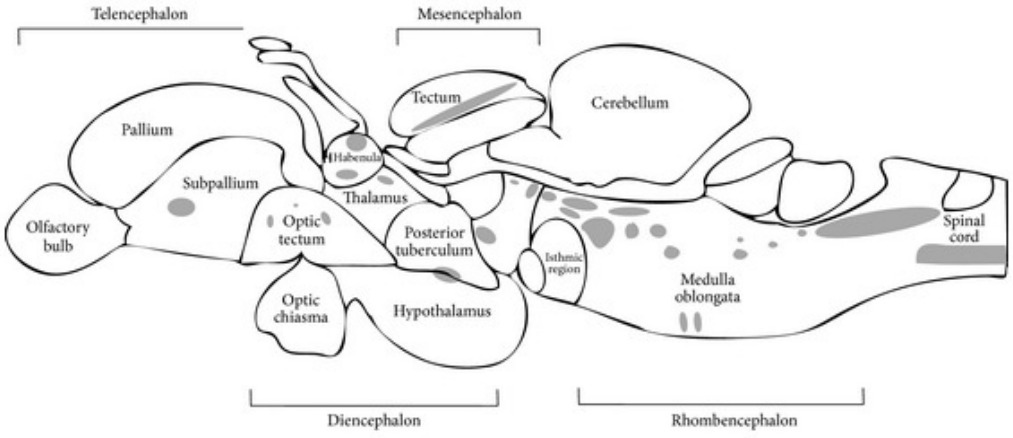

Figure 2.3. Adult Zebrafish Brain. Sagittal view of an adult zebrafish brain. Figure adapted from Toledo et al. (2013).

2.3.1 *Area Ventralis Telencephali*

The ventral subdivision of the telencephalic lobes (vTel), also known as subpallium, is an important integrative center in the teleostean CNS [105]. As seen in Figure 2.1 A, neuroanatomical and hodological studies suggested homologies between teleosts and rodents primarily in intersecting areas of the SDN and areas from the MRS, exclusively [66].

More specifically, the ventral nucleus of the ventral telencephalon (Vv) is considered to be homologous to the lateral septum (LS) while evidence suggests the supracommissural nucleus of the ventral telencephalon (Vs) is an homologue of medial amygdala (meAMY) and medial bed nucleus of the stria terminalis (BNST). Furthermore, the striatum (Str) and the nucleus accumbens (NAcc) are putative homologues of the dorsal and central nucleus of the ventral telencephalon (Vd/Vc), respectively [66].

On a different note, both cholinergic and dopaminergic pathways have neural populations in the ventral telencephalic region of the zebrafish brain.

Thus, the vTel is a great candidate to study not only incentive-motivated behaviors but also social cognition-typed behaviors such as social attention [103].

2.3.2 *Area Preoptica, Posterior Tuberculum, Rostral Hypothalamus*

These three diencephalic areas are mostly related to endocrine regulation of sex-associated social behaviors.

In detail, the preoptic area (POA) is the most rostral part of the diencephalon. It is considered to be a highly conserved region across vertebrates [69] and it has been implicated in the regulation of stress responses, social approach, subordinance, aggression, courtship and parental care [33].

In mammals, the VTA is a MRS hub that plays a significant role in regulating reward, motivation, cognition, and aversion [81]. Its putative homologous structure in the zebrafish brain is the posterior tuberculum (PT) [66]. This area is involved in the MRS with dopaminergic projections to the vTel [85].

The anterior hypothalamus and the ventromedial hypothalamus are respectively homologous to the ventral tuberal nucleus (VTN) and the anterior tuberal nucleus (ATN). These areas are part of the ventral hypothalamic zone, located at the most rostral region of the hypothalamus. Accordingly, these two structures are considered nodes of the SBN. Their particular role in zebrafish behavior has not been explored, yet in mammals they are known to be involved in control of aggressive behavior, reproduction and parental care [66].

3 | NTR/MTZ-Mediated Ablation of Neuronal Cells

Chemogenetic ablation is a non-invasive procedure for conditional genetic manipulation.

In the coming sections, we will briefly cover the system to generate transgenic lines. Subsequently, we will review the basis to drive controlled genetic expression, through a chemical approach, in zebrafish.

3.1 GAL4/UAS System

The Gal4/UAS system is a binary technique that manipulates gene expression in specific targeted cells [21].

In detail, Gal4 is a transcriptional activator found in yeast. Its sequence can be inserted into the genome, under the control of a tissue-specific enhancer. In parallel, the upstream activating sequence (UAS) is a Gal4 binding site which, when bound to the promoter, drives the expression of a given gene [22][21].

Accordingly, a transgenic line can be created, as illustrated by Figure 3.1. Firstly, a construct containing Gal4 and an enhancer for a determined region of interest, is built and injected into the genome of a zebrafish embryo. The tissue-specific driver line is crossed with a UAS line fluorescently tagged. Ultimately, a new product line is generated, in which the reporter gene is expressed solely in locations where Gal4 is present [5].

This system is a powerful genetic tool that allows the manipulation of gene expression in selected cells and tissues. Furthermore, we can drive targeted cells to express toxic genes and induce cell death exclusively in the desired areas.

3.2 NTR/MTZ System

Nitroaromatic compounds such as metronidazole (MTZ), are reduced by nitroreductase enzymes (NTR) which can be found in *Escherichia coli*. The reaction mechanism of NTR/MTZ has a cytotoxic activity mainly due to two metabolites formed during the process. These products have the power to oxidize DNA chains and form covalent DNA adducts, inducing cell death [6].

3.3 NTR/MTZ-Mediated Ablation

Most systems are formed by cooperative units. In order to understand their function in the global scheme, one can remove single elements and observe the changes introduced to the system. Subsequently, the ability to induce conditional cell death in an animal model such as the zebrafish, is a powerful tool to study both development and

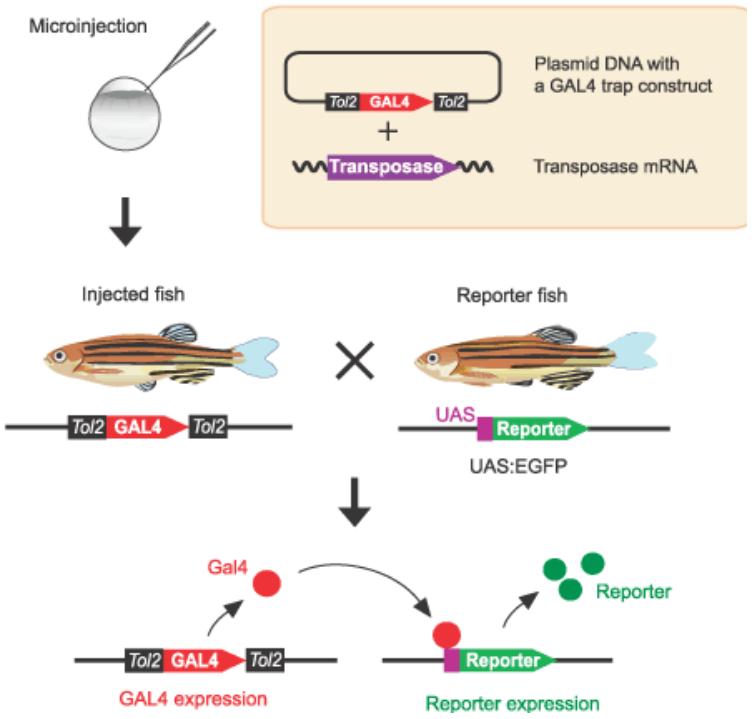

Figure 3.1. Gal4/UAS System in Zebrafish. Generation of a transgenic Gal4 line. A DNA plasmid containing a Gal4 construct and the binding enzyme transposase are injected in an embryo, through microinjection. Subsequently, a reporter fish carrying a fluorescent protein gene (reporter/EGFP) downstream of Gal4 recognition sequence (UAS), is crossed with the injected fish. As a result, if carrying both Gal4 and UAS constructs, their progeny will express the reporter in the targeted regions. Figure adapted from Asakawa et al. (2008).

regeneration [78]. To that end, finding the appropriate genetic ablation protocol is a requirement. It has to allow for an accurate selection of the region of interest, while avoiding leakage to neighbouring areas. It also needs to hold the advantage of being temporally controllable, transmissible to the later generations and reversible [21].

Over the years many different protocols were designed with the attempt to fulfill the previous conditions [74][96][47]. Most methods use a GAL4/UAS system to promote the expression of a prodrug converting enzyme, in a tissue-specific manner. In theory, this entitles the treatment of an experimental fish with the proper prodrug, at a desired time. Consequently, the incubation should promote cell death in enzyme expressing cells, as explained in sections 4.1 and 4.2. However, an additional concern to be considered is whether the ablation occurs in any cell population and at any stage. Otherwise, it may be necessary to restrict the ablation to specific cell types. Therefore, it is important to chose the protocol better suited to each project.

The NTR/MTZ system has been widely applied for it best complies with the requirements specified above and it does not regard the cycle status of the cell. There are other NTR substrates such as CB1954 (5-(aziridin-1-yl)-2,4-dinitrobenzamide), which

has been commonly used for these assays. Yet, it exhibited a 'bystander effect', affecting neighbouring cells along with the targeted ones [13]. Hence, MTZ has been the preferred prodrug for cell ablation purposes.

Figure 3.2 summarizes the results from ablation studies performed in Curado et al. (2008). Larvae at 80 hours post fertilization (hpf) were treated either with MTZ or DMSO, a reagent which helps solubilize MTZ, for a period of 24 h. The lack of fluorescence of the targeted cells, designated as β, suggests a successful ablation. Interestingly, following a recovery of 24h, the β cells start to regenerate.

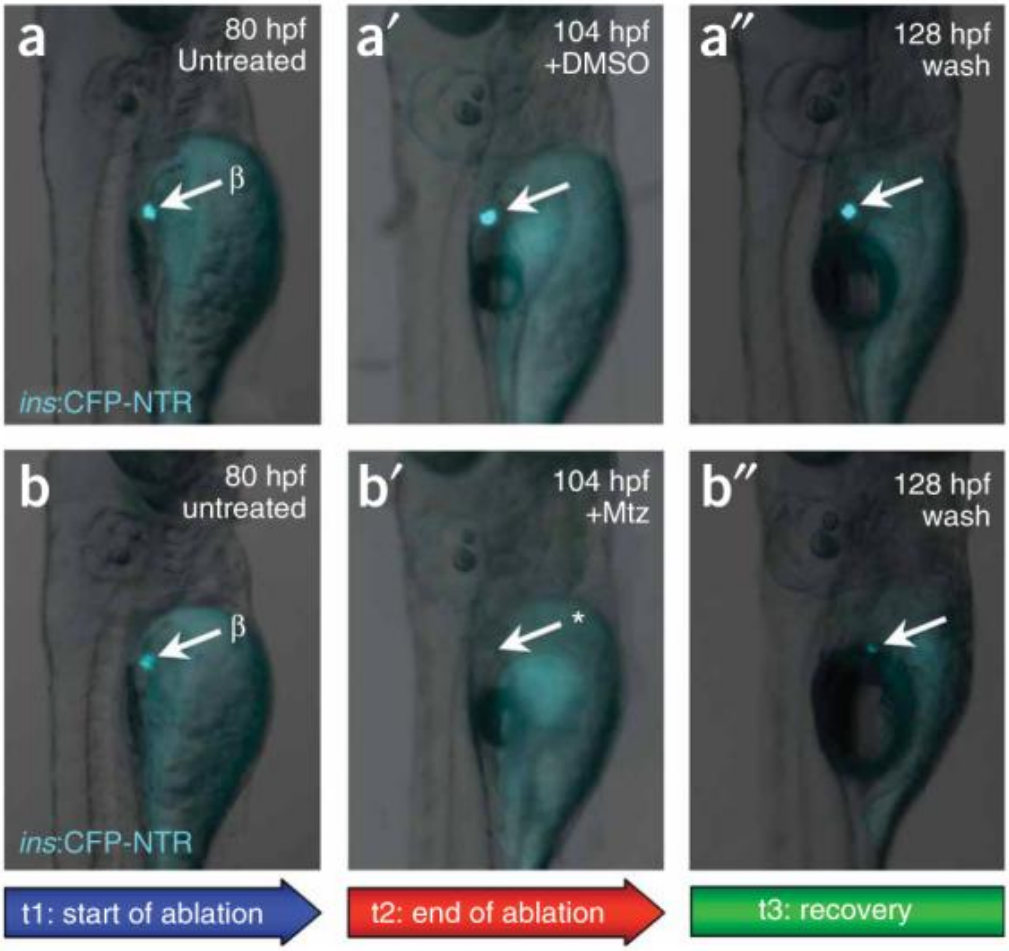

Figure 3.2. Chemo-genetic Ablation in Zebrafish Larvae. Visual monitoring of CFP expression in β cells of Tg(ins:CFP-NTR)s892 larvae. (a, a', a") Stages of control treatment through the incubation in DMSO solution. (b, b', b") Stages of ablation treatment through incubation in MTZ solution. (t1, t2, t3) Stages of treatment when the expression of CFP was recorded. Figure adapted from Curado et al. (2008).

The advantages of having zebrafish as a model for cellular ablation have been clearly

stated. However, it should be added the administration process of the prodrug, directly through the water. The substance enters the organism through diffusion, facilitating the uptake. Moreover, the fusion of a fluorescent marker to the NTR allows for a continuous monitoring over the evolution of the regeneration process in larvea/embryos (Figure 3.2), and for validation in older fish such as juvenile or adult fish [21].

There are limitations associated to these methods. The success of the ablation on the cell population might depend on the accessibility of the targeted tissue to the prodrug. Furthermore, the rate to which the tissues respond to the loss of cells might be different, requiring different exposure and recovery times to reach the desired effects [21]. A great number of variables can be manipulated to optimize the ablation protocol to different developmental stages and particular characteristics of the organisms which may arise.

3.3.1 *y321* GAL4 Transgenic Line

In the current work, we used the transgenic GAL4 line *y321* [52] and the construct UAS-*nfsB*-mCherry. *nfsB* is a gene found in *E-Coli* that encodes for the enzyme nitroreductase. The addition of the fluorescent protein *m-Cherry* allows for a visual confirmation of the locations in which NTR is being expressed. As indicated by the brain views presented in Figure 3.3, this line targets a great portion of the ventral telencephalon and mainly the far end regions of the preoptic area. We can also find signal in the rostral hypothalamus and the posterior tuberculum, although considerably low.

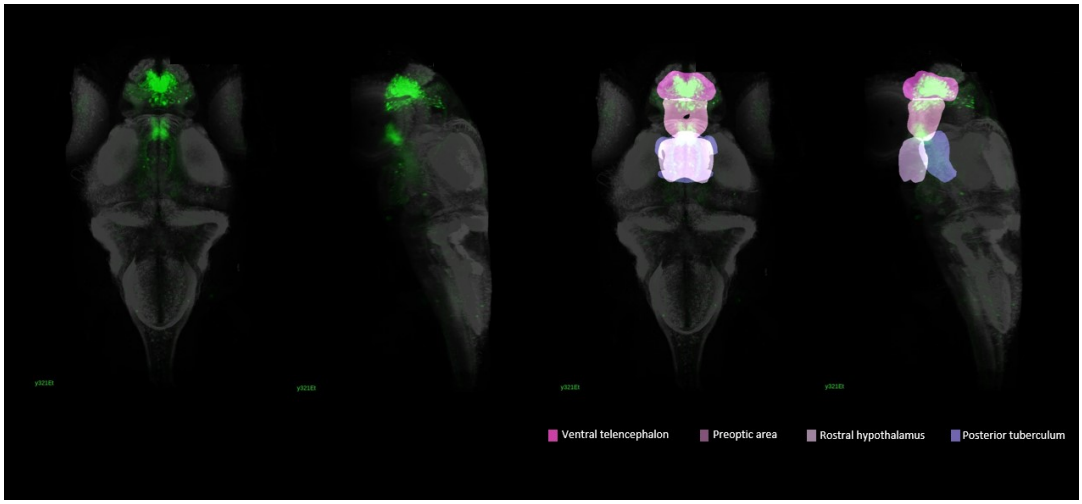

Figure 3.3. Transgenic GAL4 Line *y321*. Horizontal and lateral views of the transgenic line *y321*. Fluorescent signal in targeted areas of the larvea brain (green) and respective anatomical regions covered- ventral telencephalon (dark pink), preoptic area (pink), rostral hypothalamus (light pink) and posterior tuberculum (purple). Figure designed in the Max Planck Zebrafish Brain Atlas platform- mapzebrain. Source: `https://fishatlas.neuro.mpg.de/`.

4 | Collective Behaviour in Zebrafish

Collective behavior is a set of strategies animals developed as a group to overcome unpredictably. For example, birds fly in flocks to help foraging and ants become part of self made bridges to adapt to the terrain [83]. Varieties of these behaviors lead to the emergence of complex patterns [99].

However, it has come to light that instead of a globally orchestrated phenomenon, these occurrences are the result of local dynamics. As it happens, shoaling fish adjust their behavior according to the position, speed and orientation of their neighbours, having a repulsion area within their immediate surroundings, followed by an attraction zone where fish tend to close the distance with their neighbours [20][19][38].

In the present chapter, we will review grouping behaviors that are characteristic of fish collectives, such as shoaling and schooling. We will also explore in more detail the local interactions that occur within a shoal.

4.1 Fish Move Together

Shoaling is a complex social behavior in which fish tend to aggregate in a cohesive group, for social purposes [80].

While the onset of shoaling behavior happens at early post embryonic development, larvae only begin to display social preference towards other fish at two weeks old. This behavior becomes more robust when they reach three weeks [27][25][40]. Shoal mates are chosen mainly through visual preference, with co-specifics of similar phenotype and from the same kin as a preferred choice [89][25][59].

The structure and dynamics of shoaling are not only visually-mediated but also greatly depend on the sensory information collected by a mechanosensory system known as lateral line. It consists on a network of superficial sensory nerves located at the surface of the skin, which senses changes in vibration and pressure [72][29].

A shoal might change its conformation with external or internal factors, conferring a plastic quality to the aggregates which depends on the integration of these two conditions, simultaneously. Although a group of fish introduced to a new environment leads to the formation of a highly cohesive shoal, it will fade with prolonged exposure. Note that cohesiveness is an important feature measured by the inter-individual distances between group elements. As fish learn about their surroundings and start to habituate, distances between individuals increase and the shoal becomes less dense. On a different note, food deprived fish tend to form looser shoals as their attention turns to searching for food instead of maintaining a safe environment against possible predators [57].

Schooling can be thought of as a particular conformation of shoaling, in which fish swim in a polarized and coordinated manner. Fish collectives can easily transition between these two states of polarization, schooling or shoaling, as needed [57][102]. In a study focused on the effects of habituation in schooling behavior, Miller et al. (2012) found that fish show less tendency to synchronize with increased familiarity of their surroundings, as indicated by the bi-modal distribution displayed in Figure 4.1. The peak for high polarization, which would represent schooling behavior, has a constant value over repeated measurements, in a range between 0.9-1. Whereas the peak corresponding to a lower polarization level, representing shoaling behavior, is mostly nonexistent in the first two days and varies between 0.5 and 0.4 in the following days, indicating an inverse relation between level of polarization and continued exposure to the same environment.

According to these findings, schooling appears to be a fixed behavior, as the polarization value is always the same. On the contrary, shoaling seemingly depends on environmental factors as the groups display different levels of disorganization as a function of their level of habituation.

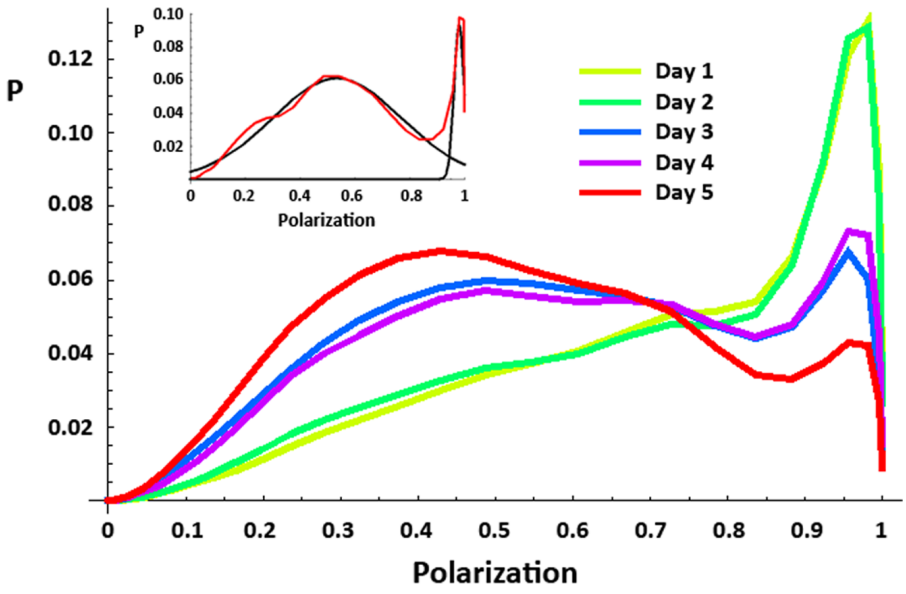

Figure 4.1. Polarization Level of the Shoal. Density distribution of polarization for repeated exposures to the experimental arena, for a period of 5 days. Bi-modal distribution with high and low polarization peaks corresponding to schooling and shoaling behaviors, respectively. The insert shows the polarization distribution over one session (red) and the decomposed modes (black). Figure adapted from Miller et al. 2012.

Nevertheless, the level of cohesion is maintained in both schooling and shoaling states. Consequently, the structure of the collective is preserved although alignment might be lost in the latter [57].

In brief, shoaling and schooling are vital behaviors which depend on the social interactions between its intervening parts. Fish rely on these for a number of primary behaviors such as foraging, mating or predator avoidance [80][57].

4.2 Local Interactions in Shoals

Social interactions between fish generate complex collective displays such as shoaling patterns. Studying the dynamics at play in these local engagements can provide valuable information in order to better understand what is happening at a macroscopic level.

Couzin et al. (2002) proposed a model in which the space surrounding a fish was divided into zones. If neighbouring fish stood too close to the focal fish, the latter would repel to avoid collisions - repulsion zone. On the other hand, if neighbours were found outside of this avoidance area, the individual would have the tendency to draw closer to the others - zone of attraction - and align - zone of orientation. Larvae tend to have a considerable repulsion zone which decreases over time. Attraction was found to start at early development (7dfp) and progress until 3 weeks, at which point the fish already swim in groups [40].

Katz et al. (2011) studied the local interactions of schooling fish, specifically the goldfish. The behavior of a focal fish has a dynamic aspect which depends considerably on the actions of its neighbours.

The relative positions of neighboring fish shape distinctive regions encircling the focal, in accordance with the model previously described (Figure 4.2 B).

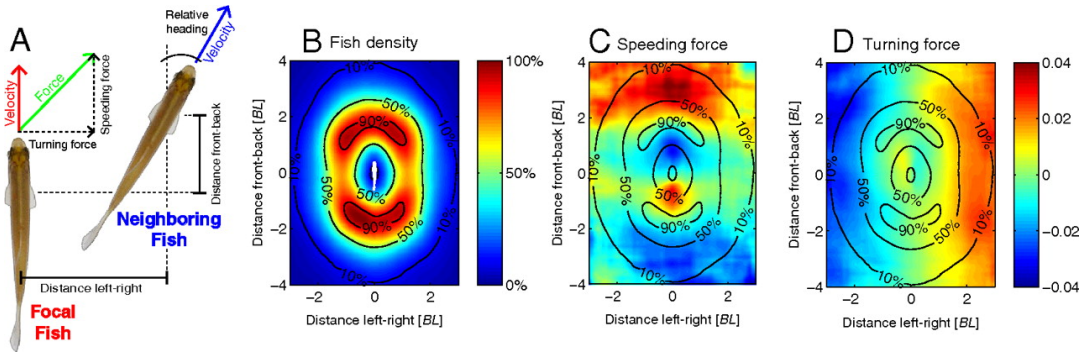

Figure 4.2. Local Interactions in Fish Dyads. Behavior adjustment of the focal fish in line with the actions of the neighbouring fish. (A) Variables considered for the calculations of the individuals relative positions. The focal fish is placed in the origin of a Cartesian plane and relative distances are measured. Acceleration (green vector) is decomposed into Turning and Speeding forces. (B) Probability of finding a neighbour at a given position with reference to the focal fish (center position). Contour of 10%, 50% and 90% represents the frequencies recorded in the bins, from lowest to highest. (C, D) Speeding and turning components of the focal as a function of the neighbours' position, respectively. Figure adapted from Katz et al. 2011.

While the probability of finding another fish in the immediate area surrounding the focal is quite small, this chance greatly increases at a inter-individual distance of about 1 to 2 body-lengths (BL), clearly indicating zones of repulsion and attraction, respectively.

Interestingly, if neighbouring fish are located in the front-back axis at a greater distance, right outside the attraction area, the focal fish will either speed up approaching the fish in front or speed down allowing the fish behind to get closer. However, the opposite situation occurs in the event that fish are found within the repulsion area (Figure 4.2 C). In a similar note, fish seem to turn toward their neighbours when they stand in the left-right axis, beyond their attraction zone (Figure 4.2 D).

These adjustments in speed and direction are a good strategy to keep neighbouring fish within the attraction zone and maintain the cohesiveness of the group. These interactions are not linear, yet they seem to capture the fundamental spacial structure found in social exchanges of larger fish schools.

Heras et al. (2019) proposed a model which captured pairwise interactions in zebrafish collectives.

As it happens, the relative positions of a focal and its neighbour strongly depend on the speed of both individuals and on the alignment between them. In situations where the speed of either animal increases, the attraction and repulsion areas gradually decrease as the alignment region increases. Note that in the example presented in Figure 4.2, alignment was not considered.

This model also provided new insights on how information flows within the collective. Fish exhibit weighted attention towards their neighbours as a function of distance. Thus, animals gain more information from fish close by and tend to ignore distant neighbours.

5 | Materials & Methods

5.1 Housing and Maintenance

The transgenic line y321:GAL4/UAS:nfsB-mCherry was imported from the University of Oregon. Animals were screened with a V8 Pentafluor Scope at 6 dpf, when the mCherry fluorescent signal was strongest. The larvae were kept in Petri dishes of 15cm diameter, inside an incubator with a 14/10 light-dark cycle at 28°C and given powder food (sera micron) three times a day. At 7 dpf, the zebrafish larvae were transferred to the main room facility and housed to be raised in tanks of system water until they reached the appropriate age for experiments. Fish were maintained by the vivarium platform at Champalimaud Research. All aspects of housing, husbandry and general animal welfare were assured, such as preservation of centralized life-support system, monitoring and optimization of water quality and feeding requirements. The system water pH, salinity and level of dissolved gases were kept under physiological conditions [54].

5.2 Chemo-genetic Ablation of Neuronal Cells

Once the fish reached 35-40 dpf, they were separated in groups of 5 individuals per tank. Each tank was incubated either in solutions of 10mM MTZ/0.2% DMSO or 0.2% DMSO, both prepared in fresh system water. In total, there were four tanks per session:

1. **DMSO Positive:** *y321:Gal4* expressing NTR and m-Cherry in the targeted areas, incubated in 0.2% DMSO solution;
2. **MTZ Positive:** *y321:Gal4* expressing NTR and m-Cherry in the targeted areas, incubated in 10mM MTZ/0.2% DMSO solution;
3. **DMSO Negative:** *y321:Gal4* **not** expressing NTR and m-Cherry, incubated in 0.2% DMSO solution;
4. **MTZ Negative:** *y321:Gal4* **not** expressing NTR and m-Cherry, incubated in 10mM MTZ/0.2% DMSO solution;

The groups consisting of negative siblings, DMSO Negative and MTZ Negative, allowed us to control for possible effects caused by differences in genotype and non-specific drug toxicity, respectively.

The solutions were renewed after 24h of incubation to maximize drug intake. Note that the MTZ is a light sensitive substance hence, every procedure had to be performed in the dark. After incubating for a period of 48h (Figure 5.1 A), the fish were transferred into new tanks with fresh system water and allowed to recover for 1 hour before proceeding to behavioural testing (Figure 5.1 B).

5.3 Behavioral Assay

In order to assess the social behavior, we recorded each group in a free swimming setting for a period of 20 minutes (Figure 5.1 C). The groups were tested at random.

We used a 30cm diameter acrylic circular experimental arena placed at the centre of a white rectangular plastic box. The latter was submerged enough to cover the arena from below to reduce reflections at the boundaries of the arena.

The videos were recorded with a Flea3 3.2 MP Color USB3 Vision (Sony IMX036) camera at an adjusted height, in which the arena covered the whole image to maximize the number of pixels per animal. The lights inside the set-up were infrared and visible LED in a ratio 12:1, to create a less stressful environment for the fish [94][73]. Using a diffuser built from white fabric sheets, we checked the homogeneity of the illumination with the FlyCapture Software Development Kit (SDK) and kept it constant throughout all experiments. Each trial consisted on 20 minutes of free swimming recorded with a frame rate of 30 frames per second (fps). The image acquisition followed a protocol built from the FlyCapture SDK and the open-source software Bonsai.

Prior to each new trial, the arena was cleaned with ethanol and system water and filled with 1L volume of fresh system water at 28°C. At the end of the trial, the fish were euthanized through thermal shock in iced water [104] and fixed in 4% PFA in 1x PBS at 4°C, overnight.

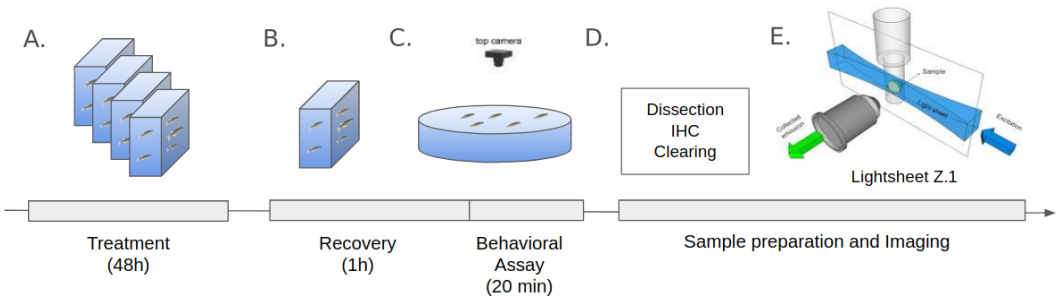

Figure 5.1. Experimental Protocol. The fish were organized in groups of 5 individuals per tank. (A) Each group was incubated for 48 h in either 10mM MTZ/0.2% DMSO solution or 0.2% DMSO, depending whether their treatment plan was MTZ or DMSO, respectively. (B) Before the behavior trial, the fish were transferred to clean tanks with fresh system water and recovered for 1 h. (C) After recovery, the group was recorded in a free swimming trial of 20 minutes and euthanized in iced water. (D) The brain samples were collected, stained and cleared and (E) each sample was imaged in the Lightsheet Z.1.

5.4 Preparation of Brain Samples

The brain tissue of a juvenile zebrafish, although maintaining some transparency when compared to adult samples, is still too opaque to allow the acquisition of quality images

regardless of the microscopic method. Therefore, it needs to undergo a clearing process which in turn could require previous immunostaining, as the clearing procedure might decrease the endogenous signal of the samples. Accordingly, we stained our samples with a standard immunohistochemistry protocol prior to clearing (Figure 5.1 D). Both methods are described in the coming sections.

5.4.1 Immunohistochemistry

The brains were collected and immunostained for tERK and mCherry. This procedure allowed us to reveal the targeted areas for the ablation and to provide a spacial orientation of their relative locations in the zebrafish brain, respectively.

In detail, the samples were washed in PBST (PBS/Triton0.25%) and incubated in 150mM Tris-HCl pH=9 for 15 minutes, at 70°C. After stopping the reaction on ice, they were washed twice in PBST and permeabilized in 0.05% Trypsin-EDTA for 5 minutes, on ice. They were then washed in PBST every 30 minutes, in a total of three times and incubated for 3 hours in blocking buffer (PBST/1% BSA/2% NGS/1% DMSO). Subsequently, they were incubated with the primary antibodies (anti-tERK mouse and anti-mCherry rabbit) in PBST/1% BSA/1% DMSO at 4°C, for 3 overnights.

After the incubation period, the samples were washed again three times, one each half hour and incubated with the secondary antibodies (anti-mouse Alexa-Fluor 633 and Alexa-Fluor 568 goat anti-rabbit), in PBST/1% BSA/1% DMSO at 4°c, for 3 overnights.

Finally, the samples were washed in PBST at least three times and stored in the same solution PBST with 0.2% Azide to prevent the appearance of fungi, until they were needed for clearing and imaging.

5.4.2 Rapid clearing method based on Triethanolamine and Formamide (RTF)

With the aim of clearing the brain tissue, we used the technique Rapid clearing method based on Triethanolamine and Formamide (RTF) [107]. As the name suggests, this method is based on the regents formamide (F) and triethanolamine (TEA), due to their inherent properties of clarity with fast action and high refractive index with suitable alkalinity, respectively. This special composition provides certain advantages such as the preservation of endogenous fluorescence signal, maintenance of the samples structures and a relatively small waiting period. In addition, it is a simple procedure that relies on applying different concentrations of the compounds at different stages.

Our protocol consisted on two consecutive incubations of 3h in the solutions RTF-1 and RTF-2, followed by an overnight exposure in the third solution, RTF-3. The compositions of each solution and the incubation times are described in Table 5.1.

Table 5.1. Exposure times and composition of clearing solutions: RTF-1, RTF-2 and RTF-3.

RTF-1	**RTF-2**	**RTF-3**
30% TEA / 40% F / 30% W	60% TEA / 25% F / 15% W	70% TEA / 15% F / 15% W
3 h	3 h	o.n.

On a separate note, it is important to mention that these solutions cannot come into contact with water otherwise, the samples become milky white. Yet, as the Lightsheet - Zeiss Z.1 microscope required the samples to be embedded in agarose 0.8% due to the refraction index (RI $\simeq$ 1.3), the samples had to be cleared while embedded in the agarose.

Therefore, each sample was mounted by being transferred into an Eppendorf tube of agarose 0.8% at 45°C and drawn into a glass capillary, with 1 mm inner diameter using a Teflon-tipped plunger. After the agarose inside the capillaries solidified, each capillary was incubated in a small Eppendorf tube containing the clearing solutions.

5.5 Imaging

As mentioned above, in the interest of verifying the effects of the NTR/MTZ-mediated ablation in the brain tissue, we used a Zeiss Lightsheet Z.1 microscope to capture the fluorescent signal from our samples (Figure 5.1 E).

5.5.1 Z-stack Acquisition

The Lightsheet Z.1 was equipped with two 5x/0.1 illumination objectives and the Plan-Neofluor 5x/0.16 detection objective. Solid state lasers, with output power of 50 mW, of 561 nm at 3% and 638 nm at 27% were used to respectively excite Alexa Fluor 568 and Alexa Fluor 633 fluorophores, using dual side illumination.

The two channels were sequentially acquired. A laser blocking filter 405/488/561/640 was used to avoid detection of the excitation light. A secondary beam splitter LP 540 together with emission filters BP 575-615 and LP 660 were used to selectively detect the two signals. Detection of emitted fluorescence was fulfilled by two pco.edge 5.5 sCMOS cameras with a pixel size of 6.5 x 6.5 μm, using an 99.87 ms exposure and outputting in 16-bit.

The acquisition area was set to 1920 x 1920 pixels, with a pixel size of 1.30 μm, at an internal zoom factor of 0.7. The thickness of the light-sheet was 13.36 μm at the center and 11.5 μm at the borders of the field of view.

Stacks with 350 μm thickness were recorded with a 2.5 μm step interval. Each sample was imaged from both ventral and dorsal sides. The imaging chamber was filled with the RTF-3 solution.

5.6 Data Analysis

With respect to the exploration of the data, both ablation and behavior analysis were written in Python 3.7 and the complete source-code for each can be found in `https://gitlab.com/renata_cruz/renata_codes.git`.

5.6.1 Ablation Analysis

The z-stacks acquired were saved in CZI format with the Zen software (Zeiss). As a first step, the images previously acquired were processed with the open-source software Fiji. Each image underwent filtering with a Median 3D (X radius = Y radius = Z radius = 2.0) and a sum Z-projection containing 80 slices. From these, 4 ROIs corresponding to the vTel, POA and two arbitrary sections were selected (Figures A.1-A.4), always following the same dimensions (338 x 356, 212 x 162, 212 x 162, 212 x 162, respectively).

Due to a high variability of auto-fluorescence and background noise, the ROI files were saved in .tif format and had to be further processed and analysed in Python 3.7. The summed ROIs were segmented using a local gradient algorithm and a background subtraction in which the segmented images were divided by their median value. From these final images, signal properties such as intensity, density and level of dispersion were analysed.

5.6.2 Behavior Analysis

As for the video files, we used the open-source and free software idtracker.ai (license GLP v.3) and the Trajectorytools package, both developed in the lab [87]. All instructions and source-code can be found in `www.gitlab.com/polavieja_lab/idtrackerai` and `https://github.com/fjhheras/trajectorytools`, respectively. With the idtracker.ai and the Trajectorytools, we acquired the trajectories of each fish which allowed not only for an analysis of the group but also of every single individual within the collective.

5.6.3 Statistical Analysis

Comparative analysis was conducted by means of the parametric tests one-way ANOVA for equality of means and the TukeyHSD post-hoc test. The underlying assumptions of a Gaussian distribution and homogeneity of variances were verified through the Shapiro-Wilk and Levene's tests, respectively. As for data which did not meet the

necessary requirements, we resorted to the nonparametric Kruskal-Wallis H method for independent samples and the Conover post-hoc test to respectively assess statistical significance and perform multiple pairwise comparisons of the groups. Statistical significance was set at $p < 0.05$ (*), $p < 0.01$ (**), $p < 0.001$ (***), $p < 0.0001$ (****).

6 | Results

The present chapter is divided into two main sections. The first part describes, in detail, the analysis of the stained samples as means to verify the level of success achieved by the ablation treatment.

Subsequently, we explore the ablation effects in the collective behavior of zebrafish. Under a free swimming context, we study the interactions between individuals within a group and which features might be particularly affected by the introduction of the disturbance.

6.1 Ablation Assessment

The regions targeted by the ablation are clearly visible in Figure 6.1 A, with the m-Cherry signal represented in green. In accordance with the information in Chapter 2, these areas correspond to the vTel (Figure 6.1, 1.), located at a position more anterior in the brain, and the rostral part of the diencephalon, including the preoptic area (POA) and a small part of the posterior tuberculum and rostral hypothalamus (Figure 6.1, 2.). These three diencephalic areas are indistinguishable within the fluorescent cluster yet the signal seems to cover mostly the POA. Therefore, we considered one unique ROI which we classified as 'POA'.

On the surface, the effects of the ablation seem to be considerable (Figure 6.1 B). Relatively to the samples treated with DMSO, the fluorescent signal following MTZ treatment appears to be dimmer, with lower density and scattered within a wider area, seemingly losing specificity to the ROIs.

Thus, in the forthcoming sections we will analyse these properties and compare them across groups in an attempt to validate the effectiveness of the ablation procedure.

6.1.1 Image Processing

As mentioned in Chapter 5, there was great variability within and between groups, due to variable levels of auto-fluorescence in the zebrafish brain samples (Figures A.5-A.12 (A)).

Accordingly, to ensure that any results from the analysis performed on the signal were not a consequence of auto-fluorescent interference, we considered two arbitrary ROIs from other regions of the brain and implemented them into our analysis.

Furthermore, the data required additional treatment to allow an adequate appraisal of the images. Figure 6.2 illustrates the adjustment of the signal after each technique was applied. The complete collection for the execution of image processing per ROI can be found in Appendix A.

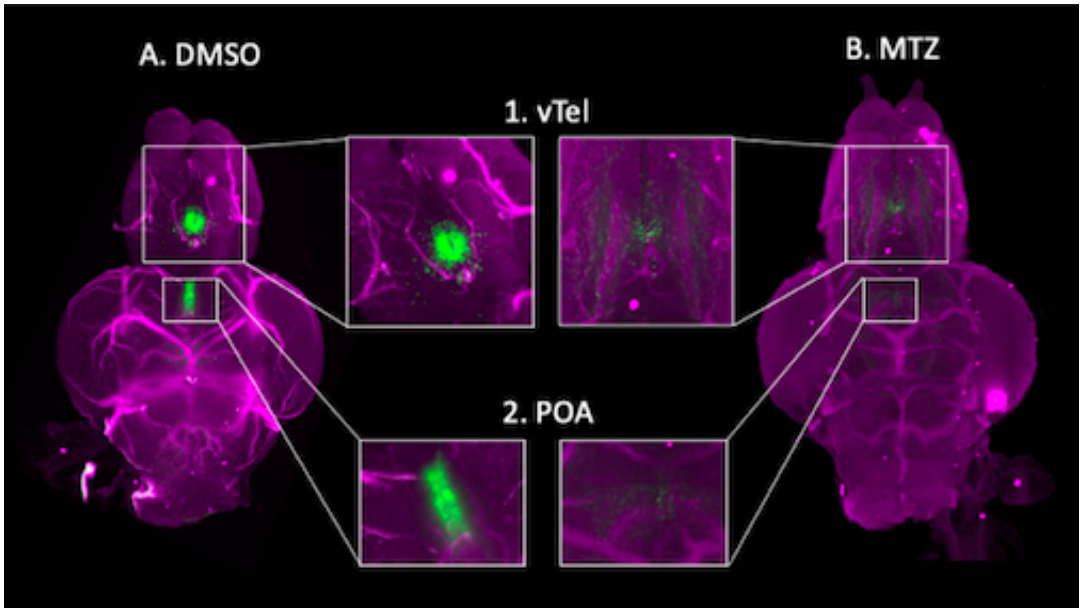

Figure 6.1. Targeted Regions for the Chemical Ablation. Brain samples stained with m-Cherry (green) and tERK (magenta) highlighting the areas marked for the ablation: (1) vTel and (2) POA. Visual effects on the m-Cherry fluorescent signal following treatment with either (A) DMSO or (B) MTZ.

Local Gradient Filter and Background Subtraction

The images in Figure 6.2 (B) display a clear improvement upon the application of the local gradient filter (LGF). As LGF subtracts the maximum local value with the minimum local value, the outcome is an image with lower edges and less sharp transitions between pixels.

Accordingly, LGF successfully filtered the majority background from the fluorescent cells and provided cleaner images for subsequent signal segmentation of all ROIs considered.

Granting these positive results, there was still some auto-fluorescence remaining which continued to challenge the analysis.

Hence, the filtered images underwent background subtraction. At length, each image was divided by their own median value. This operation ensured any trace of auto-fluorescence had minimal weight in the signal analysis.

Identification of the Peaks

Finally, the peaks of intensity were identified by retrieving the coordinates of pixels in which intensity values were higher. As revealed in Figure 6.2 (C) and Appendix A A.5-A.12 (C), the peaks detected overlaid relatively well with the signal.

Nevertheless, it is important to highlight that this segmentation precluded an accurate quantitative analysis of the m-Cherry signal. It did however provide the tools for a qualitative approach through the comparison of DMSO and MTZ treatments and thus, enabled an empirical evaluation of the ablation protocol efficiency, which remained our main intent.

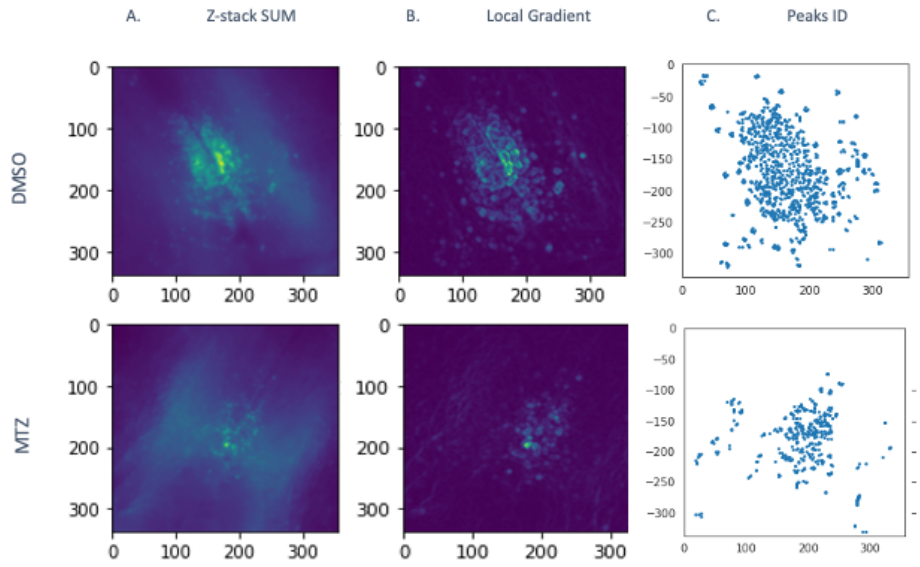

Figure 6.2. Image Processing. Sample of a vTel ROI with low auto-fluorescence to illustrate the stages of image processing. (A) Summed Z-stack of the ROI for DMSO (control) and MTZ (ablation). (B) Application of the Local Gradient Filter (LGF) to the respective ROI figures presented in A. (C) Final segmentation for identification of intensity peaks coordinates, following Background Subtraction (BS) of the filtered images. A complete record of all ROIs and respective side views processed can be found at Appendix A A.5-A.12.

6.1.2 Properties of the Fluorescent Signal

The effects on m-Cherry fluorescence following NTR/MTZ-mediated ablation are easily recognizable (Figure 6.2 and Appendix A A.5-A.12). In a purely observational preliminary analysis, the signal found in MTZ groups appears to be dimmer, spreading over almost the entire ROIs and with greater distance between peaks of intensity. In respect to DMSO groups, the signal seems to be more cohesive and compact.

Intensity

In parallel, Figure 6.3 presents a comparison on the average intensity values per pixel, for the vTel and the POA.

As expected, the intensity is reduced in samples treated with MTZ in both ROIs, regardless of the view.

There seems to be a contrast regarding the variability level on the ventral view of the POA, relatively to its opposite side. In addition, the level of significance appears

to change accordingly, with the dorsal view displaying a lower level of variance and holding higher statistical significance. However, this observation does seem accurate for the vTtel. Indeed, the overall range of the data is lower and exclusively the group treated with DMSO has visible variability. Yet, this does not resemble an association with the side view. If any relation between these variables exists, it is not apparent.

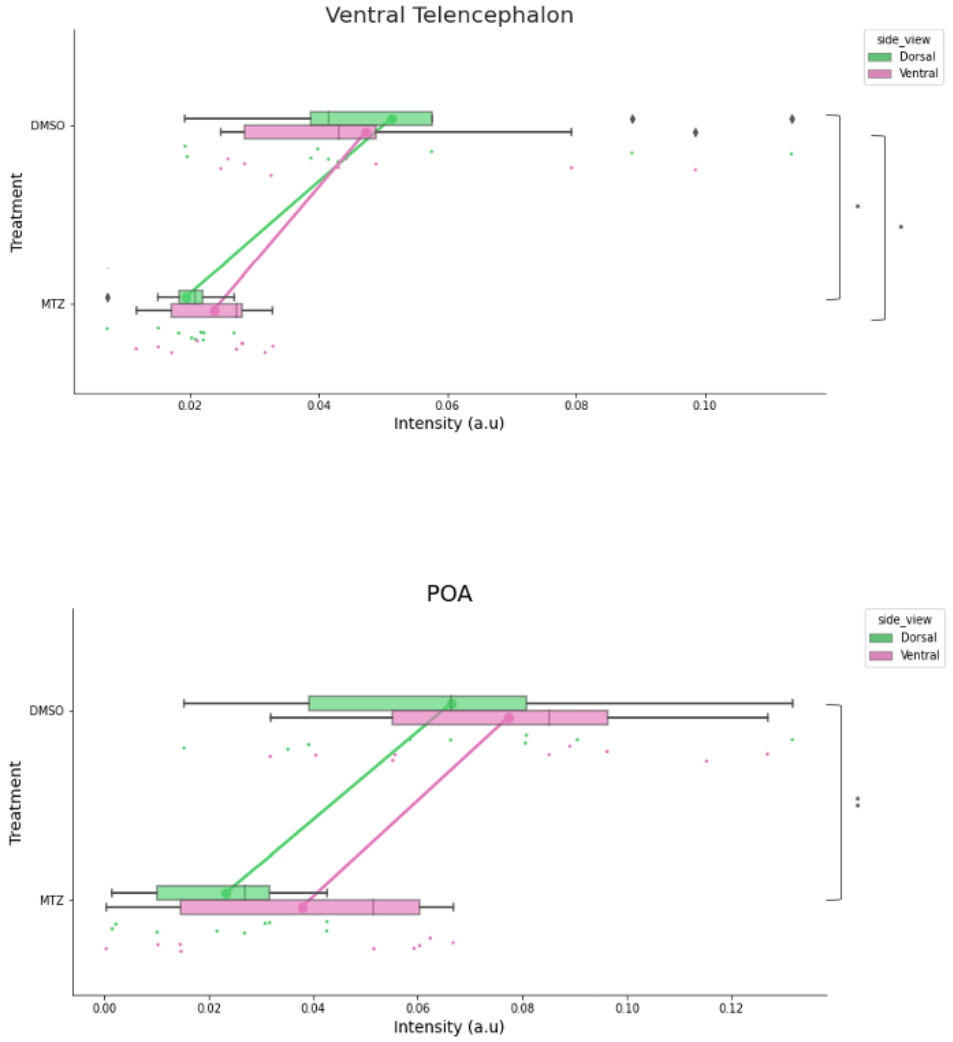

Figure 6.3. Signal Intensity. Comparison of the intensity per pixel between groups treated with DMSO (control) and MTZ (ablation), in the vTel and diencephalon (top and bottom panel, respectively). Within each treatment both side views, dorsal and ventral, were also compared. Boxplots displaying the intensity, accompanied by jittered data. Means are represented with a large dot (•) and connected between comparable groups. Each group had a collection of 9 images (n=9). Statistical significance was set at * $p<0.05$ and ** $p<0.01$, Conover post-hoc test.

Nevertheless, there is a clear decline of m-Cherry signal within animals treated with MTZ in the vTel as well as the POA. Particularly in the vTel, both dorsal and ventral views differ significantly between the two treatments.

As for the side views, no significant differences were found between dorsal and ventral sides within the same treatment, either for the DMSO or the MTZ groups.

Furthermore, analysis on the arbitrary ROIs (Figure A.13) showed no significant differences between the groups, indicating auto-fluorescence should not be influencing the results.

In other words, the decline of the signal intensity from ablated samples is consistent in both vTel and the POA.

Density

As means to study the density of the signal, we measured the number of intensity peaks per pixel in each image. Figure 6.4 displays the plotted data for signal density on both ROIs.

There is a significant decrease in the density values in MTZ treated samples, which is consistent in all groups compared.

In the vTel, apart from a pair of outliers in each view, the majority of the data is concentrated within a rather small range, yet both treatment groups seem to overlap slightly. Whereas, the level of variability found in the POA is apparently greater, with data spread into a larger range in both treatments. Notwithstanding, DMSO and MTZ groups appear to be more distant, with less overlapping.

There are no evident differences between dorsal and ventral side views.

It should be noted that the differences found between DMSO and MTZ groups are not due to auto-fluorescence. As can be indicated by Figure A.14, no significant distinctions between groups in the arbitrary ROIs were observed.

In short, the ablation treatment seemingly decreased the m-Cherry signal density in the targeted areas.

Dispersion

Finally, we evaluated the scattered nature of the fluorescent signal by calculating the weighted distance between intensity peaks. The information is represented in Figure 6.5.

When compared, the two treatments were found to be significantly different from one another in terms of euclidean distance, regardless of the view. The views themselves seem to share no significant distinctions, in agreement with previous results.

Apropos, the comparison between treatments in the vTel is seemingly more clear while still contemplating some outliers.

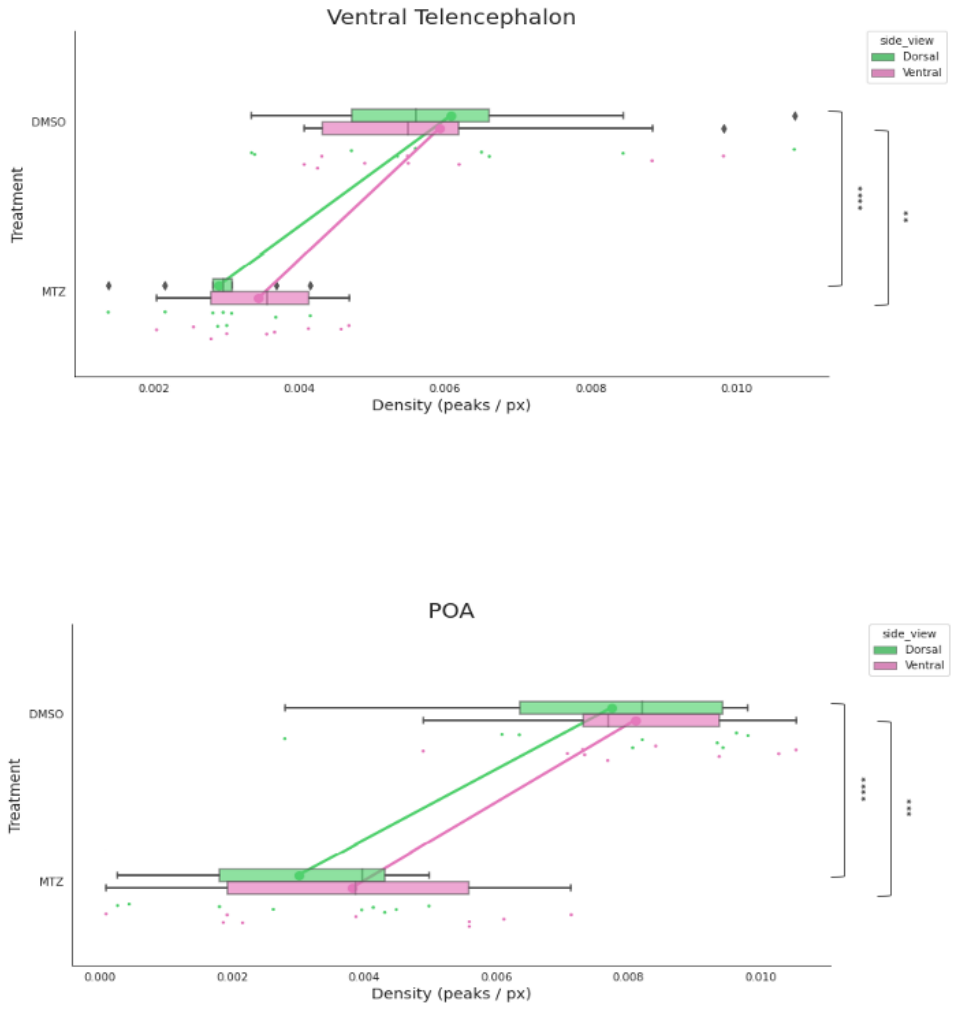

Figure 6.4. Signal Density. Comparison of the signal density between groups treated with DMSO (control) and MTZ (ablation), in the vTel and diencephalon (top and bottom panel, respectively). Density was measured as the number of peaks per pixel. Within each treatment both side views, dorsal and ventral, were also compared. Boxplots displaying the density, accompanied by the respective jittered data. Means are represented with a large dot (•) and connected between comparable groups. Each group had a collection of 9 images (n=9). Statistical significance was set at ** $p<0.01$, *** $p<0.001$, **** $p<0.0001$, Conover post-hoc test.

Along the same lines as the previous plots (Figures 6.3 and 6.4), the discrepancy of range where vTel and POA data are inserted is unmistakable. However, the distance between high density regions of data is shorter in the vTel, with higher overlap while the opposite is observed in the POA.

In conclusion, both ROIs sustained an increase in signal dispersion accompanied by a decrease in intensity and density values.

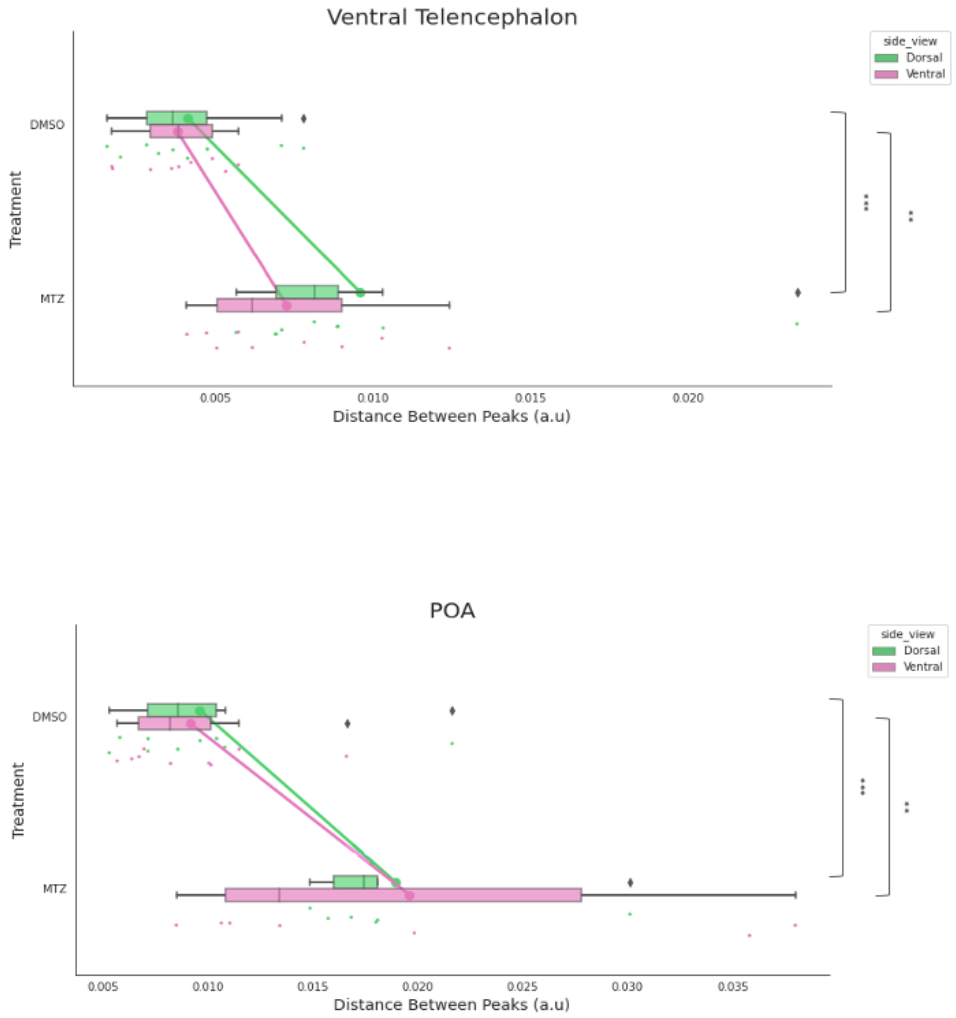

Figure 6.5. Dispersion Level. Comparison of the signal dispersion between groups treated with DMSO and MTZ, in the vTel and diencephalon (top and bottom panel, respectively). Dispersion level was measured as the distance between peaks. Within each treatment both side views, dorsal and ventral, were also compared. Boxplots displaying the distance distribution, accompanied by the respective jittered data. Means are represented with a large dot (•) and connected between comparable groups. Each group had a collection of 9 images (n=9). Statistical significance was set at ** $p<0.01$, *** $p<0.001$, Conover post-hoc test.

6.2 Behavioural Framework

Following ablation treatment, we studied the behavior of free swimming fish considering particular traits underlying the collective behavior of teleosts, as described in Chapter 4. Thus, not only did we explore their local interactions with neighboring fish, but also thoroughly analysed their shoaling behavior.

6.2.1 Kinematic Parameters

Initially, we examined some general features of the individual trajectories. We sought to assess if there were differences not directly related to complex social behavior but rather to overall motor performance. Specifically, we focused on the speed and acceleration of each animal, as displayed in Figure 6.6.

Curiously, there is a clear decrease in the speed of MTZ treated animals. The distribution seems to be bi-modal, with the first peak close to zero, probably due to a set of fish exhibiting low or minimal movement. The second peak is shifted to higher speed values but still quite low in comparison to the distributions from DMSO groups. Also, while significant differences were found between strains, they are not apparent in the distributions. These may be due to small variations between the individuals and not necessarily to actual distinctions between the groups.

The acceleration also declines following MTZ treatment. Similarly, it appears a fraction of fish hardly accelerates, represented by the first peak of the distribution. Presumably, these animals correspond to the set described above. Again, differences were found between strains treated with DMSO, yet they were not evident in the distributions.

In brief, both speed and acceleration are greatly affected by the MTZ treatment. However, this influence seems to be a side effect of the drug and not a consequence of the ablation per se.

6.2.2 Exploration of the Arena

In order to have a general view of the trajectories taken by the collectives and how exactly they explored the arena, we plotted their global positions in Figure 6.7.

It is clear that groups treated with DMSO spend more time in the borders of the arena, whereas groups treated with MTZ are mostly in the centre.

While MTZ negative are apparently concentrated within a smaller area in the center, there is some intermediate density close to the borders. MTZ positive show a larger high density area in the center of the arena yet the borders seem to be avoided. However, these differences are feeble when compared to DMSO animals.

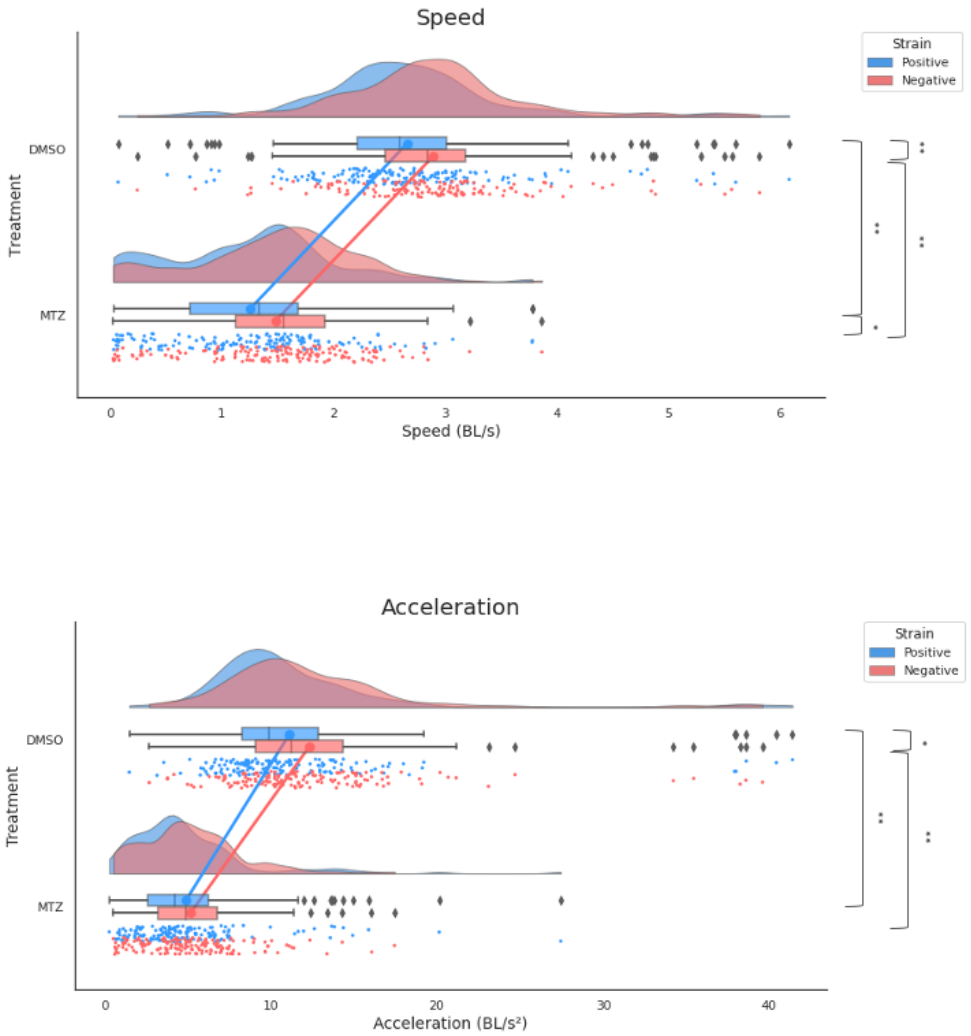

Figure 6.6. Kinematic Parameters. Comparison of the speed and acceleration of fish treated with DMSO (control) and MTZ (ablation) (top and bottom panel, respectively). Within each treatment both strains, positive and negative for the expression of *ntr*, were also compared (see Chapter 5 for a complete description of the groups). Boxplots displaying the median speed and median acceleration of each individual, accompanied by their density distributions and jittered data. Means are represented with a large dot (•) and connected between comparable groups. Statistical significance was set at * $p<0.05$, ** $p<0.01$, Conover post-hoc test.

This major dichotomous behavior is most likely a general effect of the drug. Instead, the disparities found in the MTZ strains, should provide specific information on the behavioral implications following ablation.

On a different note, trajectories from groups treated with DMSO appear to be biased towards the right side of the arena. As it happens, the set-up door, which consisted on a thick sheet to allow easier access during experiments, is positioned on that side. Thus, there might be some external disturbances to which the fish might be

particularly sensitive.

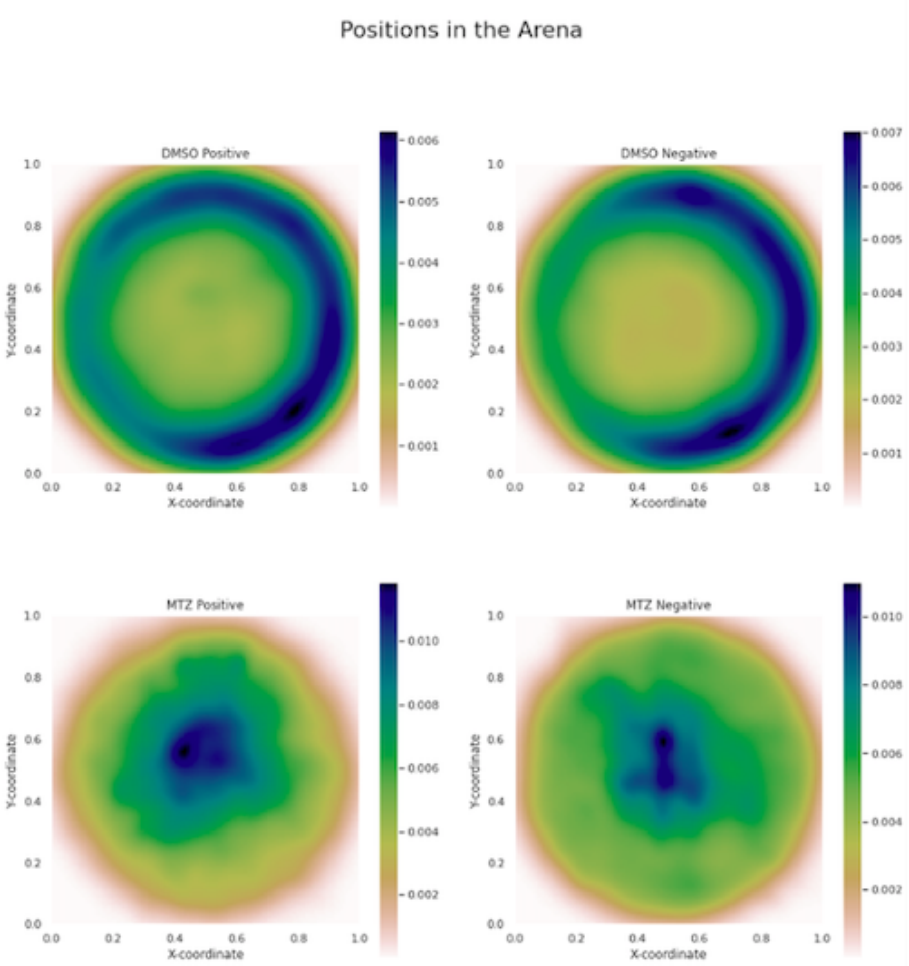

Figure 6.7. Exploration of the Arena. Density plot calculated by the median group positions (n=5) measured at each frame. The color code maps the density at each bin according to the colorbar scale.

6.2.3 Local Fish Dynamics

As an essential part of social behavior, we studied the local interactions between individuals and the extent to which they might be affected by the ablation. The results are summarized in Figures 6.8-6.10.

The relative positions of neighbouring fish, in animals treated with MTZ, appear to be opposite between strains. While the negative strain has higher density in surrounding the focal, the positive strain exhibits the opposite effect in comparison with DMSO treated groups (Figure 6.8).

Indeed, subtraction plots from DMSO and MTZ groups show an inverse difference regarding the strain, with positive and negative directions for positive and negative strains, respectively. In addition, the subtraction between the two MTZ groups show a clear positive difference at the same location (Figure 6.8, middle panel). These

distinctions seem to be complemented with a general significance (Figure 6.8, bottom panel). No considerable differences were found between strains treated with DMSO.

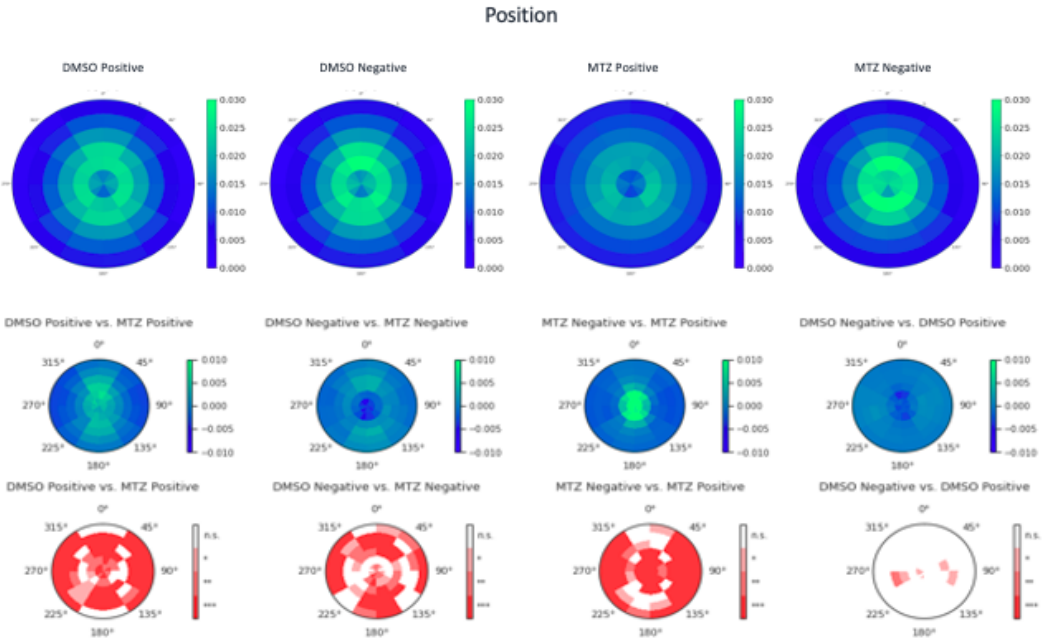

Figure 6.8. Local Interactions With Neighbouring Fish- Positions. Polar plot of the relative positions of neighboring fish surrounding a focal fish (center position). Probability of finding an individual at a given position with reference to the focal fish (top panel). Subtraction of the polar plots according with the paired groups referred in their respective labels (middle panel). Plots representing the significance associated with the statistical inference performed at each bin of the polar plots (bottom panel). Statistical significance was set at * $p<0.05$, ** $p<0.01$, *** $p<0.001$, **** $p<0.0001$, Conover post-hoc test.

We then calculated the turning and forward accelerations of focal fish, as a function of neighbours positions (Figure 6.9 and 6.10, respectively). Interestingly, the general pattern found in both features seems to be maintained with MTZ treatment, yet with values ranging in a lower scale. Indeed, animals still seem to turn in the direction of their neighbours and adjust their own acceleration according to the relative positions of the others. Differences found in the subtraction and significance plots appear to represent this general scaling decrease.

On the other hand, positive MTZ seems to decrease further in regard to the negative strain. While this distinction is more prominent in the turning component, forward acceleration exhibits some significant differences in the vertical axis as well. Some differences were also found between strains treated with DMSO yet for the turning component, they are minor. Strangely, in the forward acceleration, the significance plots are rather similar.

In short, these local dynamics seem to be generally altered following ablation. Nevertheless, the discrepancies observed in the position plots might be an indication of a

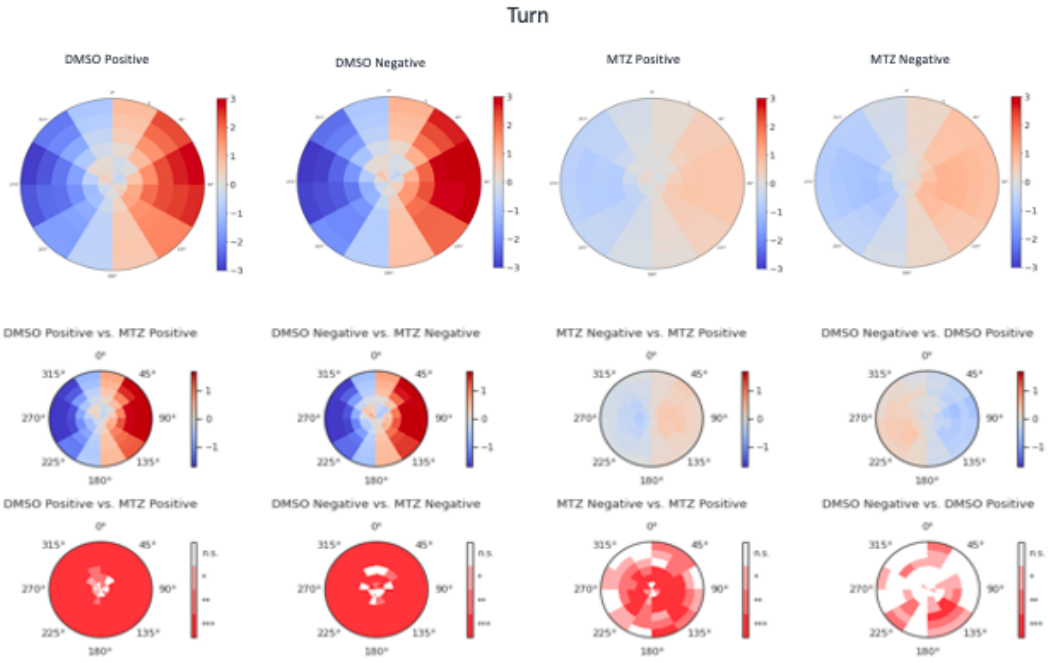

Figure 6.9. Local Interactions With Neighbouring Fish- Turning Acceleration. Mean values of the forward acceleration of the focal (central position) relative to the neighbours positions (top panel). Subtraction of the polar plots according with the paired groups referred in their respective labels (middle panel). Plots representing the significance associated with the statistical inference performed at each bin of the polar plots (bottom panel). Statistical significance was set at * $p<0.05$, ** $p<0.01$, *** $p<0.001$, **** $p<0.0001$, Conover post-hoc test.

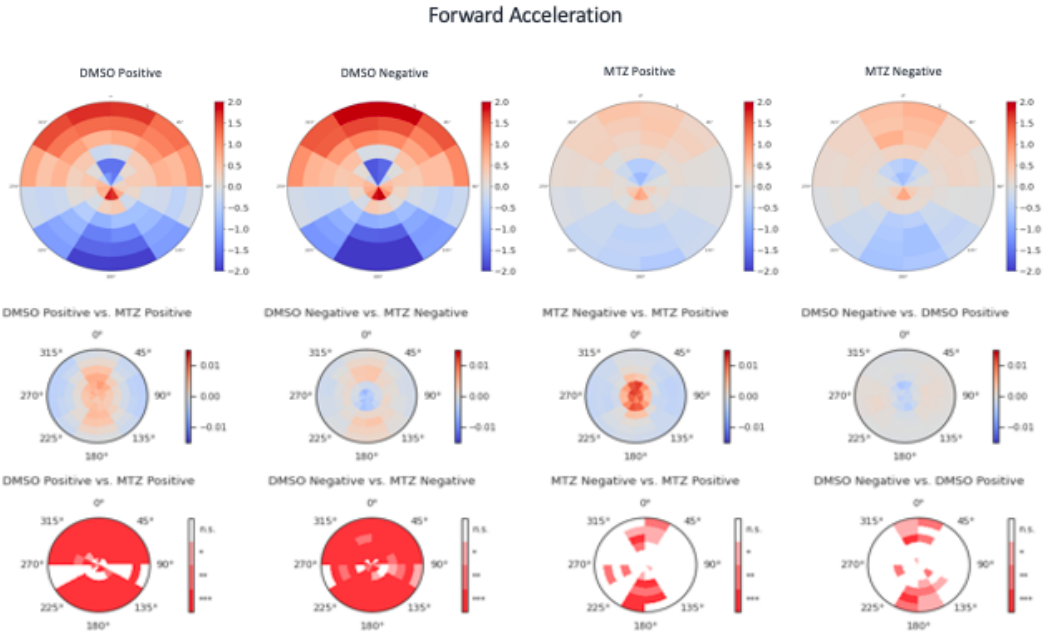

Figure 6.10. Local Interactions With Neighbouring Fish- Forward Acceleration. Mean values of the forward acceleration of the focal (central position) relative to the neighbours positions (top panel). Subtraction of the polar plots according with the paired groups referred in their respective labels (middle panel). Plots representing the significance associated with the statistical inference performed at each bin of the polar plots (bottom panel). Statistical significance was set at * $p<0.05$, ** $p<0.01$, *** $p<0.001$, **** $p<0.0001$, Conover post-hoc test.

specific behavioral adaptation to the treatment.

6.2.4 Shoaling Behavior

Fish have a tendency to aggregate and form shoals, even in small groups with a low number of individuals. Such is the present case, in which the collectives consisted exclusively on five elements each.

Consequently, we explored different features inherent to shoals. In particular, we studied inter-individual distances between its constituents and their orientation towards their neighbours. Such measurements should provide the necessary information to infer about the overall cohesion and polarization, respectively.

Inter-individual Distances

Under MTZ treatment, inter-individual distances (IID) seem to increase slightly. However, this shift is not so evident, as shown in Figure 6.11.

Furthermore, distributions from MTZ groups are more broad indicating a higher level of variability (Figure 6.11). Although the distribution peak of the MTZ negative group seems to be around the same value as the peaks for DMSO treated groups, there is a shift in the MTZ positive peak towards greater IID values. This difference between strains is also present in the averaged data presented in Figure 6.11, yet it is not significant.

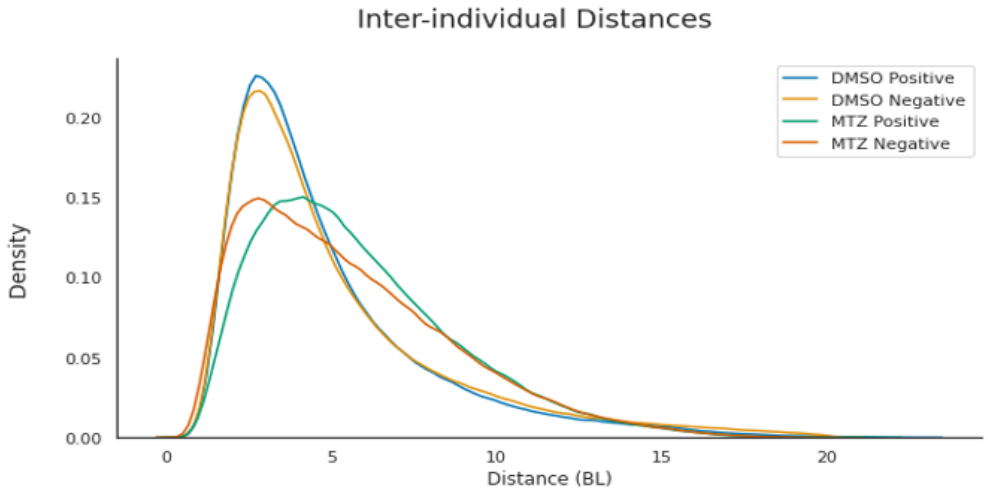

Figure 6.11. Distributions for Inter-individual Distances (IID). Comparison of the IID of groups treated with DMSO (control) and MTZ (ablation). Within each treatment both strains, positive and negative for the expression of *ntr*, were also compared (see Chapter 5 for a complete description of the groups). KDE plots of the median IID value of each collective (n=5) per frame- *g*.

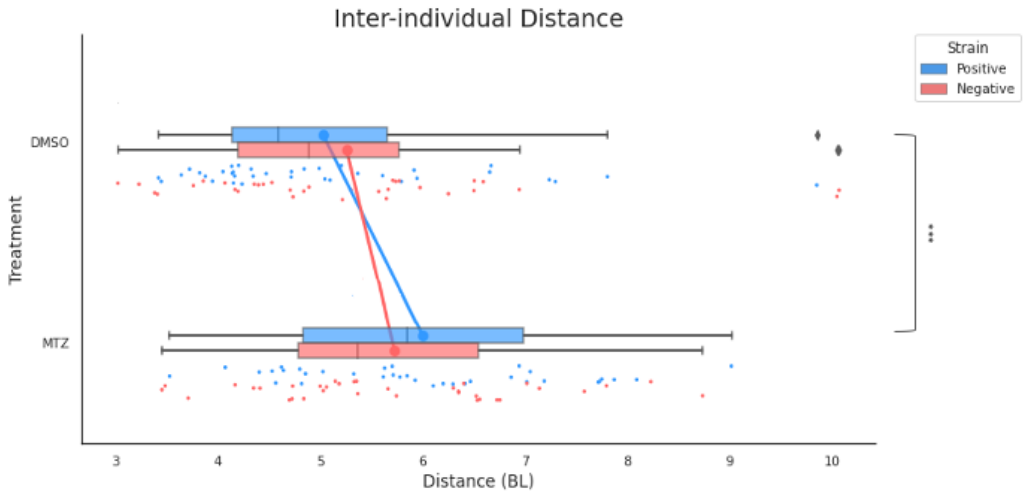

Figure 6.11. Inter-individual Distances (IID). Comparison of the IID of groups treated with DMSO (control) and MTZ (ablation). Within each treatment both strains, positive and negative for the expression of *ntr*, were also compared (see Chapter 5 for a complete description of the groups). Boxplots displaying the mean of g (median IID value of each collective per frame) per video, accompanied by their jittered data. Means are represented with a large dot (•) and connected between comparable groups. Statistical significance was set at *** $p<0.001$, Conover post-hoc test.

Nevertheless, while the IID of MTZ treated animals is significantly different from DMSO groups in positive strains, the distinctions are not so prominent in the negative strain. In addition, no differences were found between strains treated with DMSO.

Meanwhile, to ensure this result was consistent throughout the entirety of the trial, we plotted the IID distributions over time.

As displayed in Figure 6.12, the distributions do not change overall in either of the tested groups. However, the variability found above in animals treated with MTZ also appears to be consistent over the extent of the session, regardless of the strain.

Local Alignment

Lastly, as means to understand if the polarization behavior of the collective changed after ablation, we studied the local alignment of the individuals.

As illustrated by Figure 6.13, the local alignment of animals treated with DMSO forms a bi-modal distribution with peaks at low and high levels of alignment.

Interestingly, the peak representing high alignment seems considerably reduced in groups treated with MTZ. Furthermore, while the negative strain seems to maintain a small peak, the positive strain seemingly loses it entirely.

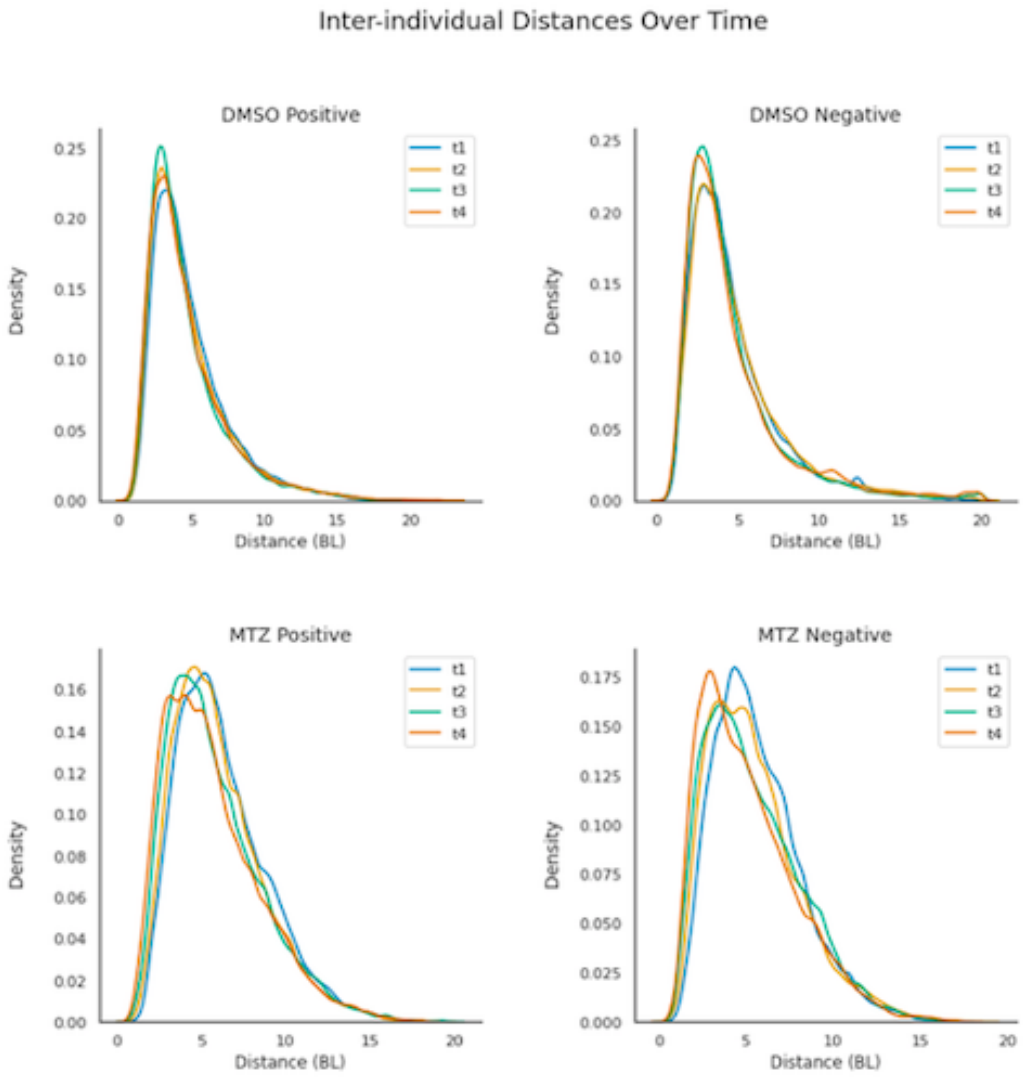

Figure 6.12. Inter-individual Distances (IID) Over Time. Comparison of the IID evolution over time of groups treated with DMSO (control) and MTZ (ablation). Within each treatment both strains, positive and negative for the expression of *ntr*, were also compared (see Chapter 5 for a complete description of the groups). The KDE plots display the IID distributions over four consecutive time periods of 15 minutes each- *t1*, *t2*, *t3*, *t4*.

Additionally, note the decreased density found in the higher alignment mode is contrasted with the increased density at lower alignment values.

No differences are apparent between strains treated with DMSO.

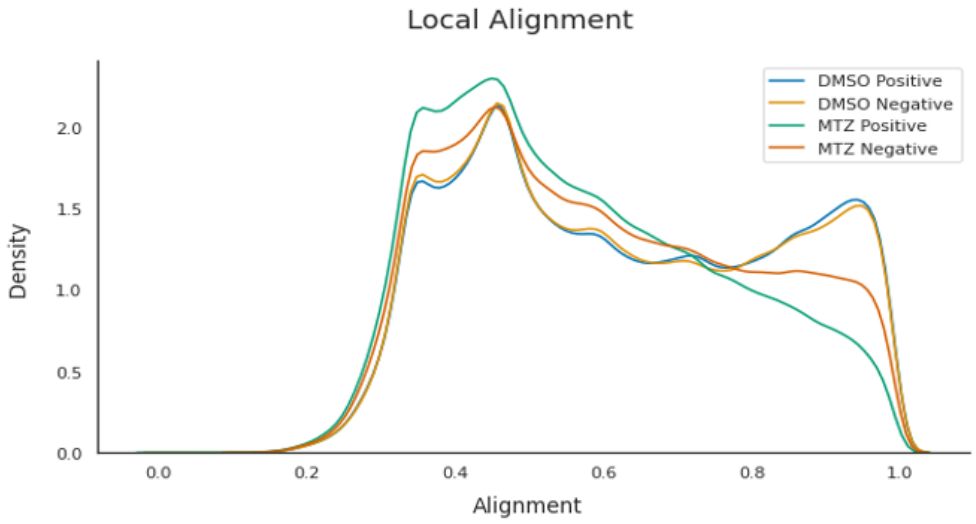

Figure 6.13. Local Alignment Between Fish. Comparison of the local alignment in groups treated with DMSO (control) and MTZ (ablation). Within each treatment both strains, positive and negative for the expression of *ntr*, were also compared (see Chapter 5 for a complete description of the groups). KDE plots of the local alignment values for all experiments.

Consequently, to visualize said alterations in time, we plotted the local alignment over four time intervals. The results are displayed in Figure 6.14.

As expected, the alignment tends to gradually decrease over time in groups under DMSO treatment, regardless of the strain.

However, groups treated with MTZ do not show the same tendency. In realty, MTZ negative groups appear to maintain a stable low peak which resembles the shape of *t3* found in DMSO groups over the first three time periods. This peak declines at the final stage (*t4*), similarly to control groups.

As for the ablated group, the peak at high alignment is minimal and the density at lower values is likewise increased. This shape is preserved throughout the four time periods analysed.

On a separate note, we considered the values of high alignment ranging from 0.7 to 1, with the latter being considered a perfect alignment. We then measured the time each group spent in high alignment mode during one session, as shown in Figure 6.15.

As it happens, there are significant differences between treatments. Nevertheless, distinctions were also found between positive and negative strains treated with MTZ

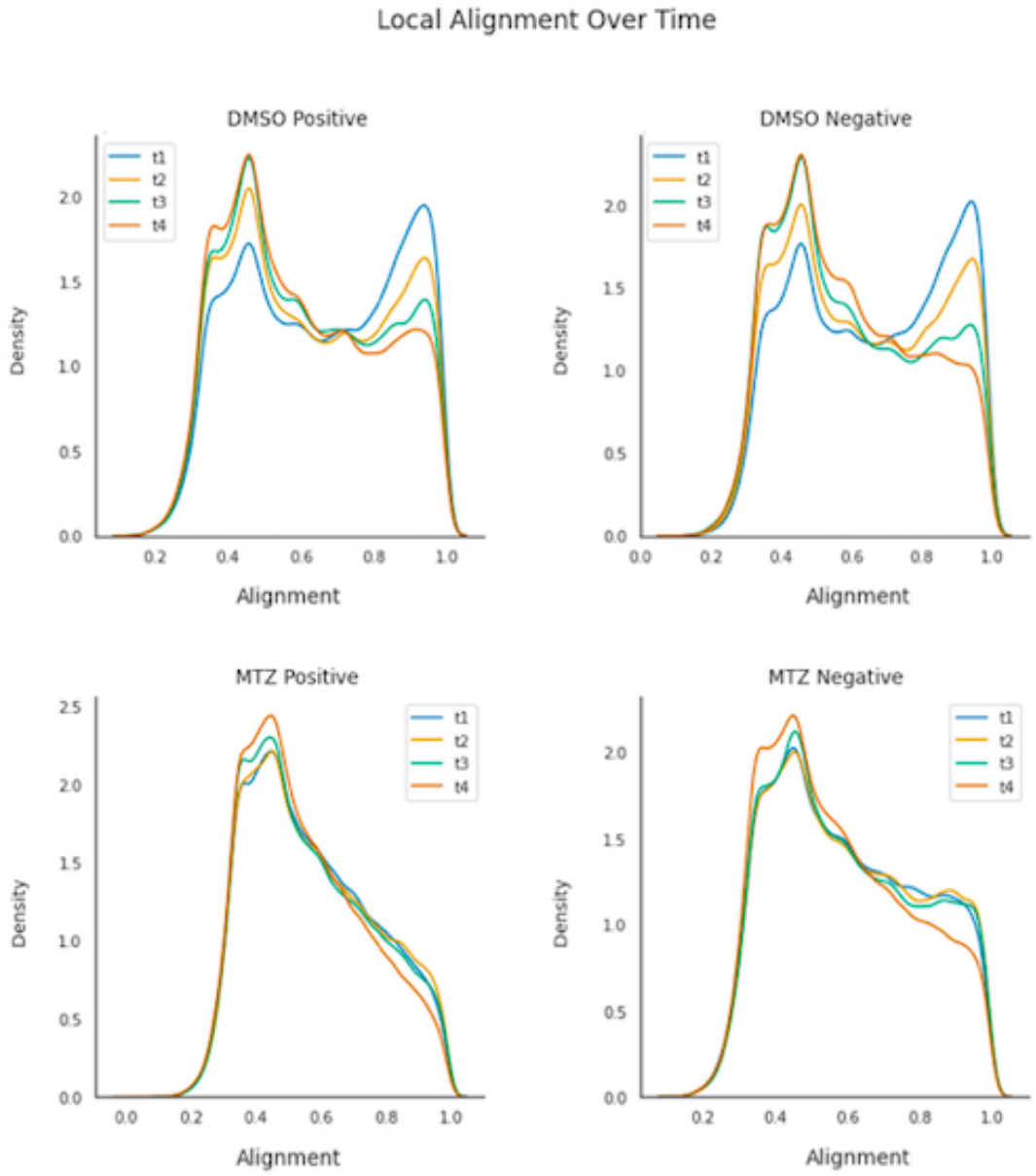

Figure 6.14. Local Alignment Over Time. Comparison of the local alignment evolution over time of groups treated with DMSO (control) and MTZ (ablation). Within each treatment both strains, positive and negative for the expression of *ntr*, were also compared (see Chapter 5 for a complete description of the groups). The KDE plots display the local alignment distributions over four consecutive time periods of 15 minutes each- *t1*, *t2*, *t3*, *t4*.

which goes in line with our previous findings. Ablated groups appear to spend less time aligned when compared to the other three groups.

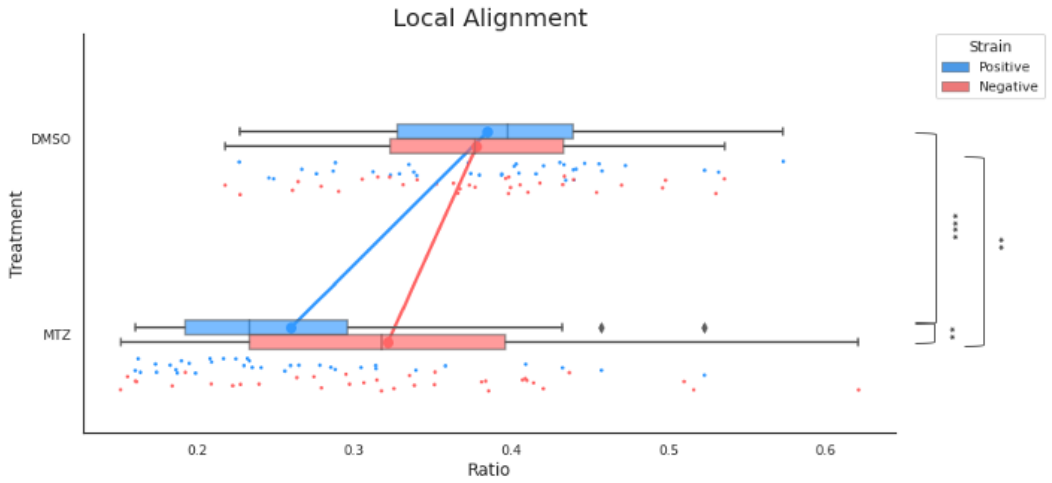

Figure 6.15. High Alignment Ratio. Comparison of the high alignment ratio of groups treated with DMSO (control) and MTZ (ablation). Within each treatment both strains, positive and negative for the expression of *ntr*, were also compared (see Chapter 5 for a complete description of the groups). Boxplots displaying the ratio of time spent in high alignment (0.7-1) over one session, accompanied by their jittered data. Means are represented with a large dot (•) and connected between comparable groups. Statistical significance was set at ** p<0.01, **** p<0.0001, Conover post-hoc test.

Finally, as groups with higher speed have the tendency to align more, we calculated the correlation between these two variables.

As shown in Figure 6.16, no disruptions were found as the moderate relationship seems to be preserved through all the tested groups.

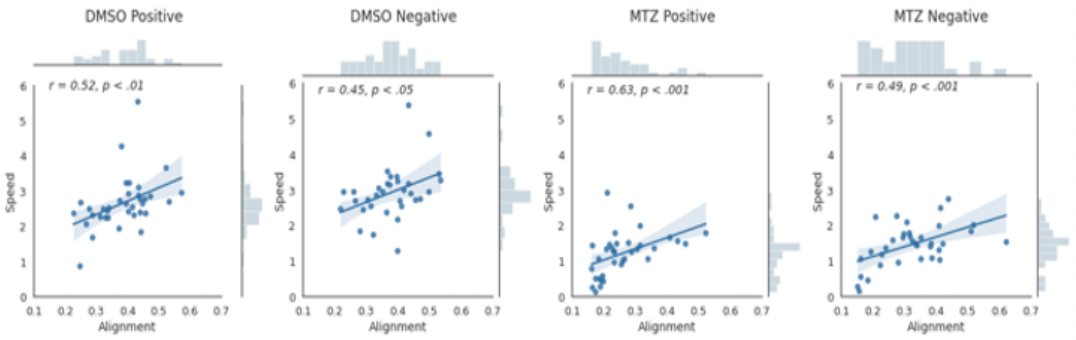

Figure 6.16. Local Alignment Ratio vs. Speed. Relationship between the local alignment and the median speed of the group. Calculated through Spearman's rank correlation coefficient.

7 | Discussion

The aim of the present thesis was to explore the role of the ventral telencephalon in socially driven interactions of zebrafish collectives.

Accordingly, we optimized an ablation protocol appropriate for fish at a juvenile stage of development, in order to chemically induce controlled cell death at a region specific level. Following treatment, we investigated social behavior in an unconstrained paradigm, in which animals could physically interact.

In section 6.1, the ablation treatment was validated through examination of the m-Cherry signal on targeted regions. Indeed, the effects of the ablation were quite extensive. The signal was clearly diminished in ablated samples yet not completely gone. These results indicated that this particular protocol lead to a partial ablation of the tissue rather than a complete one.

In section 6.2, we analysed the trajectories of the animals in a free swimming trial. As a consequence of the ablation procedure, fish presented impaired motility, evident in their general kinetic parameters. They also exhibited a slight increase in overall group cohesion. However, the most striking result was the local alignment of the individuals, which was considerably impaired in ablated groups. These results support the hypothesis that the targeted areas, in particular the ventral telencephalon, might have an important role in the local polarization of shoals.

7.1 Optimization of the Ablation Protocol for Juvenile Zebrafish

The success of a chemo-genetic ablation highly depends on a number of variables. Firstly, it is important to consider the characteristics of the individual, such as the transgenic line, target regions or stage of development. Additionally, factors directly related to the technique are also pivotal like drug concentration, exposure time and recovery time [21].

Most protocols available are designed for larvea due to their transparency and simple manipulation, which are extremely advantageous features for regeneration studies [78][22][21]. There are adaptations for juveniles [21] and reports on partial ablations achieved in adult fish, particularly in the regions of the olfactory bulb (OB) and the habenula [32][70]. These constituted an outset for possible protocols appropriate for our intended age.

We attempted a number of different protocols which differed in exposure time and recovery time, in order to have visible results of ablation efficiency while avoiding elevated drug toxicity or cellular regeneration, respectively. We started by testing a drug exposure period of 24 hours while maintaining a concentration of 10mM in

the MTZ solution. However, an overnight did not prove to be sufficient to reach observable results (data not shown). Therefore, we chose to increase the exposure time to 48 hours to ensure maximum ablation in the targeted areas. In addition, we observed that a recovery period of at least 24 hours showed already a high level of regeneration. Therefore, we reduced it to an interval of 1-2 hours prior to the behavioral trial.

7.2 Quality of the Signal Low Due to Variability of Auto-fluorescence

Auto-fluorescence is a recurrent challenge in microscopy. Brain tissue is particularly affected as it has a variety of cell types and accumulation of lipofuscins, which can greatly contribute to this phenomenon [92]. In addition, fixation processes can also induce fluorescence [17].

The considerable auto-fluorescence detected in the imaged tissues (Figures A.5-A.12 (A)) is present in both groups, which suggests an issue intrinsic to the samples rather than an effect of the ablation treatment.

The clearing method is also relevant as it allows to acquire a clear z-stack of the signal. We tested different clearing protocols, specifically ethyl-cinnamate and RTF, to choose which would be more appropriate for our samples. While ethyl-cinnamate was extremely efficient in clearing the samples, it failed to preserve the m-Cherry signal. On the other hand, the RTF procedure resulted in a lower quality clearing but properly conserved the fluorescence (data not shown). As the signal was located more to the periphery and not too deep within the brain tissue, the RTF clearing method proved to be adequate for our particular needs.

There might be other factors contributing to this extensive auto-fluorescence, yet no studies as to what might be the cause were conducted.

7.3 Ablation Treatment Induced Partial Cell Death in *y321* Transgenic Line

As formerly mentioned, chemical ablation is a sensitive technique highly dependent on the features of the animal model in use and the intended targets to ablate. Complete ablations are extremely difficult to achieve and most have been reported in zebrafish larvea [21][79].

Previous studies performed on adult fish, with optimized ablation protocols for brain tissues, have exclusively achieved partial ablations [32][70]. The neurogenesis rate for juvenile fish is unknown [91] and some cells may not be accessible to the drug [21].

In addition, since we are not targeting a particular group of cells, we do not know which cell types are being affected and therefore, cannot adjust the protocol to their particular properties [55]. With a long exposure period combined with short time recovery, our protocol should maximize ablation on the target regions.

In accordance, our results show that the m-Cherry fluorescent signal clearly decreased. Not only was the overall intensity lower, but the density of the signal was also reduced, as expected.

Interestingly, while the signal was locally concentrated in animals treated with DMSO, it dispersed after the MTZ treatment. Indeed, some signal was found outside the established ROIs following ablation. This phenomenon might be due to an m-Cherry release after membrane rupture, resultant of cell death.

In the future, this could be confirmed by a cell death assay such as TUNNEL or Caspase-3 [78].

In brief, evidence shows that the targeted areas were clearly affected by the treatment and the ventral telecephalon and rostral diencephalon were successfully partially ablated.

7.4 MTZ Affects Motor Function

Toxicity studies have shown MTZ to be particularly harmful to aquatic organisms [51][15]. The substance has been implicated in teratogenesis, hepatic problems and intestine damage in fish [36][37]. However, no behavioral effects have been reported thus far. At the same time, in humans, neurotoxicity associated with MTZ seems to be a rare event [48][2] yet there have been reports in which MTZ treatment caused peripheral neuropathy [12].

In our findings, kinematic parameters were significantly compromised following drug exposure. The fish showed signs of akinesia, in particular slowness in swimming and decreased dislocation, but no changes in posture were evident [43].

These non specific behavioural changes suggest MTZ toxicity is higher than expected, inducing serious impairments at the level of motor functions.

Furthermore, while significant differences were found between strains treated with MTZ, these were not evident on the distributions of kinematic parameters (Figure 6.6) nor in the general behavior displayed in video recordings (data not shown). In addition, these distinctions were not consistent between the two parameters analysed. DMSO groups reveal similar results. This analysis does not seem to be capturing real differences but rather small disparities in the data aggravated by the large sample

size. Accordingly, it appears there should be a similar level of damage to the motor functions in animals treated with MTZ, regardless of their strain.

Nevertheless, there must be a better compromise between elevated toxicity and adequate ablation achievement. A more efficient protocol must be designed in order to optimize ablations particularly for behavioral assays, in which performance is extremely important. Recent studies have introduced nifurpirinol as a less toxic alternative substrate in NTR-induced ablations [10].

7.5 Preoptic Area in Stress Response and Anxiety-typed Behavior

Similar to rodents, the open field test is a widely used paradigm designed to study behavioral phenotypes such as fear and anxiety in zebrafish [49].

Substantial information can be extracted from an open field experiment, for the appraisal of anxiety-like behavior. The feature most commonly analysed is thigmotaxis. It refers to the time spent near the walls and it is a risk assessment measurement, as the center of the arena is considered to be an aversive environment [93]. Although not so customary, shoaling can also be an anxiety measurement. In response to a possible threat, fish tend to aggregate and the cohesion level of the group increases . Thus, an enhancement on the described parameters strongly indicates anxious behavior [56][98].

In our apparatus, animals displayed clear signs of anxiety. This response was not unexpected as the trial was primarily an open field assay. Fish treated with DMSO exhibited an extremely elevated thigmotaxis (Figure 6.7) and a high level of cohesion within the shoal (Figure 6.11). In contrast, these parameters decreased with MTZ treatment. Certainly, this result is largely a consequence of the impaired motor functions found in these groups due to drug treatment. However, there is a difference between strains. Negative groups treated with MTZ seem to spend more time near the walls when compared with the ablated group. In addition, the first also shows increased cohesion, yet the difference is not significant.

Interestingly, the local interactions indicate higher level of local proximity in MTZ negative groups, as individuals show a tendency to be closer together with an increased density in the attraction zone (Figure 6.8). This effect overcomes the results found in DMSO treated fish and is mostly lost in ablated groups. The reinforced proximity observed in these groups could be an indication of additional anxiety experienced by the fish as the exposure to the drug itself and motor impairments may be considered as stressors.

As it happens, the two strains under MTZ treatment do not show the same behavioral pattern and although the difference is feeble, it could be a direct consequence of the POA/ rostral diencephalon ablation. As mentioned in Chapter 2, the POA is thought to be responsible for stress responses and anxiety regulation in zebrafish [8][11][24]. Thus, our results could be an indication that POA ablation might be a contributing factor to the disruption of normal stress response and down-regulation of the anxiety circuitry.

7.6 Local Interactions Maintained After Ablation

Collectives have rules of behavior derivative of local interactions between their constituents [44][39]. These exchanges can have a cooperative or competitive character which strongly conditions their global design [83][9]. In zebrafish we observe the former, as shoaling behavior is a cooperative strategy employed for the benefit of the whole group.

The dynamics found at a local level are the basic structures for the general pattern of a shoal. As the configurations seem to be maintained in all groups regardless of treatment or strain (Figures 6.8-6.10), their intensities are clearly different.

As formerly discussed, results indicate an antithetical level of proximity in ablated groups and control groups exposed to the drug (Figure 6.8). Also, fish are able to turn and regulate the distance toward their neighbours through the adaptation of their acceleration yet it seems they accelerate less to maintain their relative position in the shoal.

These results support that there is a clear impact in internal interactions due to akinesia but the slight difference observed in the acceleration and turning components, between the ablation group and the negative strain treated with MTZ, suggests there might be an ablated-related consequence.

7.7 Ventral Telencephalon in Shoaling Behavior

In the context of shoaling, cohesiveness and orientation have anti-predator advantages [41]. When introduced to a new environment, animals will have the tendency to be more anxious and aggregate in denser and further polarized shoals [98][57]. However, as they begin to explore their surroundings, they start to display an adaptive behavior of habituation and gradually, individuals may venture further away from the group and transitions into polarized states might become less frequent [57].

From our results, the habituation process is quite clear in the local alignment component of DMSO groups, yet no such effect is seen in the inter-individual distances.

Studies have reported that the cohesion in a shoal tends to keep within a certain range, if the internal dynamics are maintained. Still, in the presence of an external stimulus the group will rapidly adapt their inter-individual distances accordingly [58][34].

In our initial hypothesis, we proposed that the ventral telencephalon might be driving shoaling behavior in fish collectives. And if so, ablating said region could potentially compromise the groups structure in a global or local manner. These possible outcomes would imply a disruption of the overall cohesion or an adjustment in the local alignment of the individuals, respectively.

While we observed a slight increase in the distance between fish (Figure 6.11), it was not significant. The self organization patterns formed from local interactions were also preserved in the four groups under assessment (Figure 6.8-6.10). These results suggest that the cohesion of the collective remains stable following ablation treatment and that the integrity of the shoal appears to be maintained.

Simultaneously, we do find a collapse in local alignment. Groups treated with DMSO show a gradual decay in the level of alignment over time (Figure 6.14). Although our drug control group, MTZ negative, reveals a lower level of high alignment from the start, due to the toxicity effects, we still see a decrease at the last time point ($t4$). This reduction could be a delay of the same behavioral pattern displayed by the DMSO groups, but with a higher latency period. Conversely, there is no evidence of such behavioral pattern of local alignment in ablated fish. There seems to be a complete loss of high alignment values between focal fish and their neighbours, which remains unchangeable for the duration of the trial.

On a different note, speed and alignment have been reported to be correlated, as shoals with higher speed tend to show increased polarization [57]. That relationship does not change with the ablation treatment.

Our findings seem to support our original assumption that the ablation might have a local influence on shoaling behavior, yet it contradicts an effect in the global cohesion of the collective.

Interestingly, these results are in accordance with the conclusions drawn from the socially-driven visual assay conducted by Stednitz et al. (2018). As the individual with the vTel ablated spent less time orienting towards the social stimulus, we observe a similar response within the shoal. This similarity suggests that possibly, the richness of the external stimuli is not so influential for the particular behavior of social attention.

Finally, as mentioned in Chapter 2, homology studies have reported the dorsal region of the vTel as an homologous structure to the mammalian NAcc. This area has been

characterized as a facilitator to attain relevant goals, by reinforcing behavioral adjustments [30]. In the context of our experiments, the aim would be the exploration of a novel environment. If these homologies are correct, we would expect the vTel to play a role in this task, specifically promoting habituation following a continued exposure to the same physical space. Indeed, we observed a complete loss of adaptive behavior particularly in the local alignment of ablated animals, supporting the assumption that the vTel might be driving this specific behavior.

8 | Conclusion

In this thesis, we were interested in exploring the anatomical function of the ventral telencephalon, in the shoaling behavior of zebrafish aggregates. Our initial hypothesis stood on two possible scenarios: either the vTel had a local effect on the behavior, leading to changes in the individual alignment of fish, while maintaining overall group integrity; or instead, wielded influence in the global pattern of the shoal without necessarily altering the alignment.

We tackled this question by ablating the vTel and the rostral area of the diencephalon and performing free swimming trials to assess shoaling behavior.

Our findings indicated that the ablation severely disrupted the local alignment of the groups yet the cohesion remained preserved, supporting our inclination towards a local impact. However, it remains unclear the actual role of the preoptic area in these results. While both vTel and POA are prominent regions in the anxiety circuitry, the POA is mostly responsible for the regulation of social behaviors associated to sexual maturity such as parental care and aggression. In addition, evidence from anatomical studies suggest the vTel and NAcc are homologous structures, an area involved in the reward system of mammals and reported to have an important role in adaptive behavior.

We demonstrated the importance of specific ventral areas of the forebrain in social behavior plasticity. The vTel and POA might be responsible for driving shoaling behavior at a local level in social environments. We also confirmed the importance of these two structures within the anxiety circuitry.

8.1 Limitations

For our study, we had to adapt every protocol to our requirements, from the sample preparation to the imaging settings. To optimize a procedure for a new developmental stage requires time and a lot of trial and error. However, for the time we had available to conduct our experiments, we could not find the optimal solutions for these designs. Consequently, we could not find the correct balance between partial ablation and minimal toxicity, in order to prevent side effects. In addition, the clearing procedure may not have been the most effective in terms of transparency. Finally, the mounting process in the lightsheet might have led to great variability between samples.

8.2 Future Directions

A logical question raised from this project would be how the dynamics might change in an heterogeneous group, formed by ablated and 'healthy' individuals. Also, it would be interesting to consider the size of the ablated fraction and observe how the

interactions might shift if the proportion of ablated fish is lower or higher within the collective.

On a different note, it would be important to learn which cell populations are being particularly affected with the ablation. This information might shed some light on the mechanisms behind adaptive responses of shoaling behavior, particularly in local alignment.

Additionally, it is necessary to clearly distinguish vTel from POA in order to understand the role of the vTel exclusively, in social behavior. To this end, we could explore other transgenic lines that include tissue-specific enhancers in this area and perform the same experimental design.

Nevertheless, it would be fundamental to start by optimizing the ablation protocol and procedures for treatment validation, such as sample preparation and imaging. Perhaps, consideration of a different pro-drug, such as nifurpirinol, might improve the ablation and lower toxicity effects at the same time. In parallel, we should attempt new time periods for drug exposure that are not so aggressive to the fish, while still being able to accomplish good ablation results. Furthermore, it would be relevant to complement the ablation quantification with a cell death assay to enhance accuracy in our analysis. Lastly, we should find a better clearing process to achieve better imaging quality.

A | Ablation Analysis

A.1 ROIs

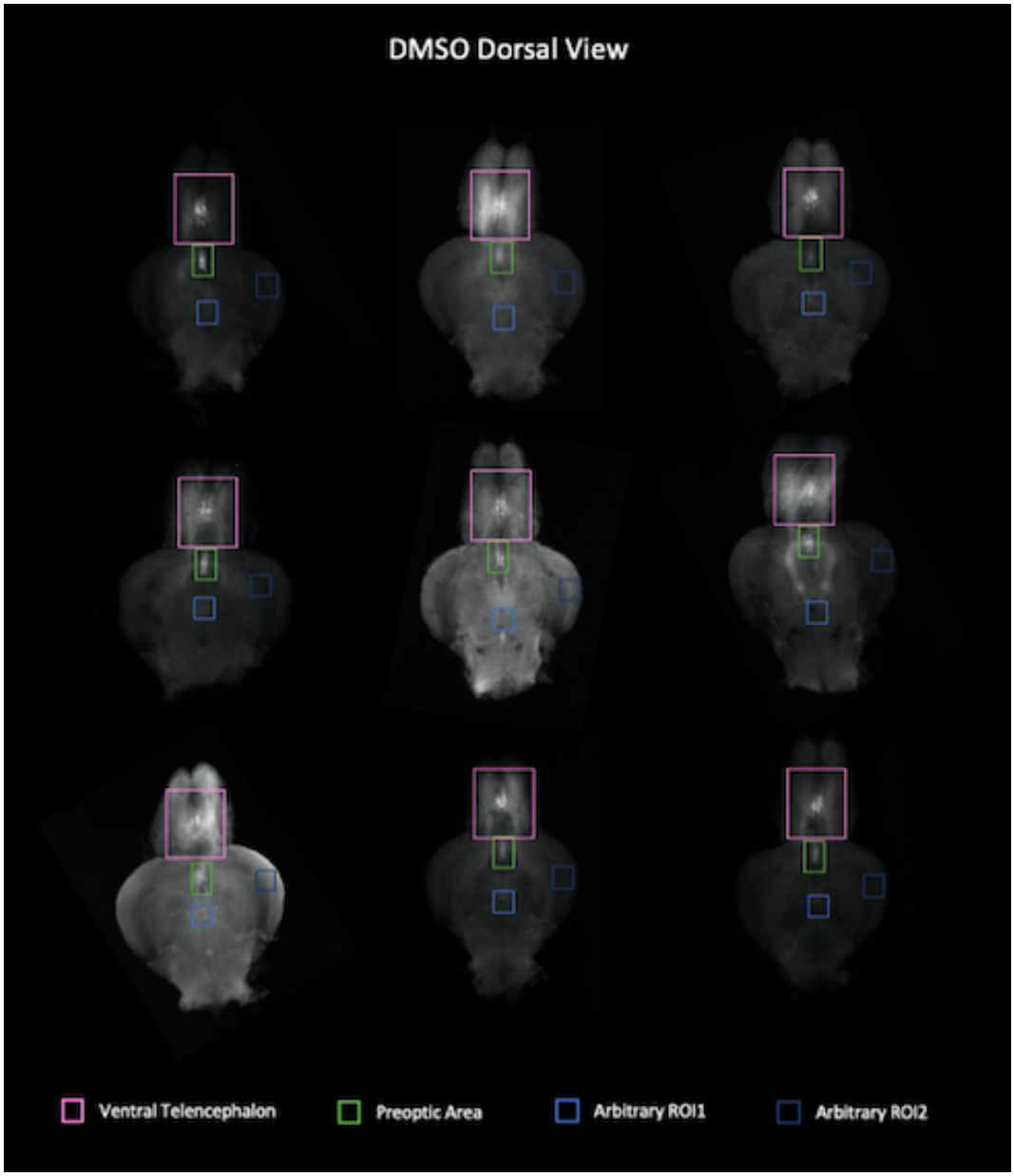

Figure A.1. ROIs for DMSO Treatment with Dorsal View. Selection of the regions of interest (ROIs) for brain samples imaged from the dorsal view and treated with DMSO.

Figure A.2. ROIs for DMSO Treatment with Ventral View. Selection of the regions of interest (ROIs) for brain samples imaged from the ventral view and treated with DMSO.

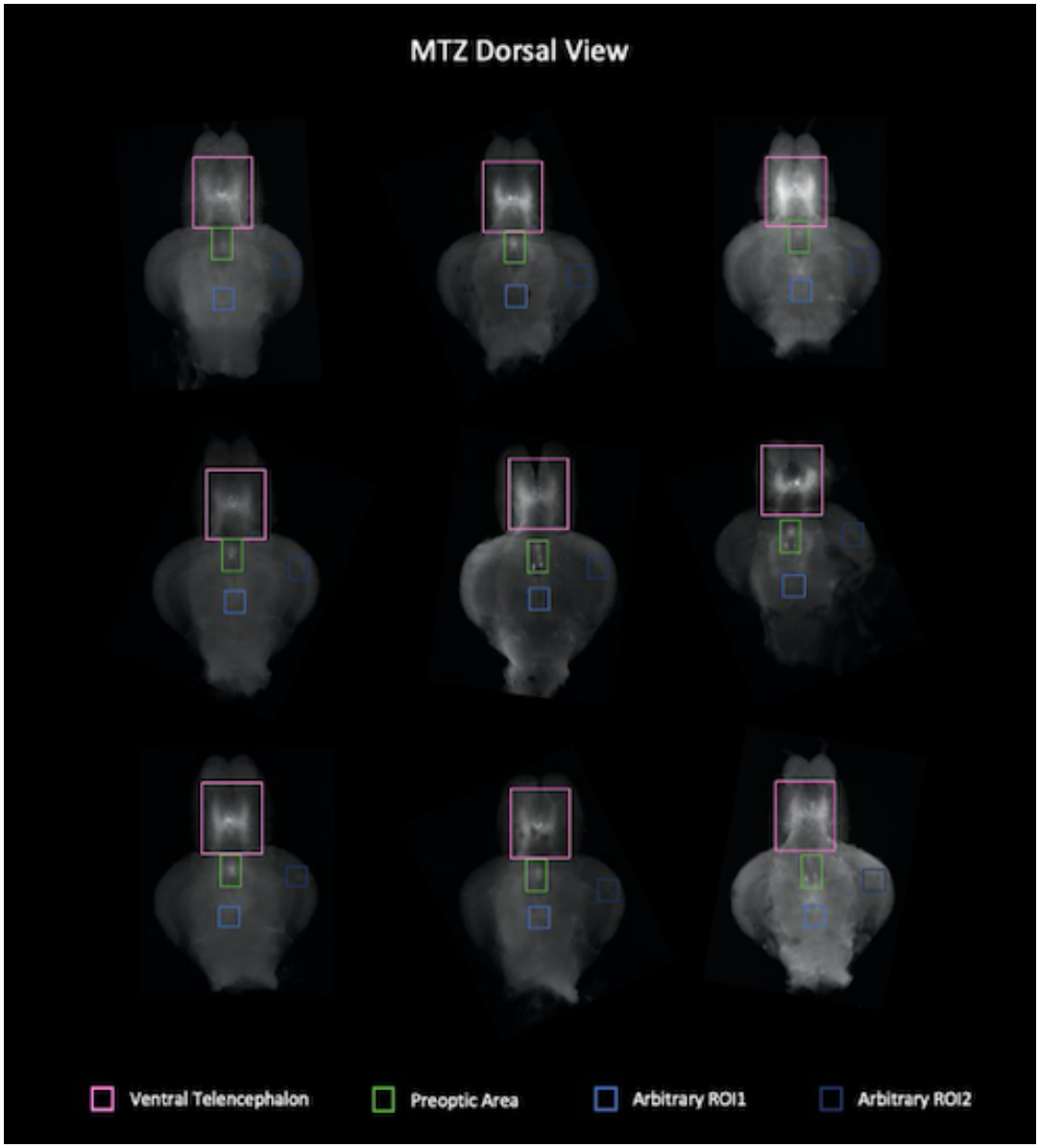

Figure A.3. ROIs for MTZ Treatment with Dorsal View. Selection of the regions of interest (ROIs) for brain samples imaged from the dorsal view and treated with MTZ (ablation treatment).

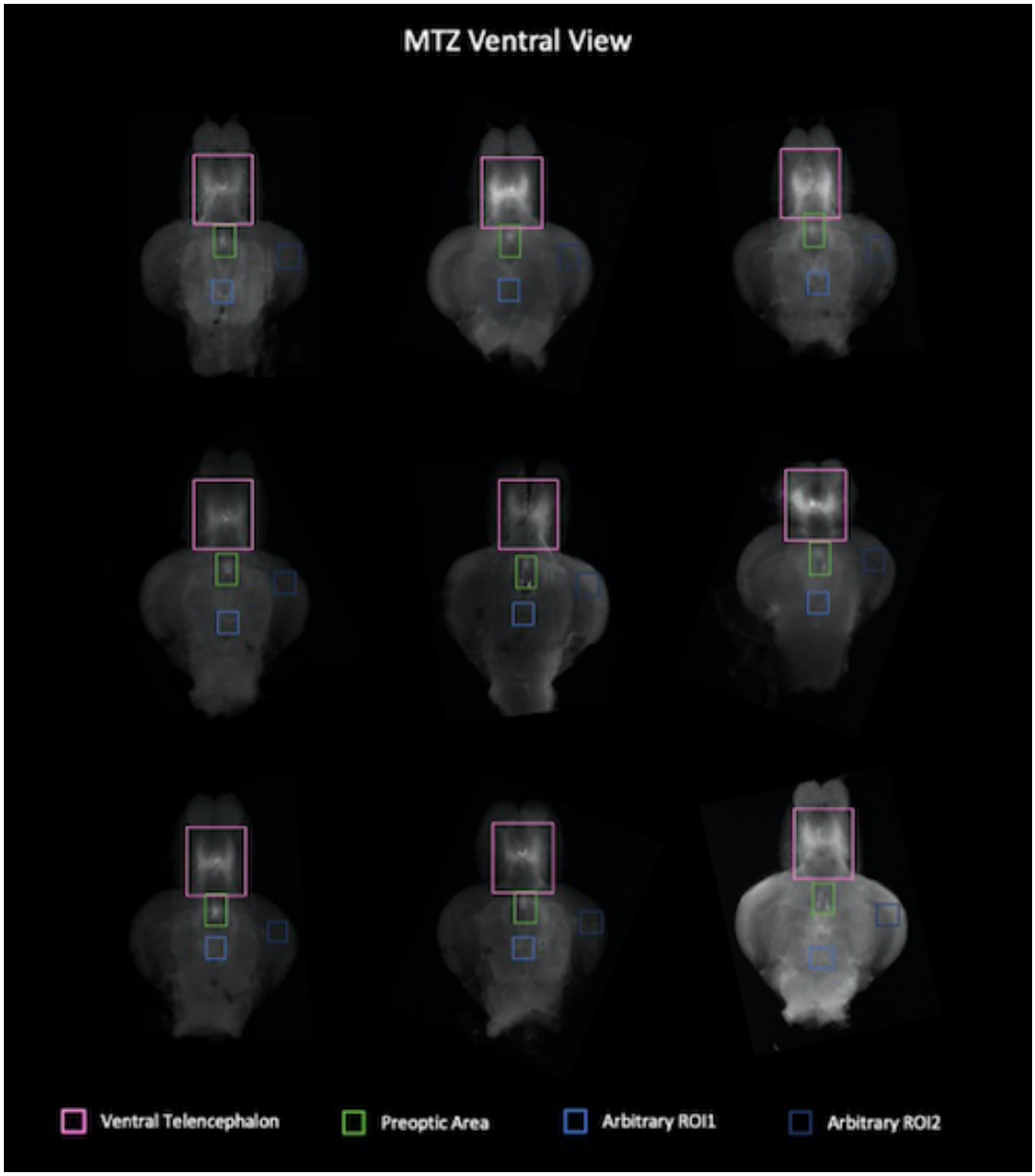

Figure A.4. ROIs for MTZ Treatment with Ventral View. Selection of the regions of interest (ROIs) for brain samples imaged from the ventral view and treated with MTZ (ablation treatment).

A.2 Image Processing

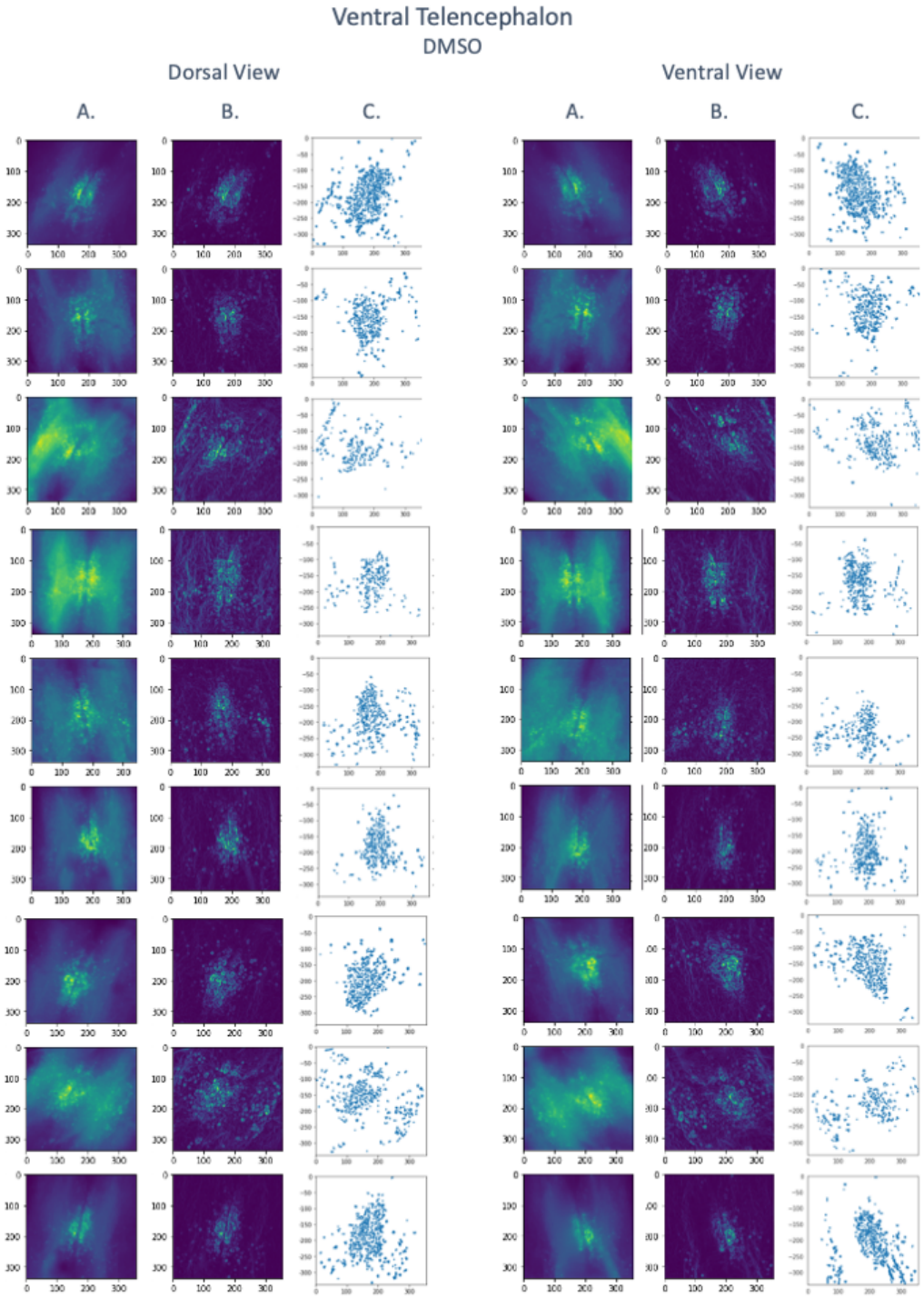

Figure A.5. vTel with DMSO Treatment. Segmentation process of the vTel images under DMSO condition.(A) Summed z-stack of the roi. (B) Resulting images after application of the local gradient (LG) filter. Background subtraction was also applied for intensity normalization. (C) Identification of the intensity peaks (threshold = 4) on normalized images.

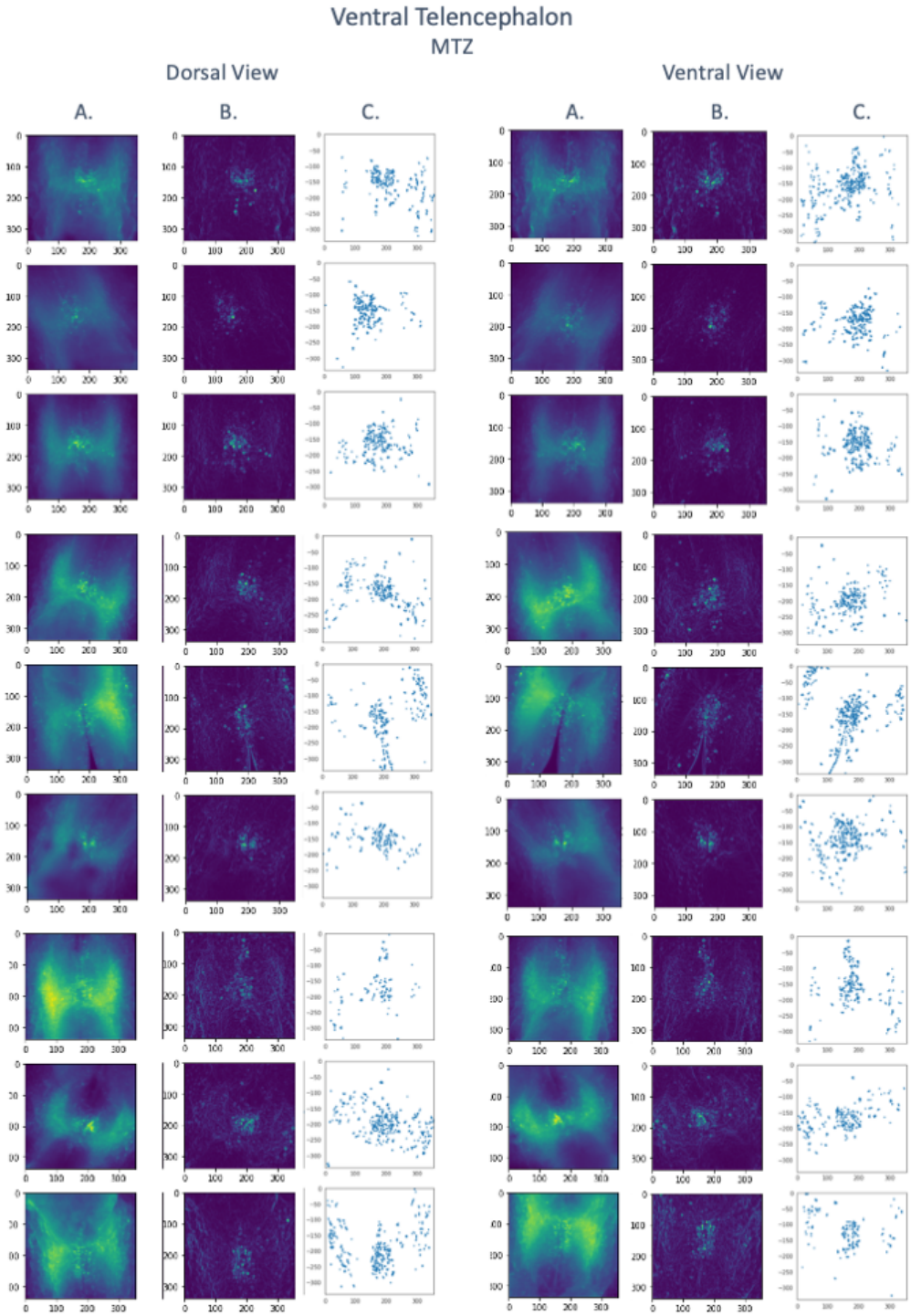

Figure A.6. vTel with MTZ Treatment. Segmentation process of the vTel images under MTZ condition.(A) Summed z-stack of the roi. (B) Resulting images after application of the local gradient (LG) filter. Background subtraction was also applied for intensity normalization. (C) Identification of the intensity peaks (threshold = 4) on normalized images.

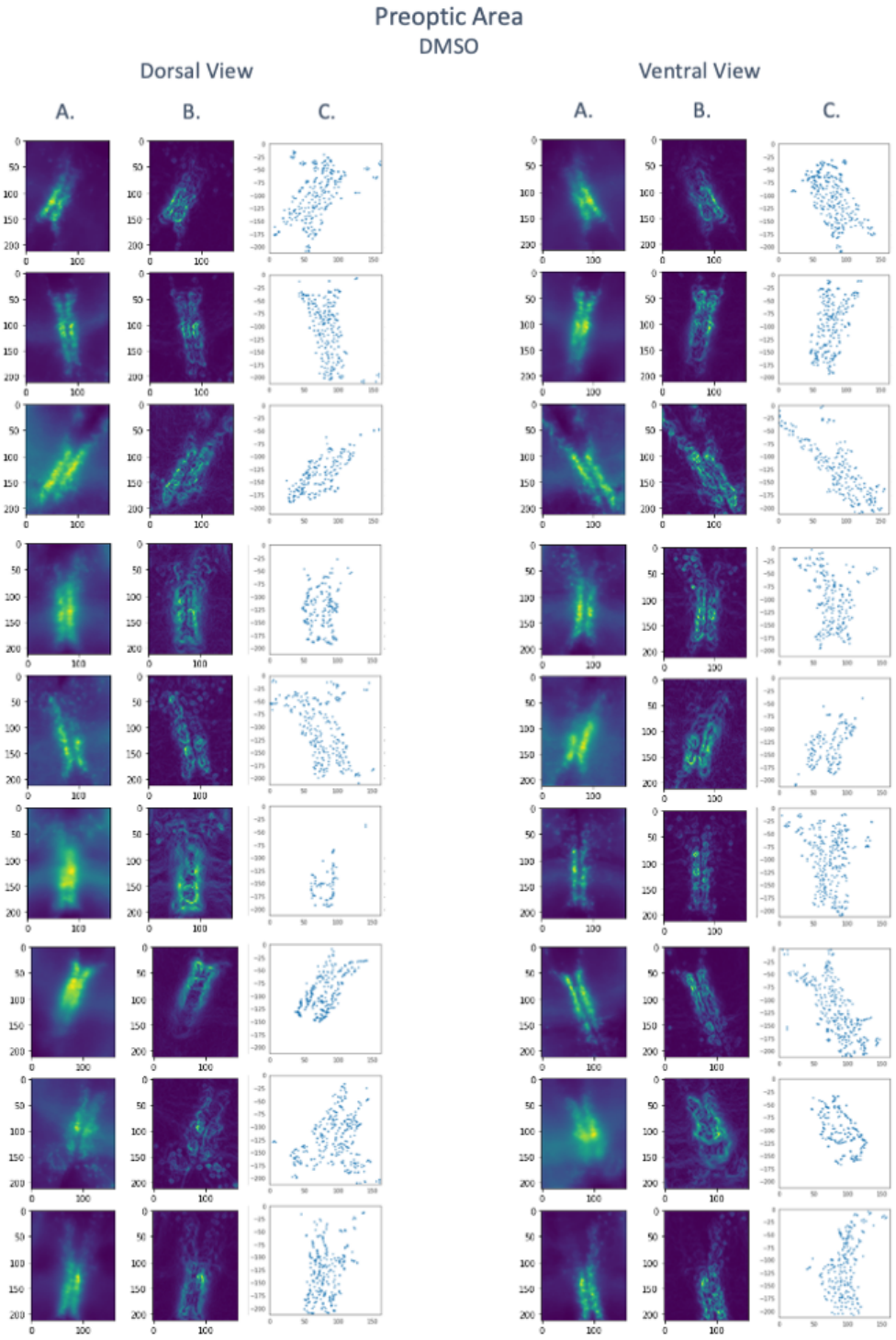

Figure A.7. Diencephalon with DMSO Treatment. Segmentation process of the diencephalon images under DMSO condition.(A) Summed z-stack of the roi. (B) Resulting images after application of the local gradient (LG) filter. Background subtraction was also applied for intensity normalization. (C) Identification of the intensity peaks (threshold = 4) on normalized images.

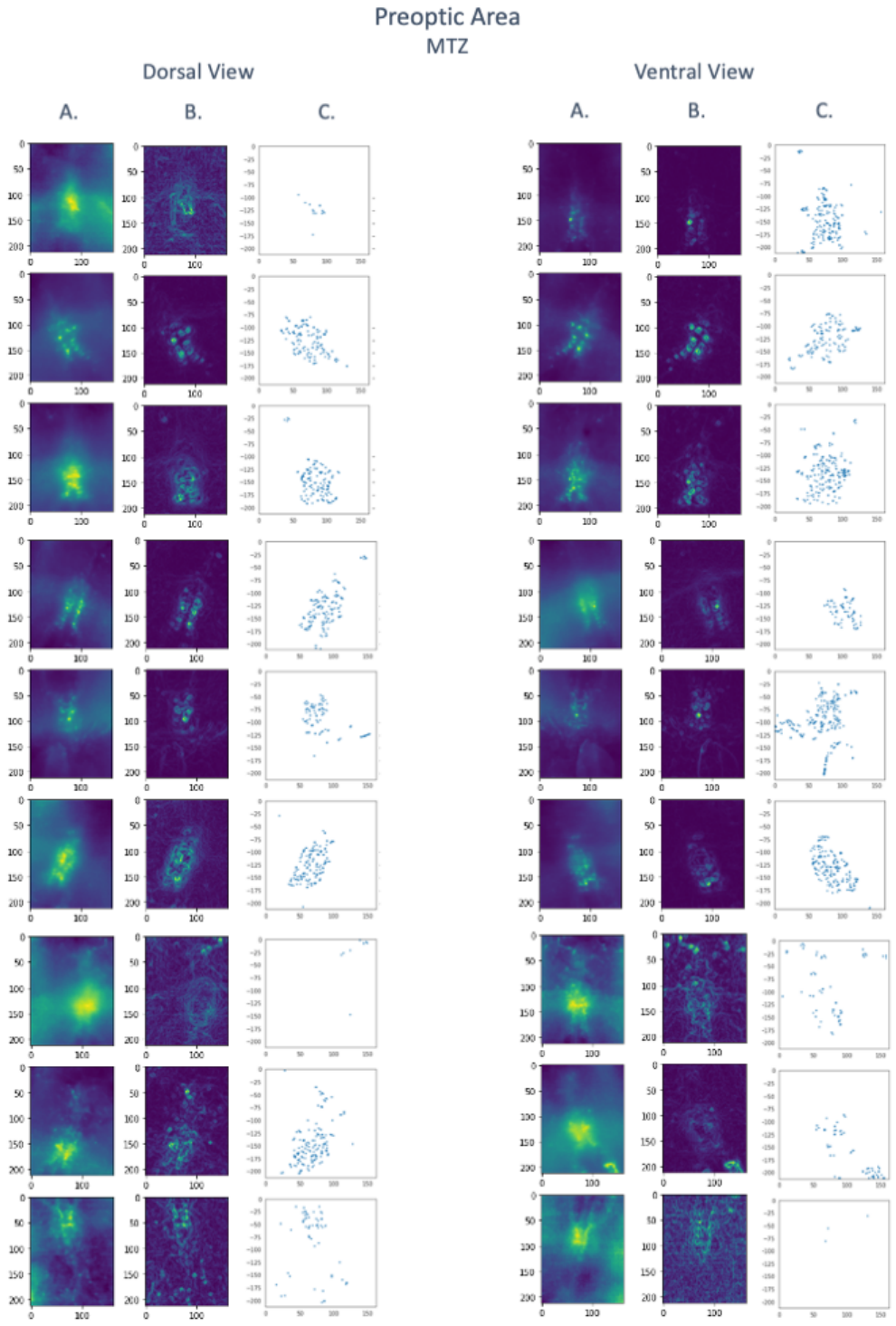

Figure A.8. Diencephalon with MTZ Treatment. Segmentation process of the diencephalon images under MTZ condition.(A) Summed z-stack of the roi. (B) Resulting images after application of the local gradient (LG) filter. Background subtraction was also applied for intensity normalization. (C) Identification of the intensity peaks (threshold = 4) on normalized images.

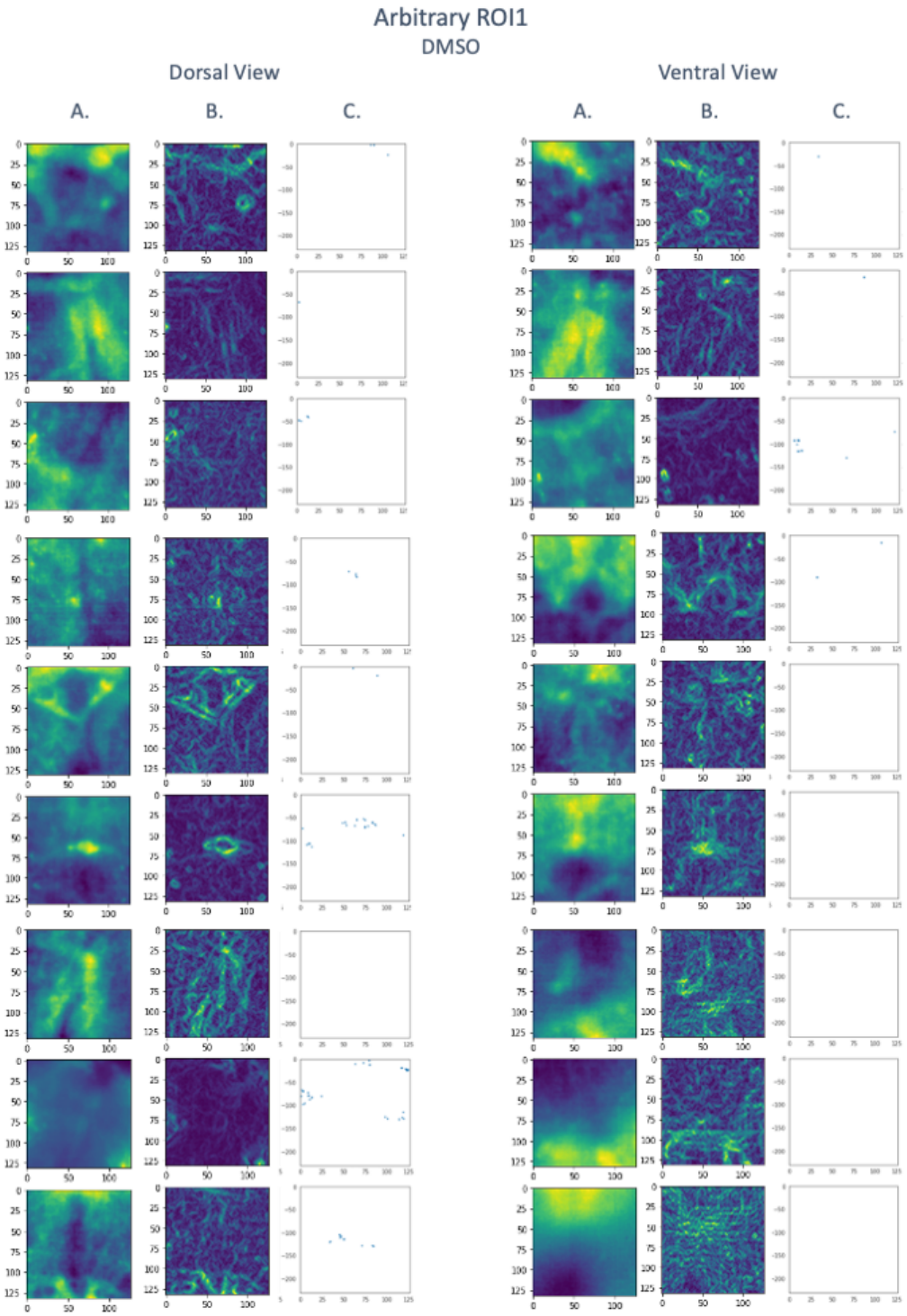

Figure A.9. Arbitrary ROI1 with DMSO Treatment. Segmentation process of the arbitrary ROI1 images under DMSO condition.(A) Summed z-stack of the roi. (B) Resulting images after application of the local gradient (LG) filter. Background subtraction was also applied for intensity normalization. (C) Identification of the intensity peaks (threshold = 4) on normalized images.

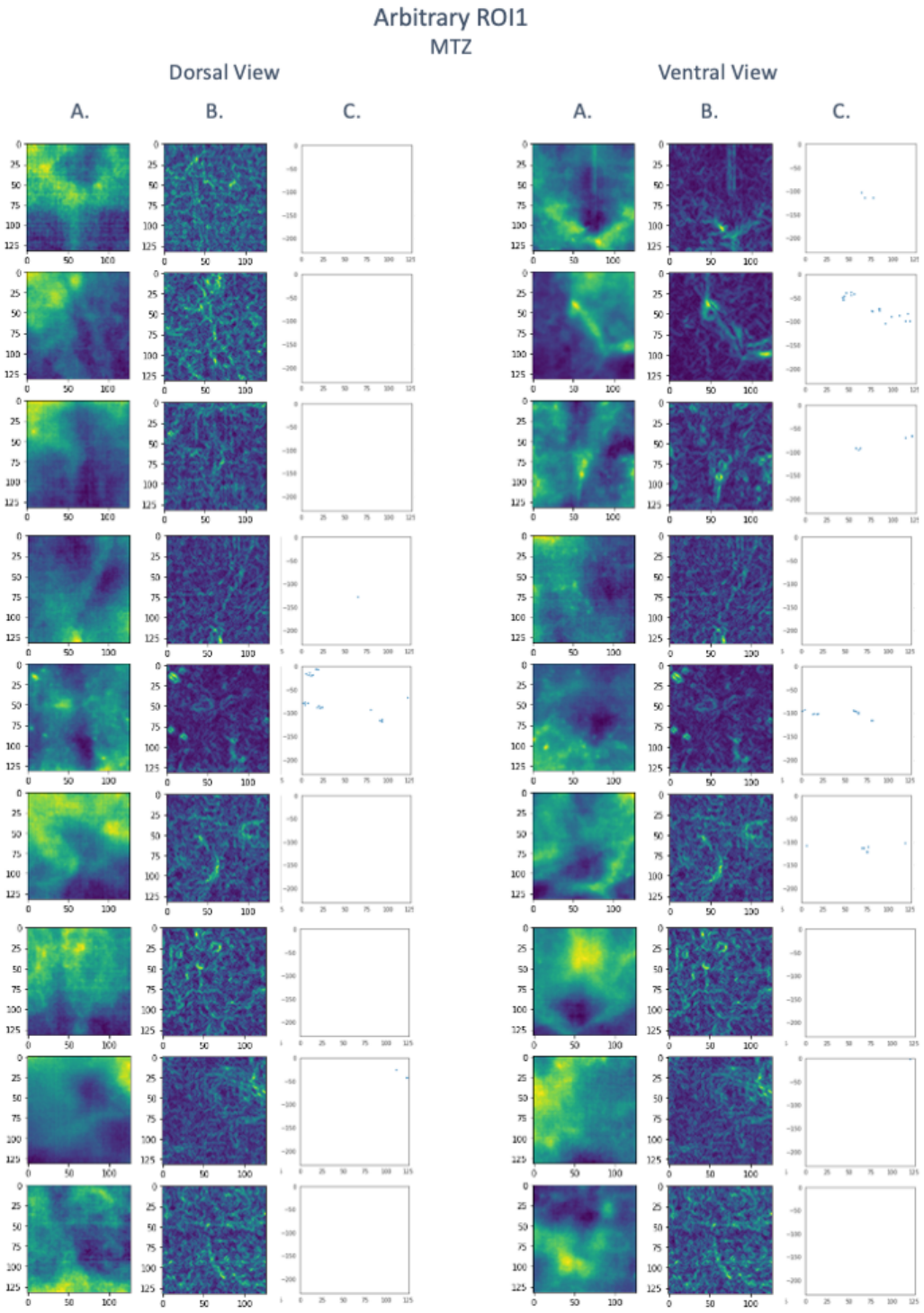

Figure A.10. Arbitrary ROI1 with MTZ Treatment. Segmentation process of the arbitrary ROI1 images under DMSO condition.(A) Summed z-stack of the roi. (B) Resulting images after application of the local gradient (LG) filter. Background subtraction was also applied for intensity normalization. (C) Identification of the intensity peaks (threshold = 4) on normalized images.

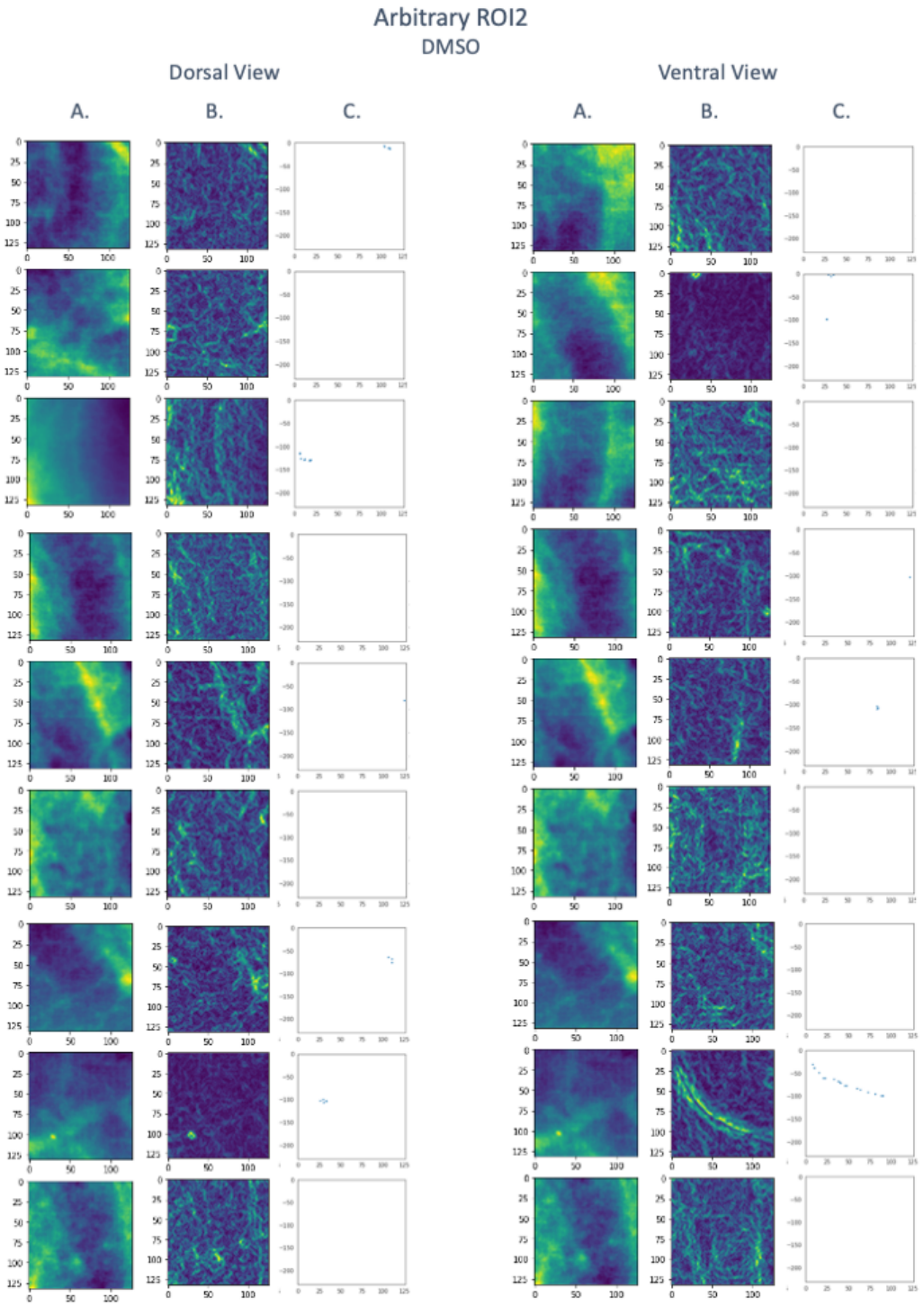

Figure A.11. Arbitrary ROI2 with DMSO Treatment. Segmentation process of the arbitrary ROI2 images under DMSO condition.(A) Summed z-stack of the roi. (B) Resulting images after application of the local gradient (LG) filter. Background subtraction was also applied for intensity normalization. (C) Identification of the intensity peaks (threshold = 4) on normalized images.

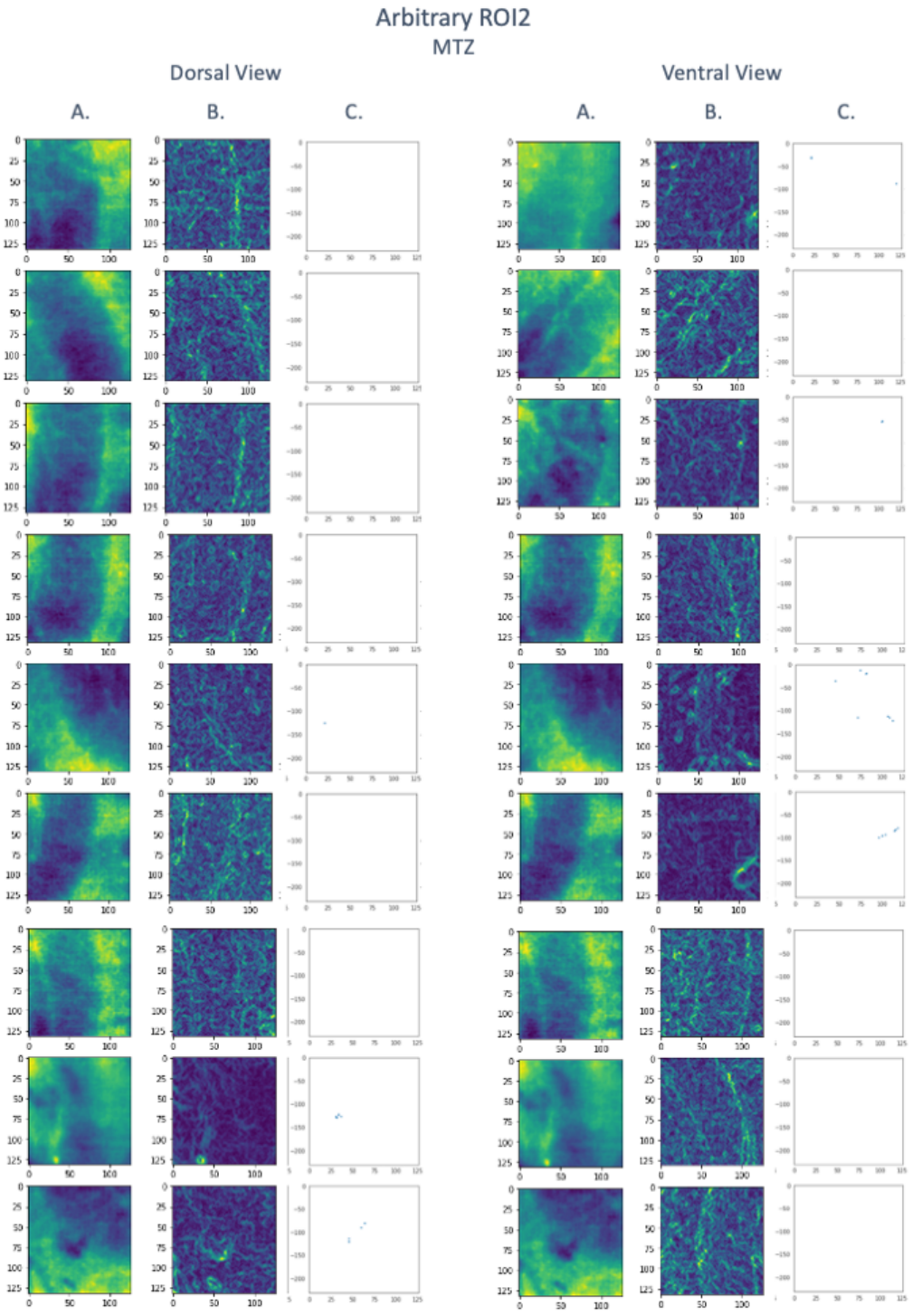

Figure A.12. Arbitrary ROI2 with MTZ Treatment. Segmentation process of the arbitrary ROI2 images under DMSO condition. (A) Summed z-stack of the roi. (B) Resulting images after application of the local gradient (LG) filter. Background subtraction was also applied for intensity normalization. (C) Identification of the intensity peaks (threshold = 4) on normalized images.

A.3 Auto-fluorescence Analysis

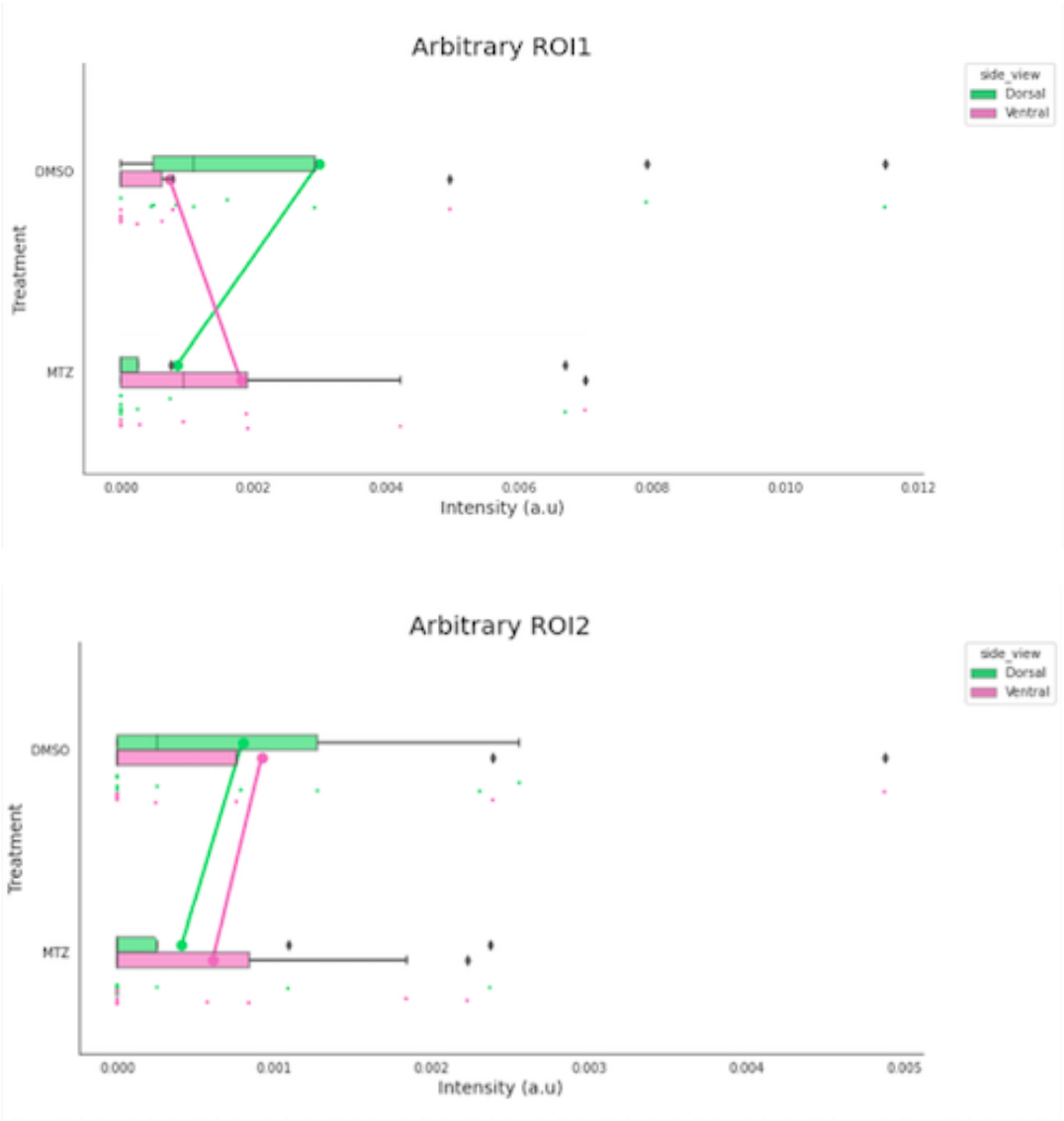

Figure A.13. Auto-fluorescence Intensity. Auto-fluorescence intensity in ROI1 and ROI2 (top and bottom panel, respectively), according to sample treatment- DMSO or MTZ. Both views, ventral (pink) and dorsal (green) are considered.

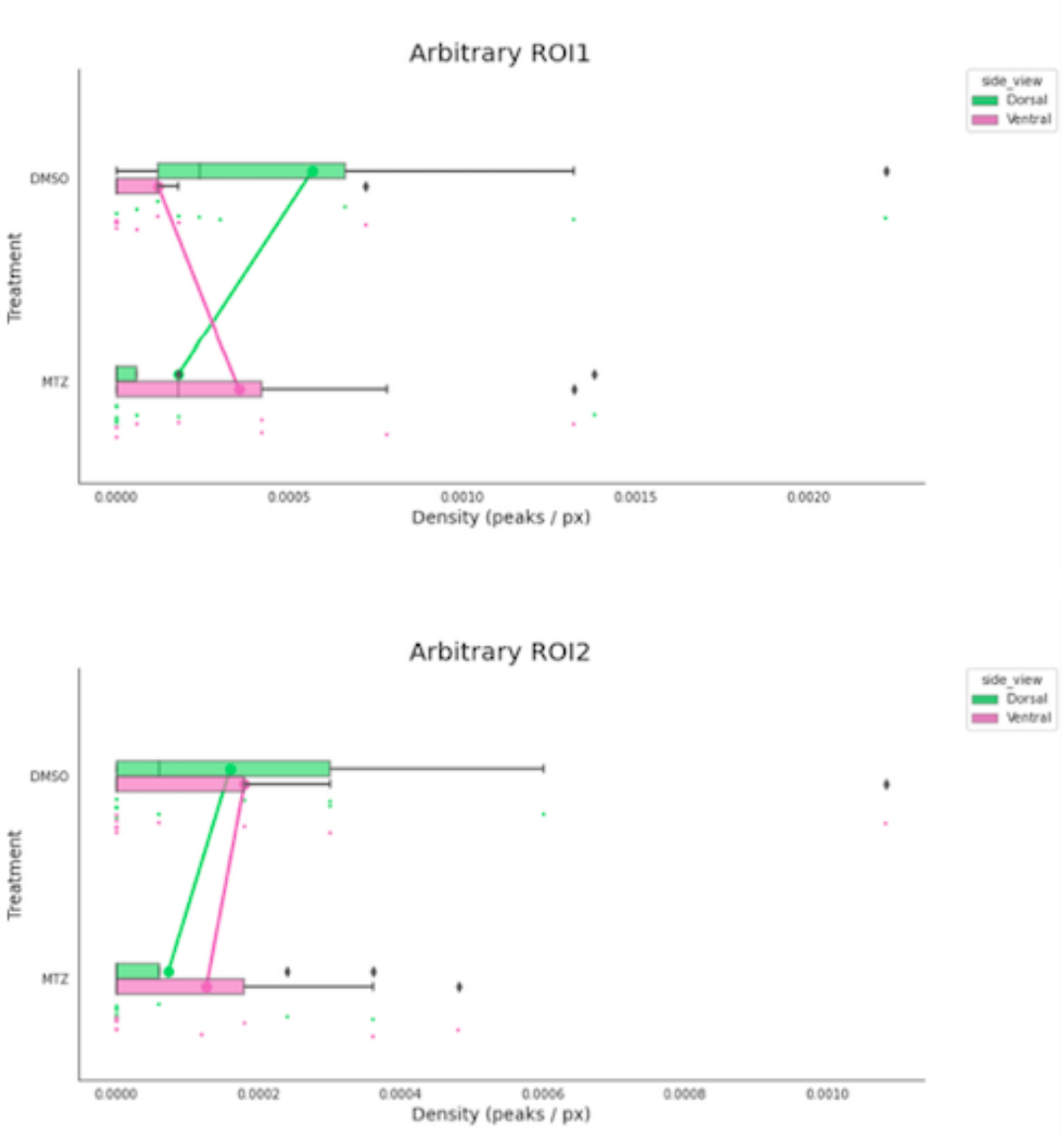

Figure A.14. Auto-fluorescence Density. Auto-fluorescence density in ROI1 and ROI2 (top and bottom panel, respectively), according to sample treatment- DMSO or MTZ. Both views, ventral (pink) and dorsal (green) are considered.

References

[1] R Adlolphs. "Cognitive Neuroscience of human social behavior". In: *Nature Reviews Neuroscience* 4 (2003), pp. 165–178.

[2] Amit Agarwal et al. "Metronidazole-induced cerebellar toxicity". In: *Neurology international* 8.1 (2016).

[3] Neelakanteswar Aluru. "Epigenetic effects of environmental chemicals: Insights from zebrafish". In: *Current opinion in toxicology* 6 (2017), pp. 26–33.

[4] Tazu Aoki et al. "Imaging of neural ensemble for the retrieval of a learned behavioral program". In: *Neuron* 78.5 (2013), pp. 881–894.

[5] Kazuhide Asakawa and Koichi Kawakami. "Targeted gene expression by the Gal4-UAS system in zebrafish". In: *Development, growth & differentiation* 50.6 (2008), pp. 391–399.

[6] Carmen Avendaño and J Carlos Menendez. *Medicinal chemistry of anticancer drugs*. Elsevier, 2015.

[7] Michael C Avery and Jeffrey L Krichmar. "Neuromodulatory systems and their interactions: a review of models, theories, and experiments". In: *Frontiers in Neural Circuits* 11 (2017), p. 108.

[8] Tobias Backström and Svante Winberg. "Central corticotropin releasing factor and social stress". In: *Frontiers in neuroscience* 7 (2013), p. 117.

[9] Sepideh Bazazi et al. "Collective motion and cannibalism in locust migratory bands". In: *Current Biology* 18.10 (2008), pp. 735–739.

[10] David Bergemann et al. "Nifurpirinol: A more potent and reliable substrate compared to metronidazole for nitroreductase-mediated cell ablations". In: *Wound Repair and Regeneration* 26.2 (2018), pp. 238–244.

[11] Nicholas J Bernier, Sarah L Alderman, and Erin N Bristow. "Heads or tails? Stressor-specific expression of corticotropin-releasing factor and urotensin I in the preoptic area and caudal neurosecretory system of rainbow trout". In: *Journal of Endocrinology* 196.3 (2008), p. 637.

[12] Walter G Bradley, IJ Karlsson, and CG Rassol. "Metronidazole neuropathy." In: *British medical journal* 2.6087 (1977), p. 610.

[13] JA Bridgewater et al. "The bystander effect of the nitroreductase/CB 1954 enzyme/prodrug system is due to a cell-permeable metabolite". In: *Human gene therapy* 8.6 (1997), pp. 709–717.

[14] John T Cacioppo et al. *Foundations in social neuroscience*. MIT press, 2002.

[15] Tolga Çavaş and Serap Ergene-Gözükara. "Genotoxicity evaluation of metronidazole using the piscine micronucleus test by acridine orange fluorescent staining". In: *Environmental Toxicology and Pharmacology* 19.1 (2005), pp. 107–111.

[16] Ruey-Kuang Cheng, Suresh J Jesuthasan, and Trevor B Penney. "Zebrafish forebrain and temporal conditioning". In: *Philosophical Transactions of the Royal Society of London B: Biological Sciences* 369.1637 (2014), p. 20120462.

[17] B Clancy and LJ Cauller. "Reduction of background autofluorescence in brain sections following immersion in sodium borohydride". In: *Journal of neuroscience methods* 83.2 (1998), pp. 97–102.

[18] Miguel L Concha. "The dorsal diencephalic conduction system of zebrafish as a model of vertebrate brain lateralisation". In: *Neuroreport* 15.12 (2004), p. 1843.

[19] Tiago Costa et al. "Automated discovery of local rules for desired collective-level behavior through reinforcement learning". In: *Front. Phys. 8: 200. doi: 10.3389/fphy* (2020).

[20] Iain D Couzin et al. "Collective memory and spatial sorting in animal groups". In: *Journal of theoretical biology* 218.1 (2002), pp. 1–12.

[21] Silvia Curado, Didier YR Stainier, and Ryan M Anderson. "Nitroreductase-mediated cell/tissue ablation in zebrafish: a spatially and temporally controlled ablation method with applications in developmental and regeneration studies". In: *Nature protocols* 3.6 (2008), p. 948.

[22] Silvia Curado et al. "Conditional targeted cell ablation in zebrafish: a new tool for regeneration studies". In: *Developmental dynamics: an official publication of the American Association of Anatomists* 236.4 (2007), pp. 1025–1035.

[23] Ke Deng et al. "Whole-brain mapping of projection from mouse lateral septal nucleus". In: *Biology open* 8.7 (2019), bio043554.

[24] Robert John Denver. "Structural and functional evolution of vertebrate neuroendocrine stress systems". In: (2009).

[25] Elena Dreosti et al. "Development of social behavior in young zebrafish". In: *Frontiers in neural circuits* 9 (2015), p. 39.

[26] Wolfgang Driever et al. "Zebrafish: genetic tools for studying vertebrate development". In: *Trends in Genetics* 10.5 (1994), pp. 152–159.

[27] Raymond E Engeszer et al. "Timing and plasticity of shoaling behaviour in the zebrafish, Danio rerio". In: *Animal behaviour* 74.5 (2007), pp. 1269–1275.

[28] Ryann M Fame, Carole Brajon, and Alain Ghysen. "Second-order projection from the posterior lateral line in the early zebrafish brain". In: *Neural development* 1.1 (2006), p. 4.

[29] Karine Faucher et al. "Fish lateral system is required for accurate control of shoaling behaviour". In: *Animal Behaviour* 79.3 (2010), pp. 679–687.

[30] Stan B Floresco. "The nucleus accumbens: an interface between cognition, emotion, and action". In: *Annual review of psychology* 66 (2015), pp. 25–52.

[31] Yijie Geng and Randall T Peterson. "The zebrafish subcortical social brain as a model for studying social behavior disorders". In: *Disease models & mechanisms* 12.8 (2019), p. dmm039446.

[32] R. Godoy, K. Hua, M. Kalyn, et al. "Dopaminergic neurons regenerate following chemogenetic ablation in the olfactory bulb of adult Zebrafish (Danio rerio)". In: *Sci Rep* 10 (2020), p. 12825. URL: `https://doi.org/10.1038/s41598-020-69734-0`.

[33] John Godwin and Richmond Thompson. "Nonapeptides and social behavior in fishes". In: *Hormones and Behavior* 61.3 (2012), pp. 230–238.

[34] Archana Golla, Henrik Østby, and Florence Kermen. "chronic unpredictable stress induces anxiety-like behaviors in young zebrafish". In: *Scientific Reports* 10.1 (2020), pp. 1–10.

[35] James L Goodson. "The vertebrate social behavior network: evolutionary themes and variations". In: *Hormones and behavior* 48.1 (2005), pp. 11–22.

[36] Beyhan Gürcü et al. "Matrix changes due to the toxic effects of metronidazole in intestinal tissue of fish (Onchorhynchus mykiss)". In: *Chemosphere* 144 (2016), pp. 1605–1610.

[37] Junyan Han et al. "Detrimental effects of metronidazole on the liver of freshwater common carp (Cyprinus carpio L.)" In: *Bulletin of environmental contamination and toxicology* 91.4 (2013), pp. 444–449.

[38] Francisco JH Heras et al. "Deep attention networks reveal the rules of collective motion in zebrafish". In: *PLoS computational biology* 15.9 (2019), e1007354.

[39] James E Herbert-Read et al. "Inferring the rules of interaction of shoaling fish". In: *Proceedings of the National Academy of Sciences* 108.46 (2011), pp. 18726–18731.

[40] Robert C Hinz and Gonzalo G de Polavieja. "Ontogeny of collective behavior reveals a simple attraction rule". In: *Proceedings of the National Academy of Sciences* (2017), p. 201616926.

[41] Christos C Ioannou, Vishwesha Guttal, and Iain D Couzin. "Predatory fish select for coordinated collective motion in virtual prey". In: *Science* 337.6099 (2012), pp. 1212–1215.

[42] Mordechai Z Juni and Miguel P Eckstein. "Flexible human collective wisdom." In: *Journal of experimental psychology: human perception and performance* 41.6 (2015), p. 1588.

[43] Allan V Kalueff et al. "Towards a comprehensive catalog of zebrafish behavior 1.0 and beyond". In: *Zebrafish* 10.1 (2013), pp. 70–86.

[44] Yael Katz et al. "Inferring the structure and dynamics of interactions in schooling fish". In: *Proceedings of the National Academy of Sciences* 108.46 (2011), pp. 18720–18725.

[45] K Kawakami et al. "Gal4 driver transgenic zebrafish: powerful tools to study developmental biology, organogenesis, and neuroscience". In: *Advances in genetics*. Vol. 95. Elsevier, 2016, pp. 65–87.

[46] Charles B Kimmel et al. "Stages of embryonic development of the zebrafish". In: *Developmental dynamics* 203.3 (1995), pp. 253–310.

[47] Ryo Kurita et al. "Suppression of lens growth by αA-crystallin promoter-driven expression of diphtheria toxin results in disruption of retinal cell organization in zebrafish". In: *Developmental biology* 255.1 (2003), pp. 113–127.

[48] Akira Kuriyama et al. "Metronidazole-induced central nervous system toxicity: a systematic review". In: *Clinical neuropharmacology* 34.6 (2011), pp. 241–247.

[49] Elana V Kysil et al. "Comparative analyses of zebrafish anxiety-like behavior using conflict-based novelty tests". In: *Zebrafish* 14.3 (2017), pp. 197–208.

[50] Aaron M Lambert, Joshua L Bonkowsky, and Mark A Masino. "The conserved dopaminergic diencephalospinal tract mediates vertebrate locomotor development in zebrafish larvae". In: *Journal of Neuroscience* 32.39 (2012), pp. 13488–13500.

[51] PF Lanzky and B Halting-Sørensen. "The toxic effect of the antibiotic metronidazole on aquatic organisms". In: *Chemosphere* 35.11 (1997), pp. 2553–2561.

[52] Gregory D Marquart et al. "A 3D searchable database of transgenic zebrafish Gal4 and Cre lines for functional neuroanatomy studies". In: *Frontiers in neural circuits* 9 (2015), p. 78.

[53] Gregory D Marquart et al. "High-precision registration between zebrafish brain atlases using symmetric diffeomorphic normalization". In: *GigaScience* 6.8 (2017), gix056.

[54] Sandra Martins et al. "Toward an integrated zebrafish health management program supporting cancer and neuroscience research". In: *Zebrafish* 13.S1 (2016), S–47.

[55] Jonathan R Mathias et al. "Enhanced cell-specific ablation in zebrafish using a triple mutant of Escherichia coli nitroreductase". In: *Zebrafish* 11.2 (2014), pp. 85–97.

[56] Caio Maximino et al. "Measuring anxiety in zebrafish: a critical review". In: *Behavioural brain research* 214.2 (2010), pp. 157–171.

[57] Noam Miller and Robert Gerlai. "From schooling to shoaling: patterns of collective motion in zebrafish (Danio rerio)". In: *PLoS One* 7.11 (2012), e48865.

[58] Noam Miller and Robert Gerlai. "Quantification of shoaling behaviour in zebrafish (Danio rerio)". In: *Behavioural brain research* 184.2 (2007), pp. 157–166.

[59] Noam Y Miller and Robert Gerlai. "Shoaling in zebrafish: what we don't know". In: *Reviews in the Neurosciences* 22.1 (2011), pp. 17–25.

[60] Cecilia B Moens and Victoria E Prince. "Constructing the hindbrain: insights from the zebrafish". In: *Developmental dynamics: an official publication of the American Association of Anatomists* 224.1 (2002), pp. 1–17.

[61] Thomas Mueller et al. "The dorsal pallium in zebrafish, Danio rerio (Cyprinidae, Teleostei)". In: *Brain research* 1381 (2011), pp. 95–105.

[62] Akira Muto and Koichi Kawakami. "Imaging functional neural circuits in zebrafish with a new GCaMP and the Gal4FF-UAS system". In: *Communicative & integrative biology* 4.5 (2011), pp. 566–568.

[63] Sarah Winans Newman. "The medial extended amygdala in male reproductive behavior a node in the mammalian social behavior network". In: *Annals of the New York Academy of Sciences* 877.1 (1999), pp. 242–257.

[64] Rudolf Nieuwenhuys, J Hans, and Charles Nicholson. *The central nervous system of vertebrates*. Springer, 2014.

[65] William Norton and Laure Bally-Cuif. "Adult zebrafish as a model organism for behavioural genetics". In: *BMC neuroscience* 11.1 (2010), p. 90.

[66] Lauren A O'Connell and Hans A Hofmann. "The vertebrate mesolimbic reward system and social behavior network: a comparative synthesis". In: *Journal of Comparative Neurology* 519.18 (2011), pp. 3599–3639.

[67] Rui F Oliveira. "Mind the fish: zebrafish as a model in cognitive social neuroscience". In: *Frontiers in neural circuits* 7 (2013), p. 131.

[68] Rui F Oliveira, Joana F Silva, and José M Simoes. "Fighting zebrafish: characterization of aggressive behavior and winner–loser effects". In: *Zebrafish* 8.2 (2011), pp. 73–81.

[69] Lauren A O'Connell and Hans A Hofmann. "Evolution of a vertebrate social decision-making network". In: *Science* 336.6085 (2012), pp. 1154–1157.

[70] Fabrizio Palumbo et al. "The zebrafish dorsolateral habenula is required for updating learned behaviors". In: *bioRxiv* (2020), p. 802256.

[71] Matthew O Parker et al. "The role of zebrafish (Danio rerio) in dissecting the genetics and neural circuits of executive function". In: *Frontiers in neural circuits* 7 (2013), p. 63.

[72] Brian L Partridge and Tony J Pitcher. "The sensory basis of fish schools: relative roles of lateral line and vision". In: *Journal of comparative physiology* 135.4 (1980), pp. 315–325.

[73] Michail Pavlidis et al. "Husbandry of zebrafish, Danio rerio, and the cortisol stress response". In: *Zebrafish* 10.4 (2013), pp. 524–531.

[74] Stella Pelengaris, Michael Khan, and Gerard I Evan. "Suppression of Myc-induced apoptosis in β cells exposes multiple oncogenic properties of Myc and triggers carcinogenic progression". In: *Cell* 109.3 (2002), pp. 321–334.

[75] Simon Perathoner, Maria Lorena Cordero-Maldonado, and Alexander D Crawford. "Potential of zebrafish as a model for exploring the role of the amygdala in emotional memory and motivational behavior". In: *Journal of neuroscience research* 94.6 (2016), pp. 445–462.

[76] Alfonso Pérez-Escudero and Gonzalo G De Polavieja. "Collective animal behavior from Bayesian estimation and probability matching". In: *PLoS computational biology* 7.11 (2011), e1002282.

[77] Alfonso Pérez-Escudero and Gonzalo G de Polavieja. "Adversity magnifies the importance of social information in decision-making". In: *Journal of The Royal Society Interface* 14.136 (2017), p. 20170748.

[78] Harshan Pisharath and Michael J Parsons. "Nitroreductase-mediated cell ablation in transgenic zebrafish embryos". In: *Zebrafish*. Springer, 2009, pp. 133–143.

[79] Harshan Pisharath et al. "Targeted ablation of beta cells in the embryonic zebrafish pancreas using E. coli nitroreductase". In: *Mechanisms of development* 124.3 (2007), pp. 218–229.

[80] Tony J Pitcher. "Functions of shoaling behaviour in teleosts". In: *The behaviour of teleost fishes*. Springer, 1986, pp. 294–337.

[81] Abigail M Polter and Julie A Kauer. "Stress and VTA synapses: implications for addiction and depression". In: *European Journal of Neuroscience* 39.7 (2014), pp. 1179–1188.

[82] Gerd-Jörg Rauch, Michael Granato, and Pascal Haffter. "A polymorphic zebrafish line for genetic mapping using SSLPs on high-percentage agarose gels". In: *Technical Tips Online* 2.1 (1997), pp. 148–150.

[83] Chris R Reid et al. "Army ants dynamically adjust living bridges in response to a cost–benefit trade-off". In: *Proceedings of the National Academy of Sciences* 112.49 (2015), pp. 15113–15118.

[84] Lesley Ricci et al. "Development of aggressive phenotypes in zebrafish: interactions of age, experience and social status". In: *Animal Behaviour* 86.2 (2013), pp. 245–252.

[85] Elke Rink and Mario F Wullimann. "The teleostean (zebrafish) dopaminergic system ascending to the subpallium (striatum) is located in the basal diencephalon (posterior tuberculum)". In: *Brain research* 889.1-2 (2001), pp. 316–330.

[86] Tobias Roeser and Herwig Baier. "Visuomotor behaviors in larval zebrafish after GFP-guided laser ablation of the optic tectum". In: *Journal of Neuroscience* 23.9 (2003), pp. 3726–3734.

[87] Francisco Romero-Ferrero et al. "idtracker. ai: Tracking all individuals in large collectives of unmarked animals". In: *arXiv preprint arXiv:1803.04351* (2018).

[88] Luiz V Rosa et al. "Three-and bi-dimensional analyses of the shoaling behavior in zebrafish: Influence of modulators of anxiety-like responses". In: *Progress in Neuro-Psychopharmacology and Biological Psychiatry* (2020), p. 109957.

[89] Cristina Saverino and Robert Gerlai. "The social zebrafish: behavioral responses to conspecific, heterospecific, and computer animated fish". In: *Behavioural brain research* 191.1 (2008), pp. 77–87.

[90] Johannes Schindelin et al. "Fiji: an open-source platform for biological-image analysis". In: *Nature methods* 9.7 (2012), p. 676.

[91] Rebecca Schmidt, Uwe Strähle, and Steffen Scholpp. "Neurogenesis in zebrafish–from embryo to adult". In: *Neural development* 8.1 (2013), pp. 1–13.

[92] Stephen A Schnell, William A Staines, and Martin W Wessendorf. "Reduction of lipofuscin-like autofluorescence in fluorescently labeled tissue". In: *Journal of Histochemistry & Cytochemistry* 47.6 (1999), pp. 719–730.

[93] SJ Schnörr et al. "Measuring thigmotaxis in larval zebrafish". In: *Behavioural brain research* 228.2 (2012), pp. 367–374.

[94] EL Serra, CC Medalha, and R Mattioli. "Natural preference of zebrafish (Danio rerio) for a dark environment". In: *Brazilian journal of medical and biological research* 32.12 (1999), pp. 1551–1553.

[95] David H Skuse and Louise Gallagher. "Dopaminergic-neuropeptide interactions in the social brain". In: *Trends in cognitive sciences* 13.1 (2009), pp. 27–35.

[96] Krasimir Slanchev et al. "Development without germ cells: the role of the germ line in zebrafish sex differentiation". In: *Proceedings of the National Academy of Sciences* 102.11 (2005), pp. 4074–4079.

[97] Sarah J Stednitz et al. "Forebrain control of behaviorally driven social orienting in zebrafish". In: *Current Biology* 28.15 (2018), pp. 2445–2451.

[98] Adam Stewart et al. "Modeling anxiety using adult zebrafish: a conceptual review". In: *Neuropharmacology* 62.1 (2012), pp. 135–143.

[99] David JT Sumpter. *Collective animal behavior*. Princeton University Press, 2010.

[100] Etsuo A Susaki et al. "Advanced CUBIC protocols for whole-brain and whole-body clearing and imaging". In: *Nature protocols* 10.11 (2015), p. 1709.

[101] GLADYS ALEJANDRA Toledo-Ibarra, ARGELIA ESPERANZA Rojas-Mayorquín, and MANUEL IVAN Girón-Pérez. "Influence of the cholinergic system on the immune response of teleost fishes: potential model in biomedical research". In: *Clinical and developmental immunology* 2013 (2013).

[102] Kolbjørn Tunstrøm et al. "Collective states, multistability and transitional behavior in schooling fish". In: *PLoS computational biology* 9.2 (2013).

[103] Ines Villano et al. "Basal forebrain cholinergic system and orexin neurons: effects on attention". In: *Frontiers in behavioral neuroscience* 11 (2017), p. 10.

[104] Chelsea K Wallace et al. "Effectiveness of rapid cooling as a method of euthanasia for young zebrafish (Danio rerio)". In: *Journal of the American Association for Laboratory Animal Science* 57.1 (2018), pp. 58–63.

[105] Mario F Wulliman, Barbara Rupp, and Heinrich Reichert. *Neuroanatomy of the zebrafish brain: a topological atlas*. Birkhäuser, 2012.

[106] Chao Yu, Minjie Zhang, and Fenghui Ren. "Collective learning for the emergence of social norms in networked multiagent systems". In: *IEEE Transactions on Cybernetics* 44.12 (2014), pp. 2342–2355.

[107] Tingting Yu et al. "RTF: a rapid and versatile tissue optical clearing method". In: *Scientific reports* 8.1 (2018), pp. 1–9.

[108] Yunsheng Zhang et al. "Optimization of the Gal4/UAS transgenic tools in zebrafish". In: *Applied microbiology and biotechnology* 103.4 (2019), pp. 1789–1799.

[109] Fernanda Francine Zimmermann et al. "Embryological exposure to valproic acid induces social interaction deficits in zebrafish (Danio rerio): A developmental behavior analysis". In: *Neurotoxicology and teratology* 52 (2015), pp. 36–41.